

2.3 Coal and Coke

The coke charged into a blast furnace plays the following roles.

- i) Heat source for combustion
- ii) Reducing agent
- iii) Spacer for maintaining gas permeability in the blast furnace
- iv) Heat-exchanging medium in a specific temperature zone to communicate heat to pig iron and slag

Of these four, the roles of heat source and reducing agent may partly be shared with liquid fuel, like heavy oil and tar, blown in from the tuyere. But, there are no alternatives of the coke so far as the spacer and heat exchanger functions are concerned, particularly in the high-temperature zone in the furnace bottom.

The coke to be charged into the blast furnace are required to satisfy all these needs and at the same time to have proper chemical composition.

In Japan, the quality of coke is controlled with emphasis placed on the coke strength at room and high temperature required of spacer function.

Given in the following are the evaluation of COLAR coal and coke, obtained by the samples and recommended measures to attain required qualities of coke.

2.3.1 Quality of COLAR coal

The coal samples which the survey mission took at site were analyzed and measured as shown in Table 2.3-1.

The samples taken were from five seams (No.5, 6, 7, 10 and 12).

(1) Proximate analysis (Table 2.3-1a)

The analysis by Kobe Steel shows far lower values of ash and phosphorus than by COLAR. As regards the ash, the samples taken by the survey mission may have been from coal seams of low ash content.

We are at a loss how to account for phosphorus in the ash. The samples taken by the mission may not represent the coal seams.

(2) Physical properties (Tables 2.3-1-b through -d)

So far as the physical properties stand, there is no significant difference between samples.

The coals were generally high in fluidity and dilatation.

(3) Microscopic measurement and ultimate analysis (Tables 2.3-1-e through -g)

Judging from the value of the mean reflectance of vitrinite which stand for the degree of carbonization and the value of fluidity, the COLAR coals seem to be akin to the high volatile coals seen in the U.S.A. (See Fig. 2.3-1)

From microscopic observations the COLAR coals show clean cross sections with less exinite similar to the Japanese high volatile coals. (American high-volatile coals show complicated cross sections with much contents of exinite and spollinite.) (Photo 2.3-1). But, from the H/C value in ultimate analysis, the COLAR coals show structures close to American rather than Japanese high-volatile coals.

(See Fig. 2.3-2). All in all, the COLAR coals are regarded as akin to the American high-volatile coals.

2.3.2 Evaluation of COLAR coal

The COLAR coals which show a low phosphorus content are expected to fully satisfy the requirement set out by Kobe Steel for the foundry pig iron coke that the phosphorus be less than 0.040%.

The ash is not too much except for the sample from No. 6 seam. Hence, no problem will arise if the coal from No. 6 seam is handled with care. Since a large discrepancy exists between COLAR's and Kobe Steel's analytical data,

it is required to check whether the samples taken by the mission are representative of the ash content of each seam.

Judging from microscopic measurement for the maceral and the reflectance of the coals, and softening and melting characteristics measured in gieseler plastometer and A.A. dilatometer, the COLAR coals resemble "Russel Fork", a high-volatile coal in the U.S.A. (See Table 2.3-2).

Judging from the C.B.I. (composition balance index) vs. S.I. (strength index) relationship prepared by Nippon Steel with respect to the characteristics of coking coals used, the COLAR coals are expected to provide coke of about 91.5% in coke strength at room temperature ($DI \frac{30}{15}$) by chamber coke ovens in Japan. (See Fig. 2.3-3) This corresponds to more than 50% in terms of tumbler stability index (T_{25}) (See Fig. 2.7-4), and it is believed that the coke strength required for the time being (1st step: $T_{25} \geq 45\%$) will be attained if the operating conditions are adjusted properly. In the second step, however, efforts should be made to increase T_{25} to more than 50%.

2.3.3 COLAR coke quality

The coke samples taken by the survey mission from the site back home were analyzed and measured. The results are as shown in Table 2.3-4. By way of reference, the properties of chamber oven coke from Paz del Rio and beehive oven coke from Bellumbi (Australia) are shown additionally. The properties of Kakogawa coke used by Kobe Steel are given in Table 2.3-3 to represent those of the coke applied to the blast furnaces of 4,000 m³ class.

- (1) Proximate analysis, JIS reactivity, microstrength, and porosity (Table 2.3-4-a)

The JIS reactivity is extremely low as compared with the coals of the same degree of carbonization.

While it may be attributable to the singularities of COLAR coal, the different conditions of carbonization may also be a cause since the coke presents to some extent a leaflet texture (most anisotropic texture) which is usually not produced by the coal as low qualified as COLAR coal.

(2) Microscopic measurement (Table 2.3-4-b)

Compared with Kakogawa coke of Kobe Steel, COLAR coke is very short of the leaflet texture (see Fig. 2.3-4) since COLAR coal doesn't contain a high qualified coal.

Accordingly COLAR coke is considered somewhat inferior to Kakogawa coke in view of coke texture. While the coke of Paz del Rio is mainly in fine mosaic texture, COLAR's shows a coarse mosaic texture.

Accordingly, COLAR coke, which is grown more in optical anisotropy, is regarded as a little better than Paz del Rio. (See Photo 2.3-2).

(3) Microscopic observations of the products carbonized in Juranek furnace

Of the samples taken by the survey mission, those from No.12 seam were carbonized to study their changes in the coking process by microscopically observing the products.

(See Photo 2.3-3). The changes during the coking process bear a resemblance to those of Mulga coal an American medium-volatile coal in the coking region, size of anisotropic texture is fine, the fibrous texture is rarely observed and coarse mosaic texture is much observed.

The cross sections of the products show large voids in the plastic zone, just as with Miike coal (a Japanese high volatile coal), Mulga coal (an American medium-volatile coal) and the like which show a high Y-index by Sapozhnikov plastometer and are high in dilatation and fluidity. It is therefore judged that COLAR coal is rich in tendencies toward softening and melting.

(4) Qualities of coke at high temperature (Table 2.3-4-c)

The mechanism that degrades the coke strength in the blast furnace is as follows.

- i) Shocks due to falling on the stock line.
- ii) Decline in particle size due to attrition to be experienced during descending from the top of shaft down.

- iii) Weakening in strength due to carbon solution reaction with CO_2 in the atmosphere and particle size reduction in the lower part of shaft.
- iv) Deterioration due to high temperature (above $1,300^\circ\text{C}$) in the sections below the belly.
- v) Deterioration due to churning and collision invigorated by a high-velocity hot blast (200 m/sec.) at the raceway ahead of the tuyere.

Of these factors, i) and ii) have been assessed in terms of coke strength at room temperature. The factors iii) through v) represent coke degrading mechanisms at high temperature, and almost all Japanese steel companies employ as a control index, coke strength after gasification which was first adopted by Hirohata Works, of Nippon Steel. In order to evaluate the qualities of COLAR coke at high temperature, coke strength after gasification was measured. The results are as shown in Table 2.3-4-c. It is found that COLAR coke is lower reactivity than that of the cokes used in any works of Kobe Steel and shows an acceptably high value of coke strength after gasification. (See Fig. 2.3-5)

2.3.4 Evaluation of the quality of COLAR coke

As it is estimated to be a high fluidity coal, COLAR coke is carbonized tight, and the microstrength with which to show the strength of the matrix is almost the same as Kakogawa coke of Kobe Steel. In addition, JIS reactivity is very low, and coke strength after gasification is also high. While the matrix of COLAR coke is carbonized tight enough, the lump size coke has many cracks, and coke strength at room temperature of the coke of the lump sizes in which range it is to be charged into the blast furnace is considered to become fragile.

Accordingly one of the major reasons why COLAR cokes have a low strength with stability index 32 to 40% in actual operation will be serious cracking of coke due to dilatation and contraction during coking process.

The stability Index of the sample cokes could not be measured, because the amount of the samples were not enough.

2.3.5 Measures for improvement of COLAR coke quality

(1) Blending the coals

- a) The coking coal used is obtained from seams No.5, 6, 7, 9, 10, 11 and 12. The coke quality seems likely to be improved with less variation if the coking coal used is classified by ash, degree of carbonization, fluidity, and other characteristic values into 2 to 3 groups, and used with the constant blending ratio of these groups. Use of the coal from No. 6 seam should preferably be limited to a minimum if at all possible.
- b) As COLAR coals are high volatile and fluidity, it is required to carbonize with enough coking time. Accordingly, improvement of coke strength will be expected by controlling the excess fluidity and making a seeds of cokes, for example, by blending inerts like petroleum coke or anthracite. In this case, however, it will be necessary to break up the coal blend to -3mm fines for about 80% and mix up evenly.
- c) There are many reports about the relationships between the characteristics of coal and the coke strength. According to N. Shapiro, R.J. Gray, G.R. Eusner, et al, it is said that the coke strength becomes high if the coal has much vitrinite with a high degree of carbonization and an optimum amount of inerts. For example, the high-fluidity Pittsburg coal (U.S.A.), if used alone, shows a stability index of as low as 38%. But if it is mixed with low-volatile coal with a stability index of 53% at a ratio of 7 to 3, the stability index of the coal blend can be improved up to 58% because of aynergy.
(See Fig. 2.3-6)

Thus, if COLAR coal is mixed with a proper type of other coals (low-volatile coal), the coke strength will probably be increased to a satisfactory level.

In this case, also, the coal blend should have contain about 80% of -3mm fines and be mixed up uniformly.

(2) Beneficiation of coal

The maceral of the coal can be divided into two parts; reactive component which melts when carbonized and inert component which does not. It is important to carbonize the coal blend with all these components mixed uniformly.

Namely, the coke strength will be improved with less variation if the coal blend is sized to -3 mm fines for about 80% and mixed up well. The crushing will reduce the bulk density, and a dust will be raised during handling. These problems will be solved effectively if oiling (addition of heavy oil) is made.

(3) Carbonization of coal

The conditions for carbonizing are dependent on the properties of coking coal and the type of coke ovens to be used.

As for the beehive coke ovens employed by the COLAR, it is recommended to take enough coking time in carbonization for the purpose of improving the coke strength. From the viewpoint of coke yield, efforts should be made to carbonize uniformly for the purpose of minimizing the solution loss. The air ratio in the coke oven is of critical importance in the attainment of these objectives. The instrumentation of coke ovens should therefore be promoted, and the optimum conditions for carbonization should be found through trial and error.

(4) Sizing of coke

It is of prime importance in keeping blast furnace operating stability to control the coke sizes to within 15 to 75 mm all the time.

The measures for improvements have been discussed above, which may be classified into two; 1st step measures which can be put to practice immediately with some modifications of the existing coke ovens and 2nd step measures which can be implemented only when a new chamber coke ovens is installed.

In passing, a new installation of chamber coke ovens is roughly estimated at ¥2,000 mil. to ¥3,000 mil. (Table 2.3-5)

2.3.6 Current operations of COLAR coke ovens

COLAR, Bellumbi Coal Co. (Australia) and Wakanabe Works of Hokkaido Tanko-Kisen (Japan) are compared with reference to their operations of beehive coke ovens (Table 2.3-6). COLAR operations are quite dissimilar to others in that the particle size of the coal blend is coarser.

2.3.7 Problems left to future study

- (1) Studies for improving the facilities and operating conditions to meet the required coke quality.
- (2) Recovery of gas.
- (3) Utilization of breeze.

COLAR COAL

Table 2.3-1-a Proximate analysis

Sample No.	Assayer	Proximate analysis						
		Water %	Ash %	V.M.% *	F.C.% *	S %	P % in Ash	CSN
Seam No.5	Kobe Steel	-	7.6	36.82	63.18	1.06	0.276	7
	COLAR	1.25	10.35	37.78	62.22	2.01	1.03	6
Seam No.6	Kobe Steel	-	28.96	36.84	63.16	1.02	0.196	4 1/2
	COLAR	1.83	16.63	38.06	61.94	1.08	0.83	6
Seam No.7	Kobe Steel	-	10.72	35.39	64.61	0.42	0.134	5 1/2
	COLAR	2.57	13.57	34.09	65.91	0.50	0.19	3
Seam No.10	Kobe Steel	-	4.72	31.11	68.89	0.53	0.159	7
	COLAR	0.50	13.70	32.98	67.02	0.73	0.109	7
Seam No.12	Kobe Steel	-	7.71	30.90	69.1	0.66	0.159	6 1/2
	COLAR	0.70	13.47	31.34	68.66	0.58	0.13	6 1/2

(* dry ash free)

Sample No.	Ash analysis (%)										
	Fe ₂ O ₃	MnO	CaO	M ₃ O	Al ₂ O ₃	SiO ₂	P	SO ₃	TiO ₂	Na ₂ O	K ₂ O
Seam No.5	11.66	0.06	0.21	0.74	16.23	56.16	0.276	0.173	1.06	0.50	1.60
Seam No.6	4.47	<0.01	0.19	0.80	15.30	65.20	0.196	0.204	1.16	0.34	1.72
Seam No.7	2.28	<0.01	0.19	0.41	19.30	58.54	0.134	0.031	1.09	-	-
Seam No.10	3.27	<0.01	0.21	0.51	15.20	66.46	0.159	0.031	1.35	-	-
Seam No.12	5.87	0.01	0.17	0.74	15.10	64.28	0.159	0.094	1.26	-	-

COLAR's analysis refers to the mean values in actual operations made from Dec. 1977 to Feb. 1978.

Table 2.3-1-b Measurements of fluidity by gieseler plastometer

Sample No.	Max. fluidity (log MFD)	Softening temperature (°C)	Maximum fluidity temperature (°C)	Solidification temperature (°C)	Melting range (°C)
Seam No.5	945 (2.98)	396	445	472	76
Seam No.6	868 (2.94)	398	445	475	77
Seam No.7	4342 (3.64)	394	446	482	88
Seam No.10	1219 (3.09)	391	447	481	90
Seam No.12	1087 (3.04)	398	449	480	92

Table 2.3-1-c Measurements of dilatation and contraction by A.A. dilatometer

Sample No.	Total dilatation (%)	Max. contraction (%)	Max. dilatation (%)	Softening temperature (°C)	Max. contraction temperature (°C)	Max. dilatation temperature (°C)
Seam No.5	88	25	63	356	420	461
Seam No.6	16	12	4	373	436	454
Seam No.7	173	25	148	341	410	472
Seam No.10	149	23	126	355	409	472
Seam No.12	139	22	117	361	412	473

Table 2.3-1-d Measurements of softening and melting characteristics by Sapozhnikov plastometer

	X-index	Y-index
Seam No.5	29	21
Seam No.6	34	13
Seam No.7	24	20
Seam No.10	13	20
Seam No.12	10	23

Table 2.3-1-e Microscopic measurement for the maceral of coal

Sample No.	Reactives (%)				Inerts (%)				Total
	Vitri- nite	1/3 Semi Fusinite	Exinite	Total	2/3 Semi Fusinite	Micri- nite	Fusinite	Mineral Matter	
Seam No.5	79.5	1.2	1.3	82.0	2.5	10.0	2.0	3.5	18.0
Seam No.6	74.0	0.3	1.9	76.2	0.5	8.7	1.9	12.7	23.8
Seam No.7	73.4	1.6	2.8	77.8	3.1	9.4	5.0	4.7	22.2
Seam No.10	71.4	2.3	0.8	74.5	4.6	15.0	3.7	2.2	25.5
Seam No.12	80.6	1.4	0.6	82.6	2.7	7.2	4.0	3.5	17.4

Table 2.3-1-f Microscopic measurement for the reflectance of vitrinite

Sample No.	Vitrinite Type (%)														Mean reflectance
	5	6	7	8	9	10	11	12	13	14					
Seam No. 5			2.2	19.5	67.4	10.9									0.94
Seam No. 6				7.1	67.9	25.0									0.96
Seam No. 7				3.3	53.4	43.3									1.00
Seam No.10					3.3	75.0	21.7								1.06
Seam No.12					15.4	73.9	9.2	1.5							1.05

Table 2.3-1-g Ultimate analysis

Sample No.	Ultimate analysis (d.a.f.)			
	C %	H %	N %	H/C
Seam No. 5	83.30	5.39	2.02	0.78
Seam No. 6	82.50	5.34	1.98	0.78
Seam No. 7	83.96	5.20	1.90	0.74
Seam No.10	85.34	4.87	1.87	0.68
Seam No.12	85.58	5.16	-	0.72

d.a.f.: dry ash free

Table 2.3-2 Comparison of the quality between COLAR coal and Russel Fork (an American high volatile coal)

	Sample No.	Characteristic values					Calculated value	
		\bar{R}_o	T.R.	T.I.	Log MFD	Total dilatation	C.B.I.	S.I.
COLAR coal	Seam No. 5	0.94	82.0	18.0	2.98	88	0.56	3.36
	Seam No. 6	0.96	76.2	23.8	2.94	16	0.79	3.60
	Seam No. 7	1.00	77.8	22.2	3.64	173	0.72	3.63
	Seam No.10	1.06	74.5	25.5	3.09	149	0.88	4.00
	Seam No.12	1.05	82.6	17.4	3.04	139	0.54	3.71
Russel Fork (An American high volatile coal)		1.07	86.6	13.4	3.67	92	0.42	3.83

\bar{R}_o ; Mean reflectance

T.R. ; Total Reactives (%)

T.I. ; Total Inerts (%)

Log MFD; Logarithm of max fluidity (D.D.P.M.)

C.B.I. ; Composition Balance Index

S.I. ; Strength Index

Table 2.3-3 Typical characteristics of coke for use in
4,000 m³ class blast furnace

(Kobe Steel, Kakogawa cokes)

a) Proximate analysis, reactivity, microstrength, porosity

Proximate analysis, (%)			JIS re-activity (%)	Microstrength		Porosity (%)	Remarks
Ash	V.M.	T.S.		>20 mesh	>42 mesh		
11.0	0.40	0.65	19	75	90	-	Chamber oven coke

b) Coke texture

Reactives (%)					Inerts (%)		
Isotropic	Fine Mosaic	Coarse Mosaic	Incomp fibrous	Leaflet	Micrinite	Fusinit	Semi Fusinit
	8.3	34.9		22.2			
78.4					21.6		

c) Coke strength at room temperature and high temperature

Coke strength at room temperature		Coke strength at high temperature	
DI 30 15	S.I.	Reactivity, %	Coke strength after gasification, %
>93.0	>55	≤30	≥65

S.I. ; Stability Index

Table 2.3-4-a Proximate analysis, and measurements of reactivity, microstrength and porosity

	Proximate analysis, %		JIS re-activity	Microstrength *		Porosity (small-lump method)	Remarks	
	Ash	V.M.		T.S.	>20 mesh			>42 mesh
COLAR coke	12.09	0.57	0.76	12	74.7	89.4	57	Beehive coke ovens
Paz del Rio coke	13.66	0.48	0.69	11	75.7	91.3	-	Chamber coke ovens
Bellumbi coke	12.57	1.15	0.35	-	-	-	-	Beehive coke ovens

* Yield (%) of +20-mesh and +42-mesh particles of a 2 gr. sample adjusted to 20 meshes and driven, together with 12 steel balls, in a specified cylinder (36 mmφ x 300 mm) at 25 rpm for 800 revolutions.

Ash analysis (%)										
	Fe ₂ O ₃	MnO	CaO	MgO	Al ₂ O ₃	SiO ₂	P	SO ₃	TiO ₂	K ₂ O
COLAR coke	7.01	0.21	0.32	0.57	21.89	60.19	0.141	0.016	1.22	0.58
										0.74

Table 2.3-4-b Microscopic measurement for coke texture (mineral free)

	Reactives (%)					Inerts (%)			
	Isotropic	Fine Mosaic	Coarse Mosaic	Incomp fibrous	Leaflet	Micrinite	Fusinite	Semi Fusinite	
	-	2.1	76.6	5.2	1.7	5.3	9.1	0	
COLAR coke			85.6				14.4		
	-	52.2	17.6	0.3	0.5	8.8	19.5	1.1	
Paz del Rio coke			70.6				29.4		

Table 2.3-4-c Coke strength of COLAR coke after gasification

n	1	2	Average
* Reactivity, %	14.3	15.3	14.8
* Coke strength after gasification, %	76.0	75.5	75.8

Sample: 20 ± 1 mm, 200 g (about 40 pcs.)

Reaction temperature: 1,100°C x 120 min.

CO₂ gas: 5 lit./min.

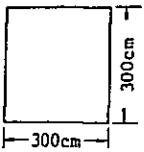
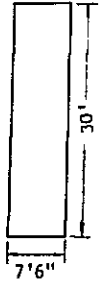
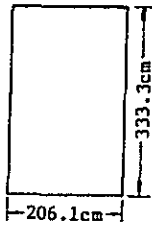
* Reactivity = $\frac{\text{Weight of sample after gasification}}{200\text{g}} \times 100$

Coke strength after gasification = $\frac{\text{Weight of +10 mm particles of the sample after gasification and 600 revolutions in a specified cylinder}}{\text{Weight of sample after reaction}} \times 100$

Table 2.3-5 An example for estimation of cost for installation of chamber coke ovens

	Details	Remarks	
Chamber coke ovens for producing lump coke for blast furnace at 200 tons a day.			
Ovens specifications	Type	Otto (single type) Tentative	
	Dimensions	430mm(W) x 14,000mm(L) x 4,000mm(H) Effective capacity, 21 m ³	Determined in consideration of coke oven operation efficiency.
	Number of ovens	15 to 20 200 tons/day: Lump coke produced 308 tons/day: Coal blends used. *1 16 tons/oven: Coal capacity per oven.*2 Availability 100%: 20 ovens (308 ÷ 16) Availability 130%: 15 ovens(308÷16÷1.3)	*1 200 tons ÷ 0.65 (yield of lump coke) *2 21 m ³ x 0.76 (bulk density of the coal blend)
	Pollution control facilities	—	—
	Plant for by-products	Exhauster, cooler, tar decantor	Recovery of tar alone; approx. 40% of coke oven gas to be recovered as a fuel for carbonization, the remaining being dissipated after burning.
	Manning	14 to 15 workers/shift	Yard: 2 workers/shift Coke ovens: 11 to 12 workers/shift Overseeing: 1 superintendent/shift
Cost estimate	<p>1. Coverage Beneficiation → Coke Battery and operating machine ~ Wharf → Plant for by-products (exhauster, cooler, tar decantor) ↳ Within the scope of estimate</p> <p>2. Cost per oven if installed in Japan ¥140 mil. to ¥150 mil.</p> <p>3. Construction cost ¥2,000 mil. to ¥3,000 mil. (140 x 15 - 150 x 20)</p>		

Table 2.3-6 Overview of beehive coke oven operations by various companies

Company	COLAR	Bellumbi	Hokkaido Kisen, Wakanabe Works
Application	Foundry pig iron	Foundry pig iron, nonferrous	Foundry pig iron
Construction of coke oven (a ground plane)	<p>A depth of coal-bed is 36 cm</p> 	<p>Tapered Designed to carry out carbonizing with enough coking time</p> 	<p>3° slope provided to facilitate coke unloading and water flow.</p> 
Number of ovens and coal charge	3.3 tons/oven	45 ovens	30 to 40 ovens/battery 2.0 to 2.7 tons/oven
Oven temp.	1,000°C	-	around 1,000°C
Cycle time (total carbonizing time)	60 ~ 72 hrs.	72 ~ 96 hrs.	48 hrs.
Air ratio control	Control of air port in the oven door.	Control of air port in the oven door.	<ul style="list-style-type: none"> ° Position of air tuyere is important. ° With the progress of carbonization, the inclination and area of tuyere are adjusted while watching the oven inside in order to regulate the air ratio.
Quenching	Squirting within the oven	<ul style="list-style-type: none"> ° Wollongong Works: Squirting at quenching station ° North Wollongong Works: Squirting within the oven 	<ul style="list-style-type: none"> ° Squirting within the oven <p>Optimum ratio: 1.4 ton of coke to 1.2 ton of water</p>
Particle size of coal	-12 mm	-1/8", 90~95%	-3 mm, more than 85%
Oiling	nil	Addition of industrial oil	-
Remarks		<ol style="list-style-type: none"> 1. Coke is screened into 7", 5" and 2 1/2" before use. 2. Coal is reclaimed and used by types. 	

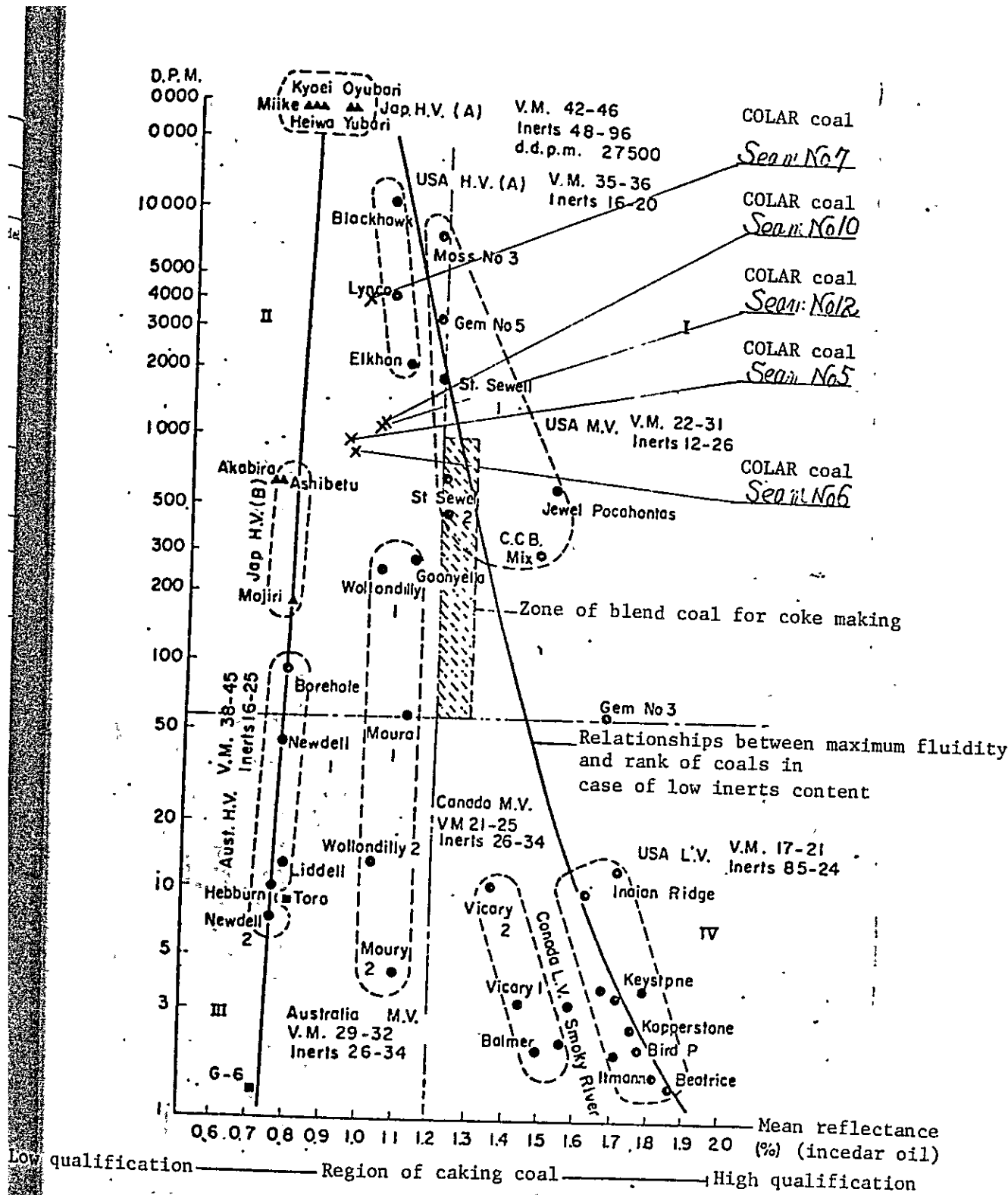


Fig. 2.3-1 Relationship between maximum fluidity and rank of coals
 [Excerpted from the Nenryo Kyokai Shi (Journal of Fuel Engineering Association), June 1978]

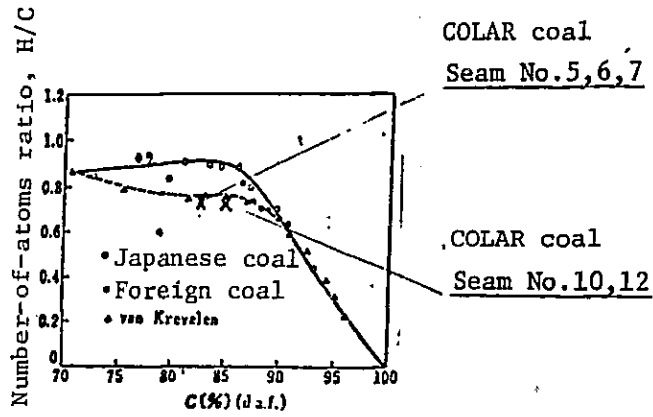


Fig. 2.3-2 Relationship between qualification and H/C
[Excerpted from Shin-pan Nenryo Binran,
(Fuel Engineering Handbook)]

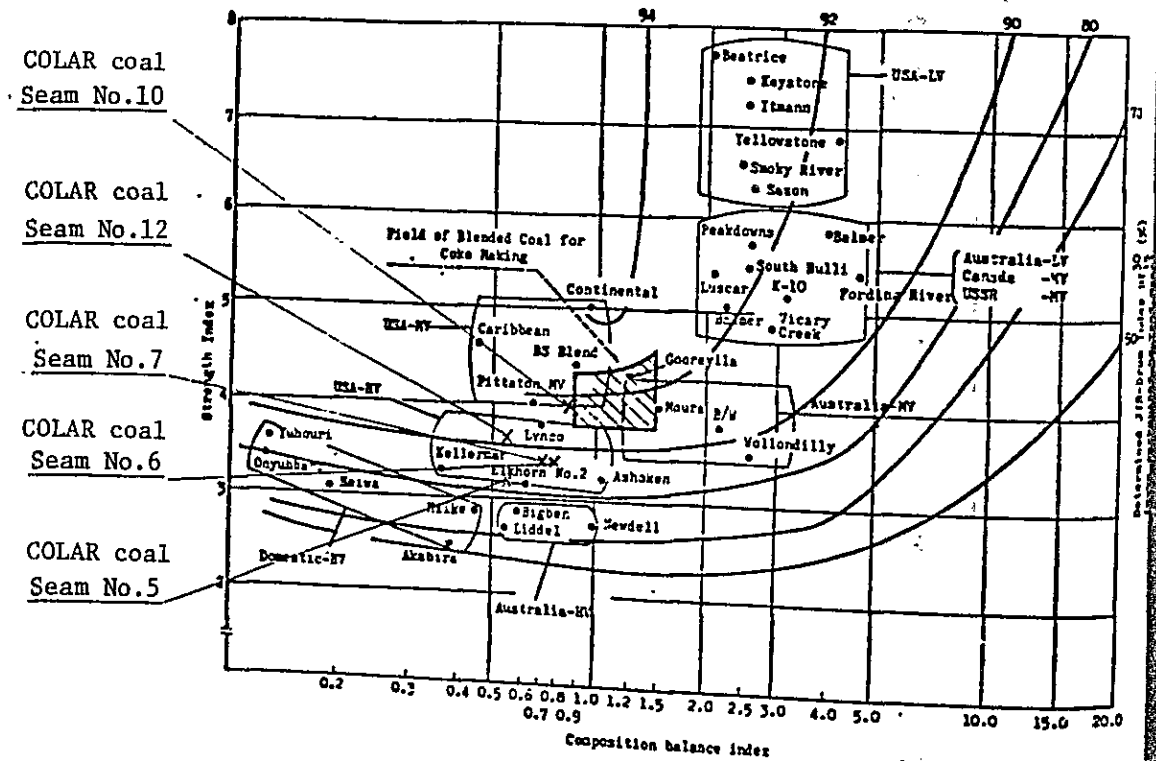


Fig. 2.3-3 Classification of single coals by C.B.I-S.I.
(Excerpted from Nenryo Kyokai Shi, June 1978)

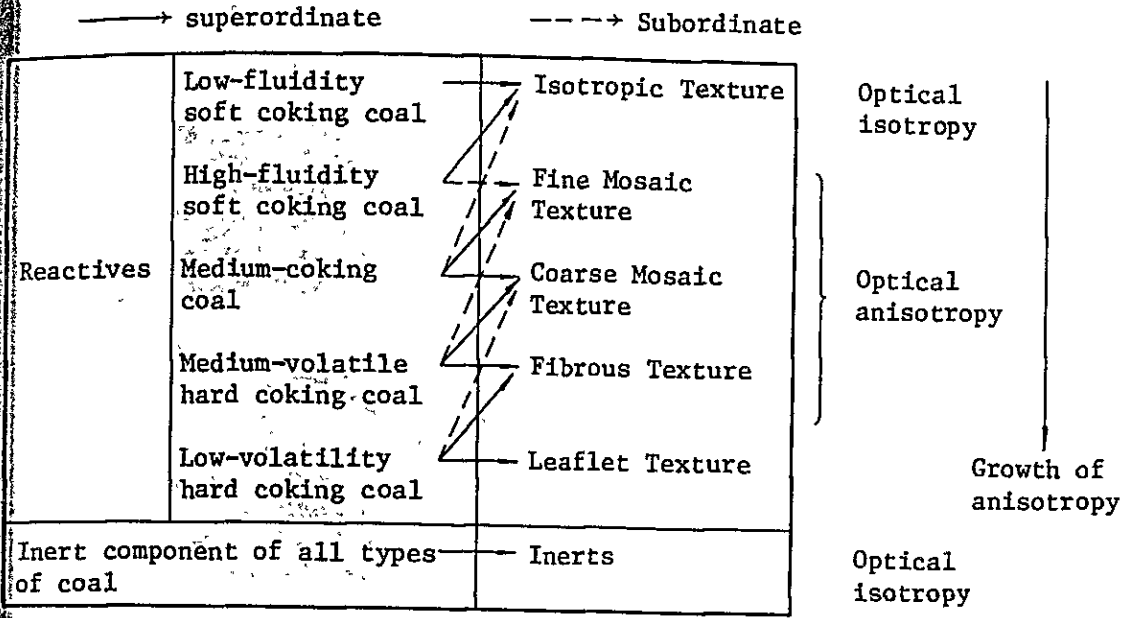


Fig. 2.3-4 Coal type and coke structure (The higher the growth of anisotropy, the lower the reactivity with CO₂.)

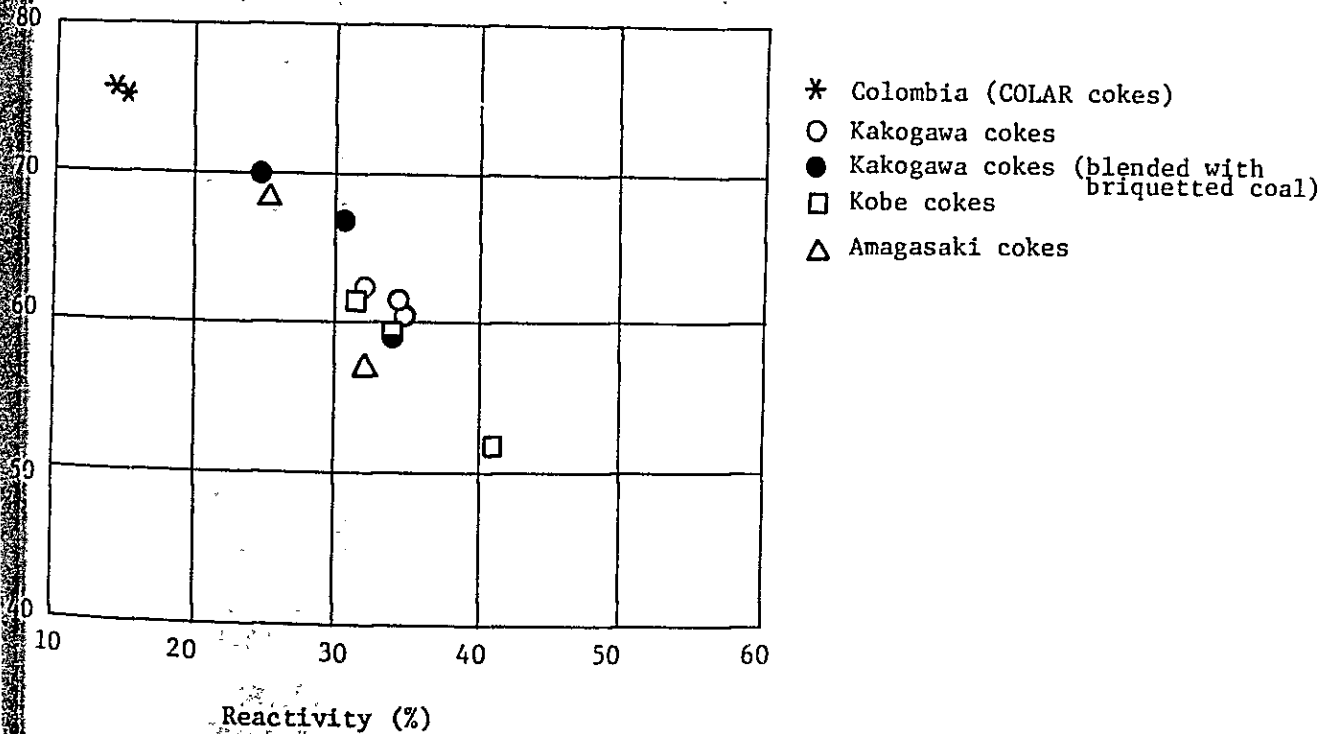


Fig. 2.3-5 Relationship between reactivity and coke strength after gasification.

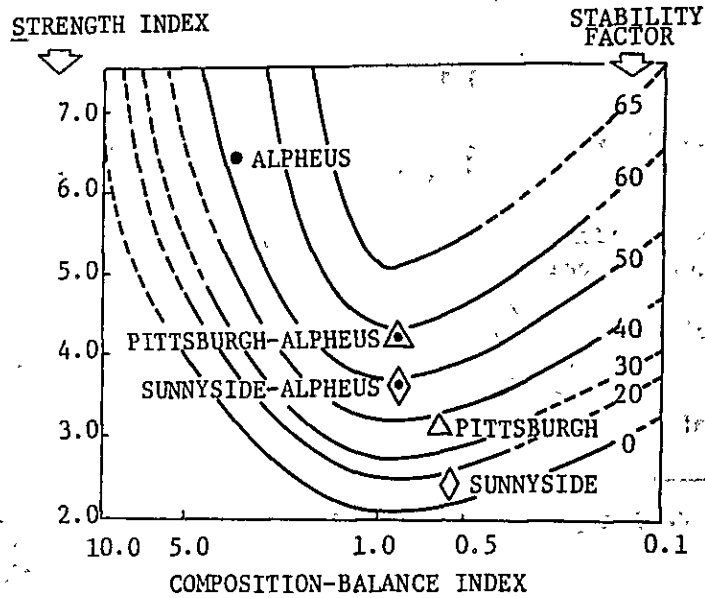


Fig. 2.3-6 Locations of a low-volatility Alpheus coal and high-volatility rank Sunnyside and Pittsburgh coals with reference to the isostability lines

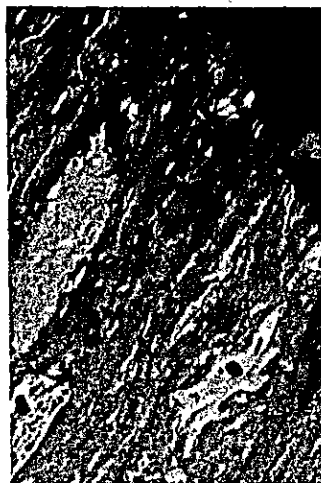
(Source: Recent Developments in Coal Petrography, by N. Schapiro, R.J. Gray, and G.R. Eusner)

Photo 2.3-1 Micrographs of COLAR coal, Takashima coal
Kellerman coal and Black Water coal (x 250)

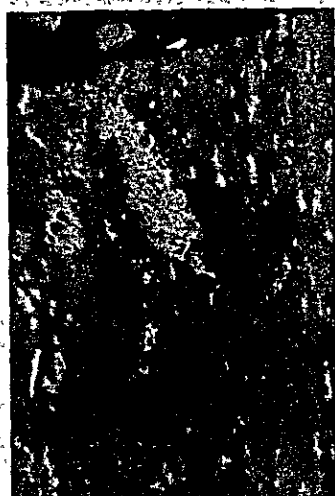
COLAR, Seam No.5



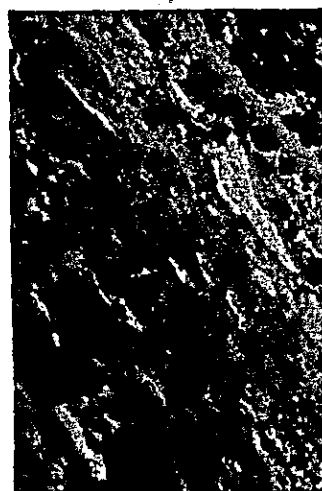
COLAR, Seam No.5



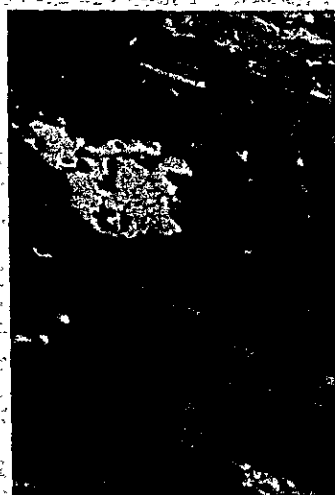
COLAR, Seam No. 6



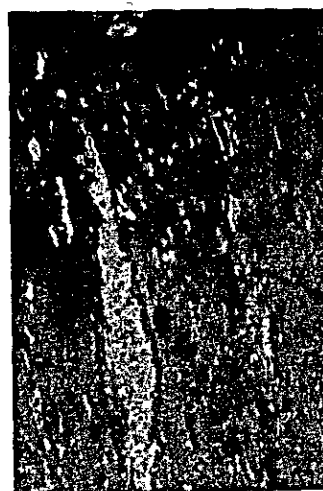
COLAR, Seam No. 6



COLAR, Seam No. 7



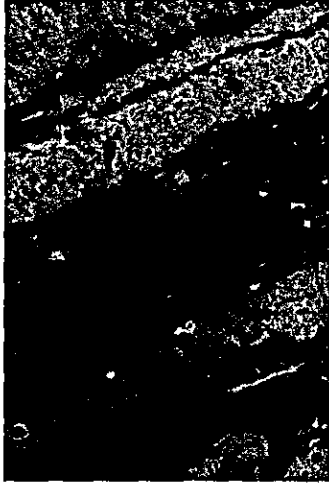
COLAR, Seam No. 7



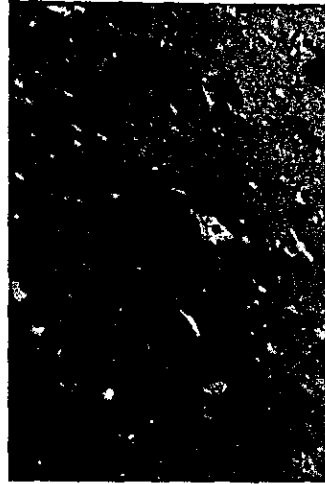
•

•

COLAR, Seam No.10



COLAR, Seam No.10



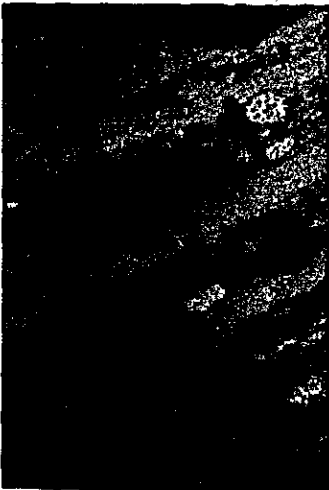
COLAR, Seam No.12



COLAR, Seam No.12



Takashima (Japan)



Takashima (Japan)



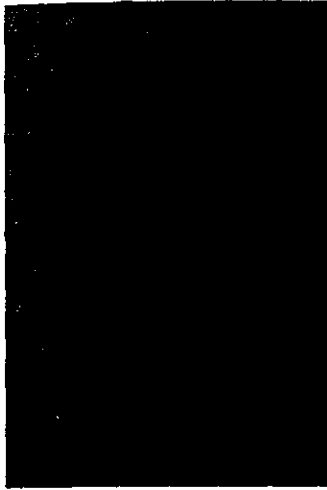
4

4

4

4

Kellerman (U.S.A.)



Kellerman (U.S.A.)

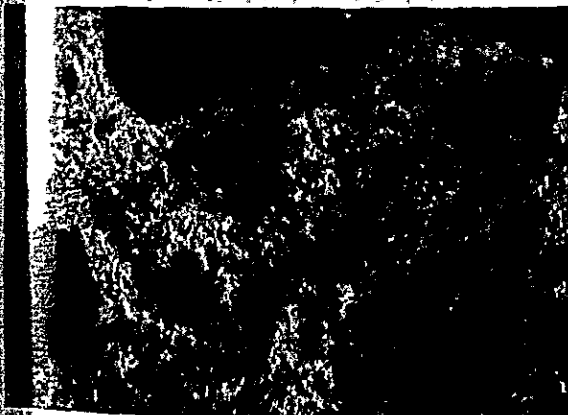


Black Water (Australia)

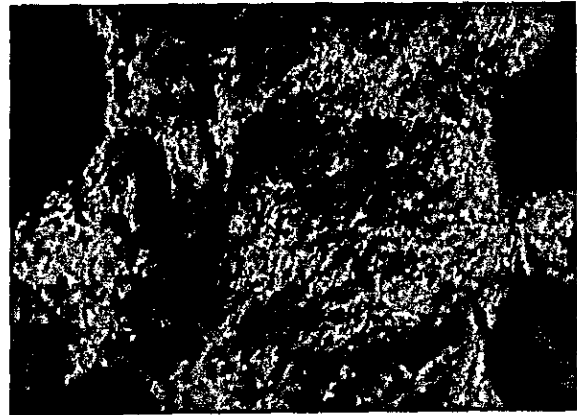


Photo 2.3-2-a Micrographs of COLAR coke

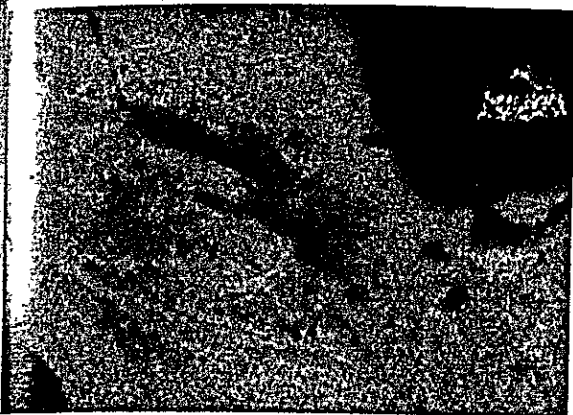
1) Coarse Mosaic Texture (x250)



2) Incomplete Fibrous Texture (x600)



3) Fine Mosaic Texture (x250)

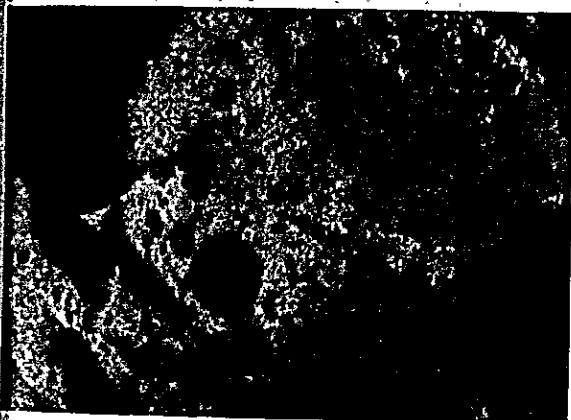


4) Leaflet Texture (x600)
Micrograph showing a part which contains bright particles visible on the coke lump with naked eye



Photo 2.3-2-b Micrographs of Paz del Rio coke

1) Fine mosaic texture (central part) and coarse mosaic texture (left below) (x250)



2) Fine Mosaic Texture (x250)

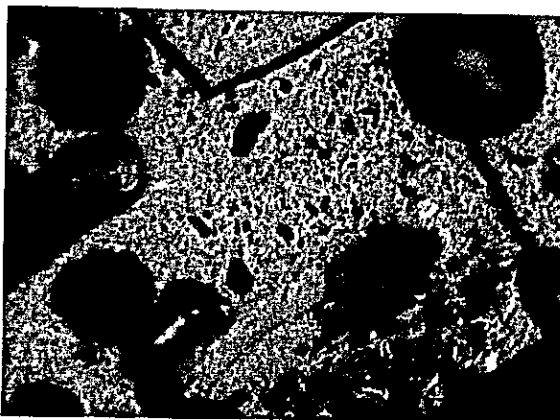
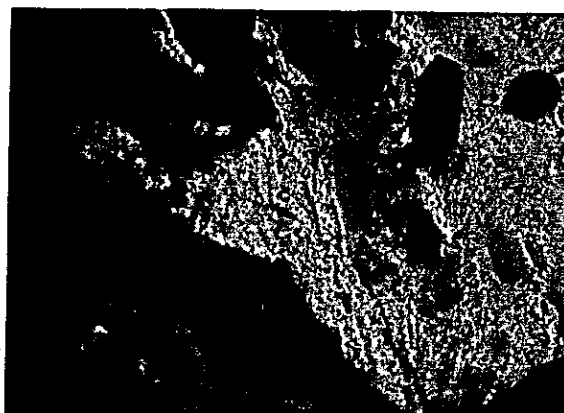


Photo 2.3-2-c Micrographs of Kobe Steel Kakogawa coke

Isotropic texture (left upper) and fine mosaic texture (central part) (x250)



2) Coarse mosaic texture (left center) and fibrous texture (center) (x250)

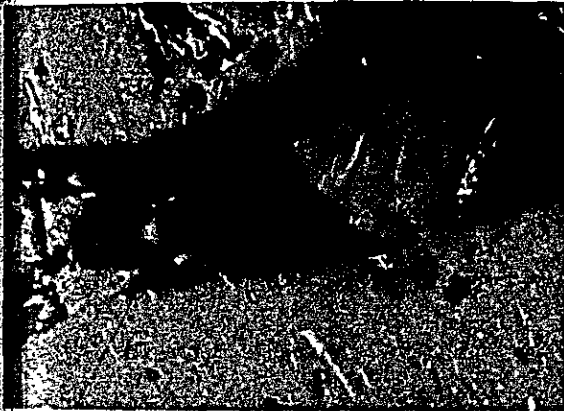


3) Fine Mosaic Texture (all over) (x250)

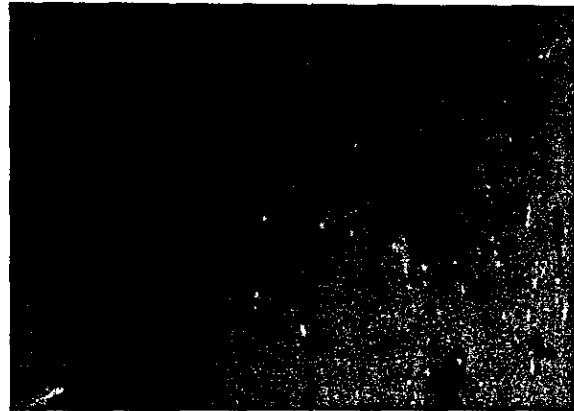


Photo 2.3-3-a Micrographs of the product carbonized the Seam No.12 sample of COLAR coal in Juranek furnace (x250)

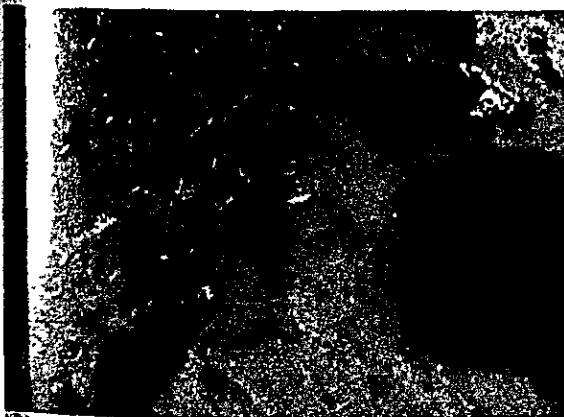
1) Inter-particle coalescence at 358°C



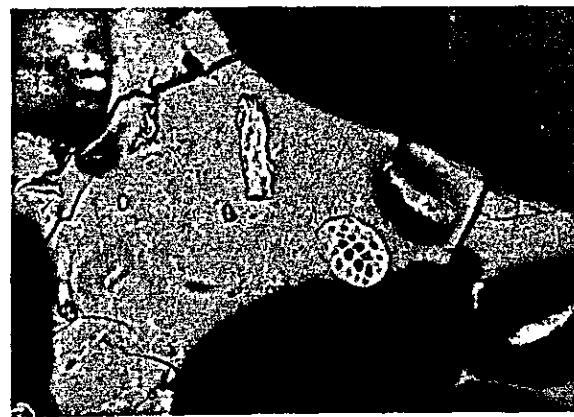
2) Degassing of volatile matter at 365°C



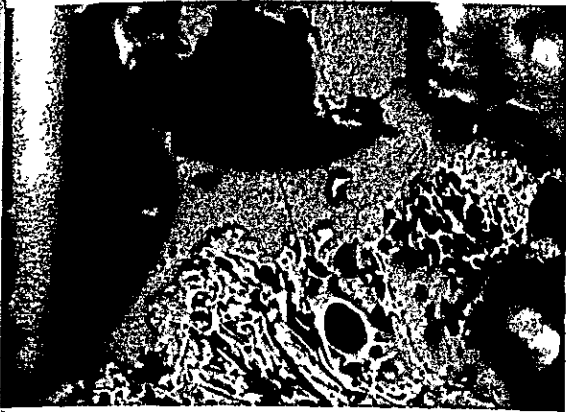
3) Start of flow at 398°C



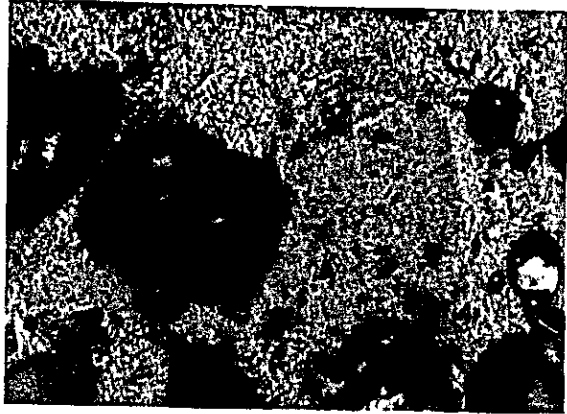
4) Briskness of flow at 426°C



5) appearance of anisotropic texture
at 478°C



6) Growth of anisotropy at 499°C
(fine mosaic texture to coarse
mosaic texture)



7) Appearance of coarse mosaic texture
and fibrous texture at 710°C

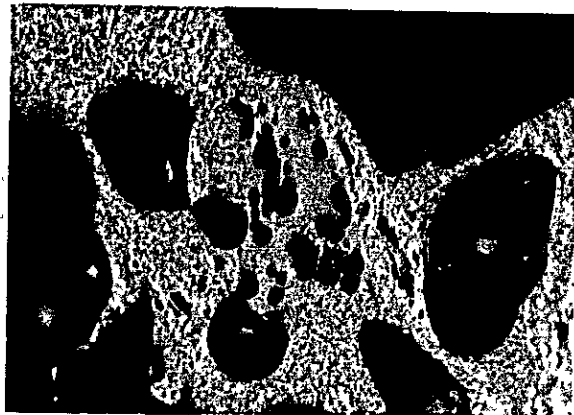
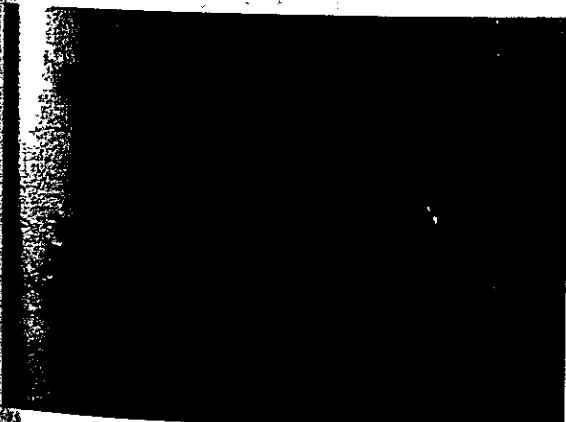


Photo 2.3-3-b Micrographs of the product carbonized Mulga
coal in Juranek furnace (x250)

Inter-particle coalescence
at 372°C



2) Degassing of volatile matter
at 390°C



3 Start of flow at 394°C



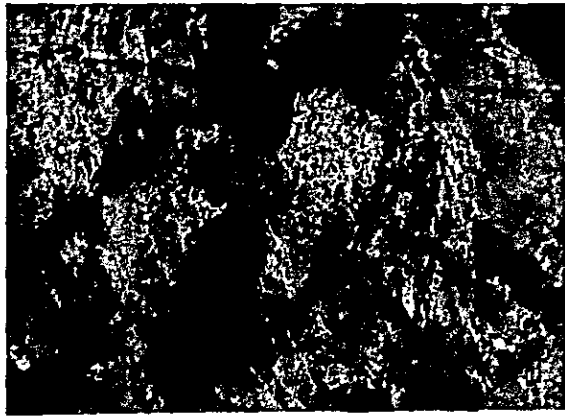
4) Appearance of anisotropy at 462°C



5) Growth of anisotropy at 504°C
(development of incomplete
fibrous texture and coarse
mosaic texture)



6) Appearance of fibrous texture
and coarse mosaic texture
at 705°C



2.4 Utilization of Fine Ore and Breeze

2.4.1 Disposal of fine ore and breeze

(1) Purpose

If the sizing of ore is carried out intensively for the purpose of increasing the blast furnace efficiency, fine ore will be increased. There have been practised various methods of collecting and making fine ore into sizable pieces from long time ago. However, the sintering method and pelletizing methods are most widely used because of their compatibility to mass production.

The sintering method is suitable for processing comparatively coarse ore such as undersized ore before the blast furnace. On the other hand, the pelletizing method is suitable for processing extreme fine ore obtainable from the magnetic ore separator at the mine or ore terminal.

The agglomerations such as pellets and sinters are added with limestone, are self-fluxed and become highly reducible. They also reduce the lime charge into the blast furnace, minimize solution loss, reduce the consumption of lump coke, increasing the pig iron output while reducing coke rate.

(2) The status quo of COLAR

At present, COLAR has no fine ore processing plant, except for an experimental direct reduction equipment.

The ore is sized at the mine in the rough and hauled to the plant. But there is no facility for screening out fine ore at Cajica Plant.

The coke is also transported from a coking plant near the mine, and there is no facility for screening out fine coke at Cajica Plant. The Dust developed by the blast furnace is dumped because no facility is installed to process it.

(3) Selection of beneficiation method

In the case of COLAR, the sintering method is regarded as best from the present state as the following conditions exist.

- i) Undersized ore obtainable through intensive sizing are coarse.
- ii) Ore is of the limonite family, and is much in ignition loss.
- iii) The processing rate is as small as 100 to 200 tons a day.
- iv) Breeze must be disposed of.

The employment of sintering method will bring about the following benefits.

- i) Blending of fine ore will reduce the variations in the chemical composition.
- ii) It is possible to obtain highly reducible sintered ore by imparting the limestone.
The limestone charge into the blast furnace can be reduced while increasing the pig iron output and reducing the coke ratio.
- iii) Efforts can be intensified for sizing the lump ore; namely, the upper limit of the size can be reduced from the present 60 mm to 30 mm, improving the gas flow in the Blast furnace.

Thus, the beneficiation and blast furnace operation can be closely combined with each other as other iron and steel manufacturers in the world are already in practice. This will lead to an increase pig iron output and a reduction in coke rate, and at the same time high-quality pig iron will be obtained.

(4) Sintering plant

The sintering plant for the COLAR should preferably be a small, inexpensive one because the furnace charge is as small as about 200 tons a day. The sintering machines now available include the following types, each being outlined in Figs. 2.4-1, -2, -3 and -4.

a) Batch type (pan type)

- i) AIB type (Allmauma Ingenious Byran) (See Fig. 2.4-1)
- ii) Greenawalt type (See Fig. 2.4-2)

b) Continuous Dwight-Lloyd type (D.L. type)

- i) Straight type (for large output) (See Fig. 2.4-3)
- ii) Rotary type (for small output) (See Fig. 2.4-4)

In Japan, the AIB type came first, but was replaced by G.W. type and then by D.L. type which is now in wide use.

This is because AIB and G.W. types are of the batch type defying mass production and are difficult in raw material charging and complicated in ignition system.

For reasons explained above, the COLAR is recommended to employ a continuous rotary sintering machine.

Compared with the continuous straight type, the continuous rotary type has the following features which recommend itself.

- i) Because of rotary scheme, the idling space can be minimized, and the effective hearth area can be maximized. Namely, the system can be arranged compact and installed in a small space. Its weight is of course light.
- ii) The building height can be reduced because the furnace height is short.
- iii) The investment cost is about 60 to 80% of the straight type's. The rotary type is most economical if the capacity is less than 30 m².

An example of the continuous rotary sintering plant is given below.

- i) Daily output : 100 tons/day (blast furnace charge ratio: 50%)
- ii) Effective area : 5.4 m²
- iii) Grating width : 600 mm
- iv) Disc diameter : 4,000 mm

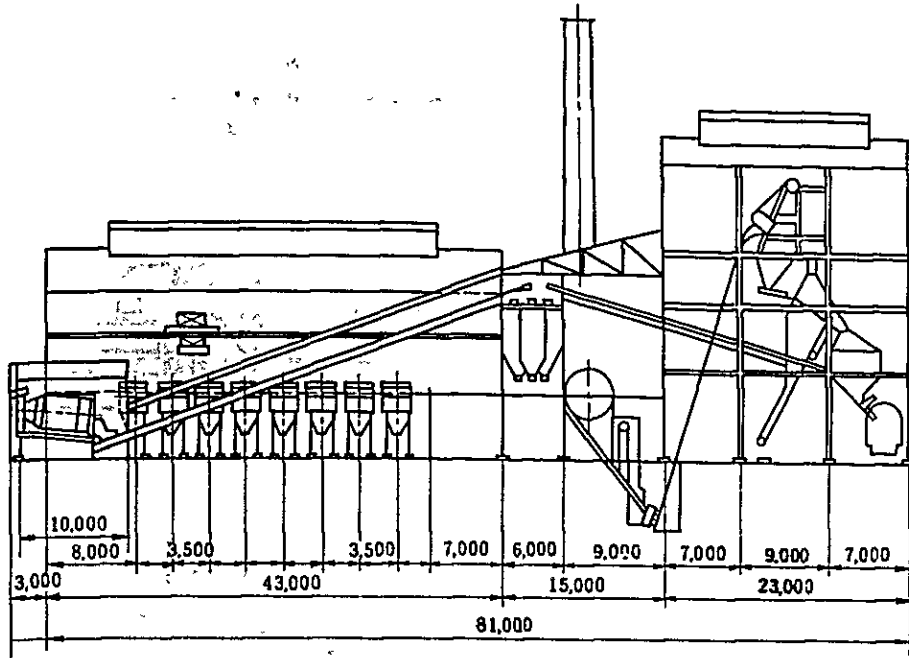


Fig. 2.4-1 AIB type sintering plant

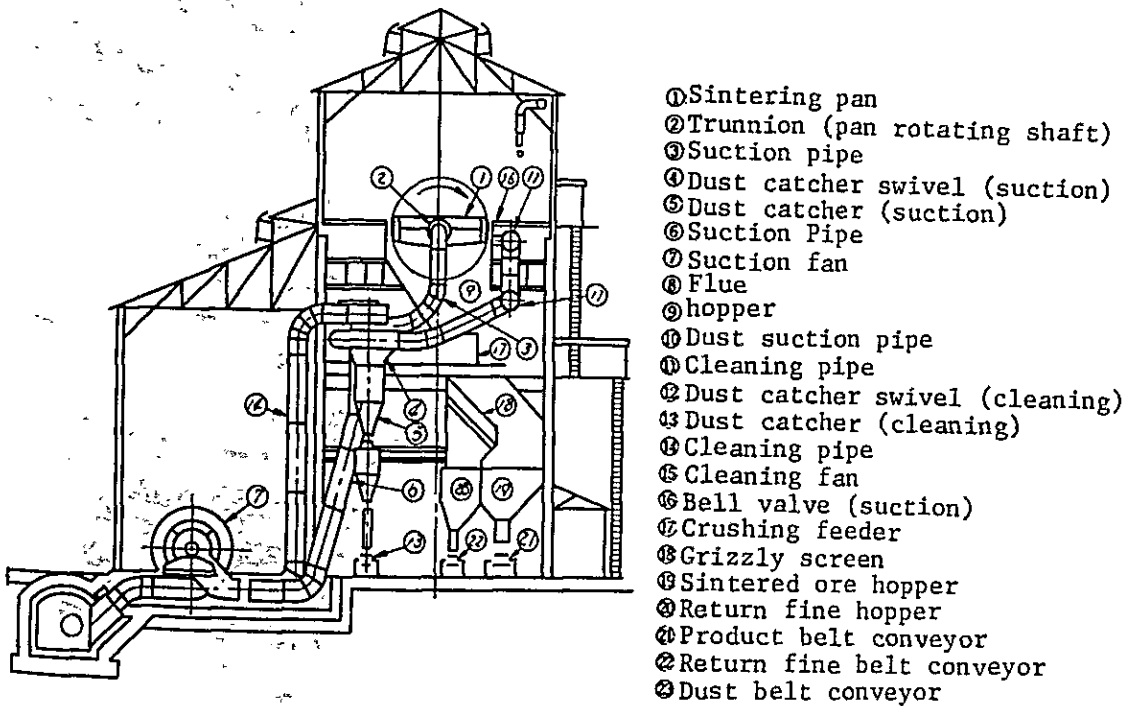


Fig. 2.4-2 Greenawalt type sintering plant

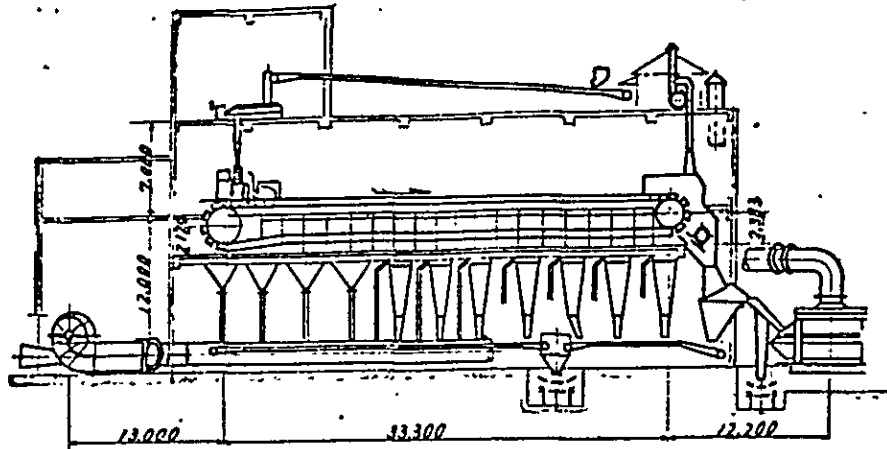
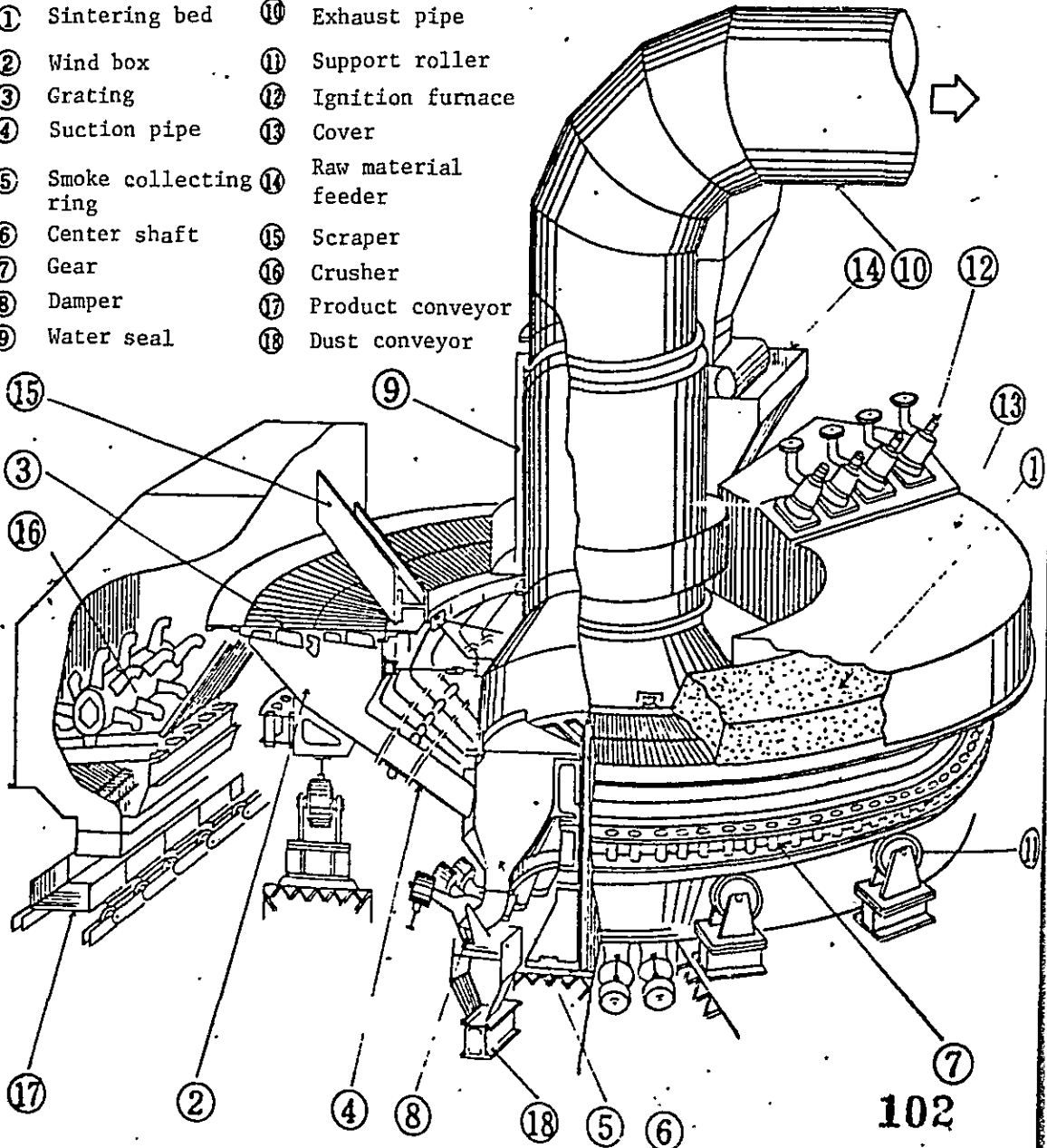


Fig. 2.4-3 Dwight-Lloyd type sintering plant

Fig. 2.4-4 Rotary sintering plant

- | | |
|-------------------------|-----------------------|
| ① Sintering bed | ⑩ Exhaust pipe |
| ② Wind box | ⑪ Support roller |
| ③ Grating | ⑫ Ignition furnace |
| ④ Suction pipe | ⑬ Cover |
| ⑤ Smoke collecting ring | ⑭ Raw material feeder |
| ⑥ Center shaft | ⑮ Scraper |
| ⑦ Gear | ⑯ Crusher |
| ⑧ Damper | ⑰ Product conveyor |
| ⑨ Water seal | ⑱ Dust conveyor |



2.4.2 Evaluation of COLAR iron ore blended sinters

The samples were turned into sintered ore on the pot test method which Kobe Steel has been practised for a long time. Because of limited volume of samples, only a single sintering test was carried out. Although it is difficult to see the whole from this bit, the sintering property of the COLAR iron ore is evaluated hereunder anyway.

(1) Features of COLAR iron ore as a sintering material

a) Chemical composition

The chemical analysis is shown in Table 2.4-1.

i) High ignition loss as compared with the iron ore used in Japan.

For the purpose of compensating for the decomposition heat of the combined water, it is necessary to increase the use of breeze.

The products are rather likely to become porous.

ii) High SiO₂ content

In order to produce self-fluxed sintered ore, it is necessary to increase the proportion of limestone.

This, together with a low Fe content in the ore, reduces the overall Fe content in the product.

b) Size

The size distribution of the samples obtained and their crushing is shown in Table 2.4-2 and 2.4-3.

It is evident that the ore is highly vulnerable to pulverization, and the sintering productivity might possibly be affected. It is therefore needed to carry out granulation of raw materials thoroughly in order to avoid this evil effect.

(2) Sintering pot test

a) Test conditions

The conditions for the test conducted are as follows.

Moisture content in the mix	:	6.6%
Breeze ratio	:	4.5% (for fresh material)
Return fine ratio	:	33.3% (for total material)
Feed ore	:	approx. 30 kg (dry weight)
Bed height of raw material	:	300 mm
Coke for ignition	:	500 gr.
Ignition time	:	60 sec.
Suction pressure in roasting	:	1,100 mmH ₂ O
Basicity of sintered ore	:	1.13
Mix proportion	:	See Table 2.4-4
Size distribution in the raw material	:	See Table 2.4-5

For an outline of the testing equipment and the methods of determining the yield, productivity and strength, refer to the sintering pan testing method on page

b) Test results

i) Chemical composition and porosity

The chemical composition and porosity of the sinters obtained are shown in Table 2.4-6. As compared the sinters obtainable from Kobe Steel production sinters, the COLAR sinters show a SiO₂ content of 12.4% or more than twice as much, and is low in Fe content. Judging from the bulk density and porosity, the COLAR sinters are very porous. This high porosity results from the combined water in material and also from slag volume. Closed pores are noticeable.

Perhaps, the slag may have blocked up the pores. The salient features of Paz del Rio sinters are a high basicity and an extremely low Fe content.

- ii) Results of sintering pot test, and characteristics of the product in the low-temperature range (below 900°C)

The results of the sintering pot test and the characteristics of product in the low-temperature range are given in Table 2.4-7. Robe River ore (Table 2.4-8) which is close in the content of the combined water to COLAR ore was put to sintering pot test, and the results are as shown in Fig. 2.4-5.

Mt. Newman (LGO) ore (Table 2.4-8) which is close in SiO_2 content to COLAR ore was also tested, and the results are shown in Fig. 2.4-6.

As compared with Robe River sinters, COLAR sinters are better in low-temperature reduction degradation index, almost par in JIS reducibility, but is inferior in yield, productivity and strength.

Probably, the SiO_2 content, basicity level (Robe River sintered ore, C/S = 1.5), etc. are influential factors. COLAR sinters are generally close in characteristics to Mt. Newman sinters

- iii) High-temperature characteristics (above 900°C)

The high-temperature reducibility and high-temperature reduction property under load of COLAR sinters, are shown in Figs. 2.4-7 and -8 in relation to Kobe Steel Production sinters.

COLAR sinters melted prematurely, and its high-temperature reduction had to be stopped by halves. As regards the softening and melting property, COLAR sinters showed a melting temperature 100°C to 200°C lower than Kobe Steel Production sintered ore. As shown in Fig. 2.2-18, it was 100°C to 200°C lower as compared with COLAR iron ore.

This will be due to the fact that SiO_2 content in sinters is high, that fayalite ($2\text{FeO} \cdot \text{SiO}_2$) which shows a low melting point in the reduction process is much produced. All these may be improved to some degree by increasing the basicity, but not to a major degree because the SiO_2 content is prohibitively high.

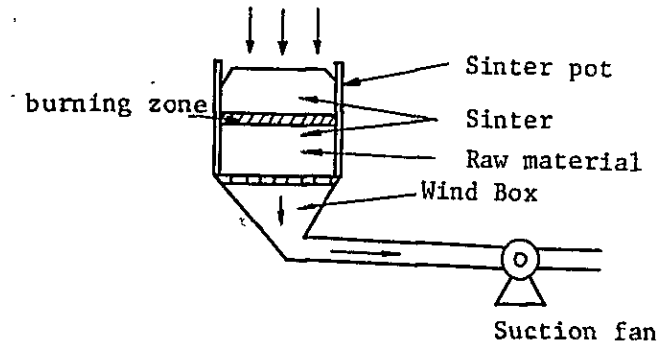
(3) Conclusion

COLAR ore were subjected sintering pot test. Because of limited availability of the samples, the test was done once only. Judging from the productivity, yield and product strength derived from the test, COLAR sinters will be quite justifiable for sintering operation. Low temperature properties such as the low-temperature reduction degradation index and JIS reducibility are fairly good. As regards high-temperature properties, however, sinters fused at a considerably low temperature because of its high SiO_2 content, betraying its inferiority to COLAR lump ore.

In using the sinters, it is therefore recommended to increase the proportion of breeze and basicity level for the purpose of improving the structure of sinters and studying its properties.

Sintering pot testing method

1. Schematic representation of testing equipment



2. Exhaust fan

- a) Type : Turbo fan
- b) Capacity : 9 to 10 m³/min.
- c) Suction pressure : 1,100 mmH₂O

3. Pot

- a) Dimensions : 325 mm ϕ (top zone) x 305 mm ϕ (bottom zone)
x 300 mm H
- b) Charge : 30 kg (dry weight)

4. Product yield = (Product quantity/Total burned quantity) x 100

Product quantity: +10 mm part of the total burned quantity having once been let to fall from a height of 2 m to shatter.

5. Productivity = Product quantity/Grating area/Sintering time (T/m²/h)

6. Shatter index

Percentage to the total product quantity of +10 mm part which is obtained by letting fall of the total product quantity from a height of 2 m 4 times.

Table 2.4-1 Chemical composition of COLAR iron ore

Ores	Chemical composition (%)							Wt. (dry.kg)
	TFe	FeO	SiO ₂	CaO	Al ₂ O ₃	MgO	Ig.loss	
Caldera	52.70	<0.1	10.69	0.01	2.83	0.01	11.22	4.03
Pacho	56.13	0.14	6.55	0.02	2.43	0.07	11.13	7.36
Citzenza	57.52	0.43	3.93	1.45	0.81	0.13	6.34	7.65
Nueva vizcaya	55.32	<0.1	0.50	0.04	0.35	0.36	7.42	2.67
Pericos (Finas)	48.84	<0.1	14.59	0.05	4.14	0.05	9.12	10.99
Pericos (Grueso)	49.59	<0.1	14.18	0.05	3.32	0.02	9.63	10.44
Raw Mix. *	52.59	0.14	9.97	0.30	2.69	0.07	9.17	

* Calculated from iron ores

Table 2.4-2 Size distribution of COLAR iron ore
at the time of acceptance (Wt.%)

Ores	Size (mm)							Moisture (%)
	75~50	50~25	25~20	20~15	15~10	10~5	-5	
Caldera	0	66.6	2.9	9.8	6.6	5.7	8.4	0.95
Pacho	41.5	41.9	1.5	4.5	4.0	2.6	4.0	1.12
Citzenza	41.3	29.3	1.9	8.9	4.6	4.3	9.7	2.56
Nueva Vizcaya	14.8	7.4	1.5	18.8	16.6	13.7	27.2	1.32
Pericos (Finas)	0	0	1.0	6.1	43.6	44.6	4.7	1.42
Pericos (Grueso)	19.2	61.6	4.3	7.3	2.7	1.5	3.4	0.71

Table 2.4-3 Size distribution and mean size of crushed material ore for sintering use

Mean size of ore mix = 1.88 mm,
-125 μ = 20.4%

Ores	Size (mm)									Mean size (mm)
	10 \sim 7	7 \sim 5	5 \sim 2	2 \sim 1	1 \sim 0.5	0.5 \sim 0.25	0.25 \sim 0.125	0.125 \sim 0.063	-0.063	
Caldera	1.6	16.0	28.7	16.1	11.0	7.6	6.1	6.4	6.5	2.47
Pacho	0.3	8.3	17.6	15.3	13.7	12.2	10.2	11.3	11.1	1.55
Citzenza	0.7	8.5	21.0	15.4	11.6	9.3	7.9	8.5	17.1	1.69
Nueva Viscaya	2.5	7.9	18.1	15.3	13.6	10.7	9.3	11.4	11.2	1.72
Pericos (Finas)	0.4	11.9	21.5	14.4	11.4	8.5	10.3	11.0	10.6	1.87
Pericos (Grueso)	1.0	12.3	24.7	16.0	12.0	8.7	9.3	8.6	7.4	2.08

Table 2.4-4 Mix proportion of materials

Ores	Weight (kg)	Ratio (%)
Caldera	1.50	7.22
Pacho	2.82	13.58
Citzenza	3.01	14.49
Queva Viscaya	0.94	4.53
Pericos (Finas)	4.13	19.88
Pericos (Grueso)	3.96	19.07
Limestone	4.41	21.23
Total	20.77	100

Table 2.4-5 Size distribution of raw material

State of raw mix	Size (mm)										Mean size (mm)
	+10	10~7	7~5	5~2	2~1	1~0.5	0.5~0.25	0.25~0.125	0.125~0.063	-0.063	
Dry	0	1.8	10.2	23.6	15.2	19.3	10.2	7.5	4.5	7.7	2.02
Wet	0	1.4	9.0	20.0	11.4	29.5	28.7	0	0	0	2.33

Table 2.4-6 Chemical composition and porosity of sinters

	Chemical composition								Bulk density (T/m ³)	Porosity		
	T. Fe	FeO	SiO ₂	CaO	Al ₂ O ₃	MgO	C/S	Total		Closed	Open	
COLAR sintered ore	48.07	6.60	12.40	14.01	3.08	0.20	1.13	1.23	26.8	15.3	11.6	
Kobe steel production sintered ore	55.27	7.07	5.75	10.21	2.16	1.40	1.77	1.63	20.8	9.3	11.6	
Paz del Rio production sintered ore	36	16	12.97	25.74	5 [~] 5.5	0.6	1.98					

* Bulk density refers to a grain size of 20 + 1 mm.

Table 2.4-7 COLAR ore sintering pot test results and low-temperature characteristics of product

Breeze (%)	No.	Max. off gas temp. (°C)	Gas flow rate (Nm ³ /min)	Yield (%)	Productivity (t/m ² /hr)	Shafter strength (%)	Low temp. disintegration (%)				JIS reduction (%)
							-10mm	-5mm	-3mm	-1mm	
4.5	1	190	6.1	67.82	1.131	70.41	55.9	24.4	14.3	6.2	
							58.6	25.7	15.1	6.2	
	\bar{x}						57.3	25.1	14.7	6.2	67.0

Table 2.4-8 Chemical composition of Robe River ore and Mt. Newman ore

	Chemical composition						
	T. Fe	FeO	SiO ₂	CaO	Al ₂ O ₃	MgO	Ig. loss
Robe River ore	57.25	0.03	5.76	0.05	2.22	0.04	9.34
Mt. Newman ore	56.00	0.202	10.97	0.13	4.20	0.04	3.46

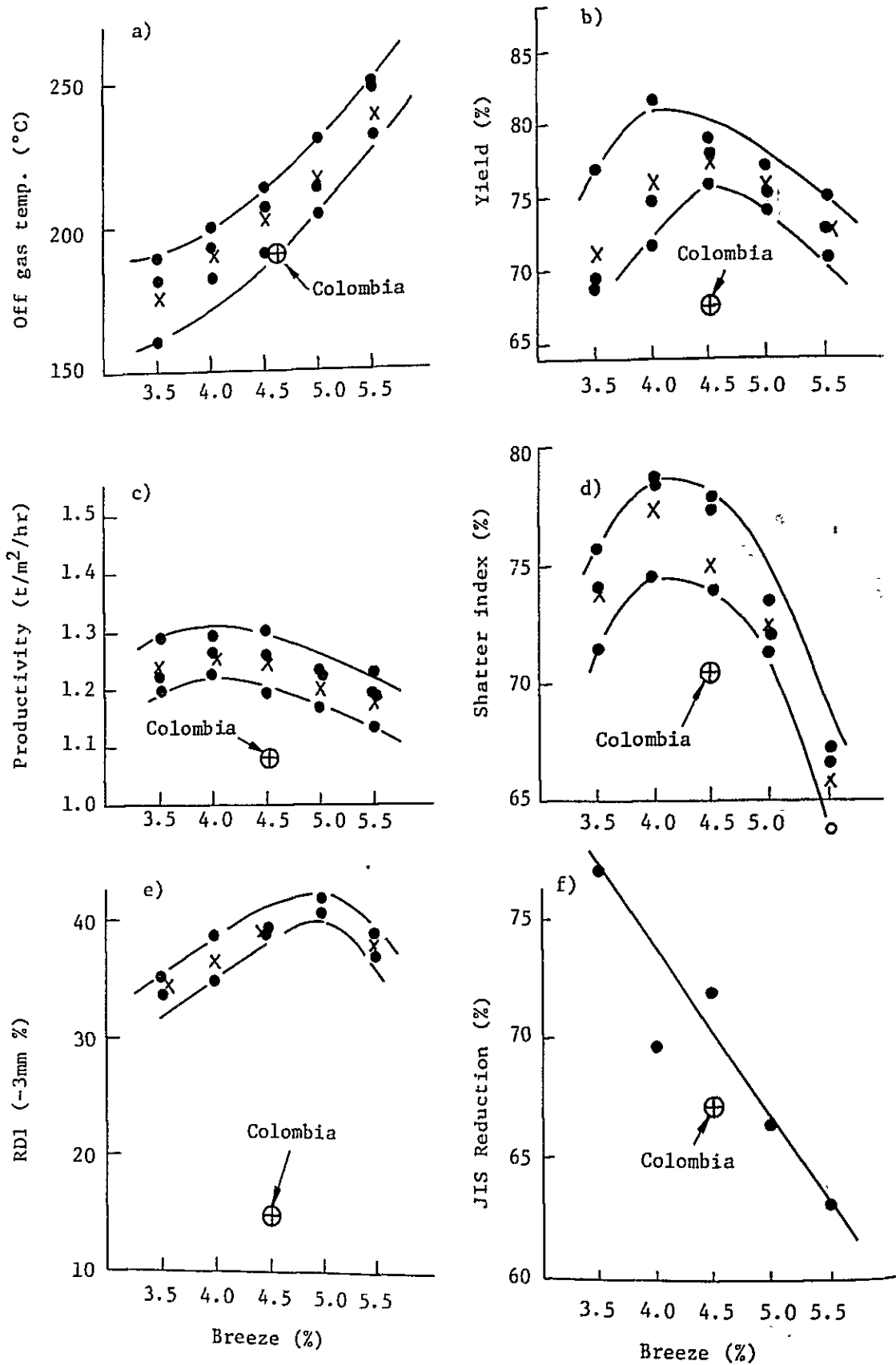


Fig. 2.4-5 Relationship between properties of Robe River sinters

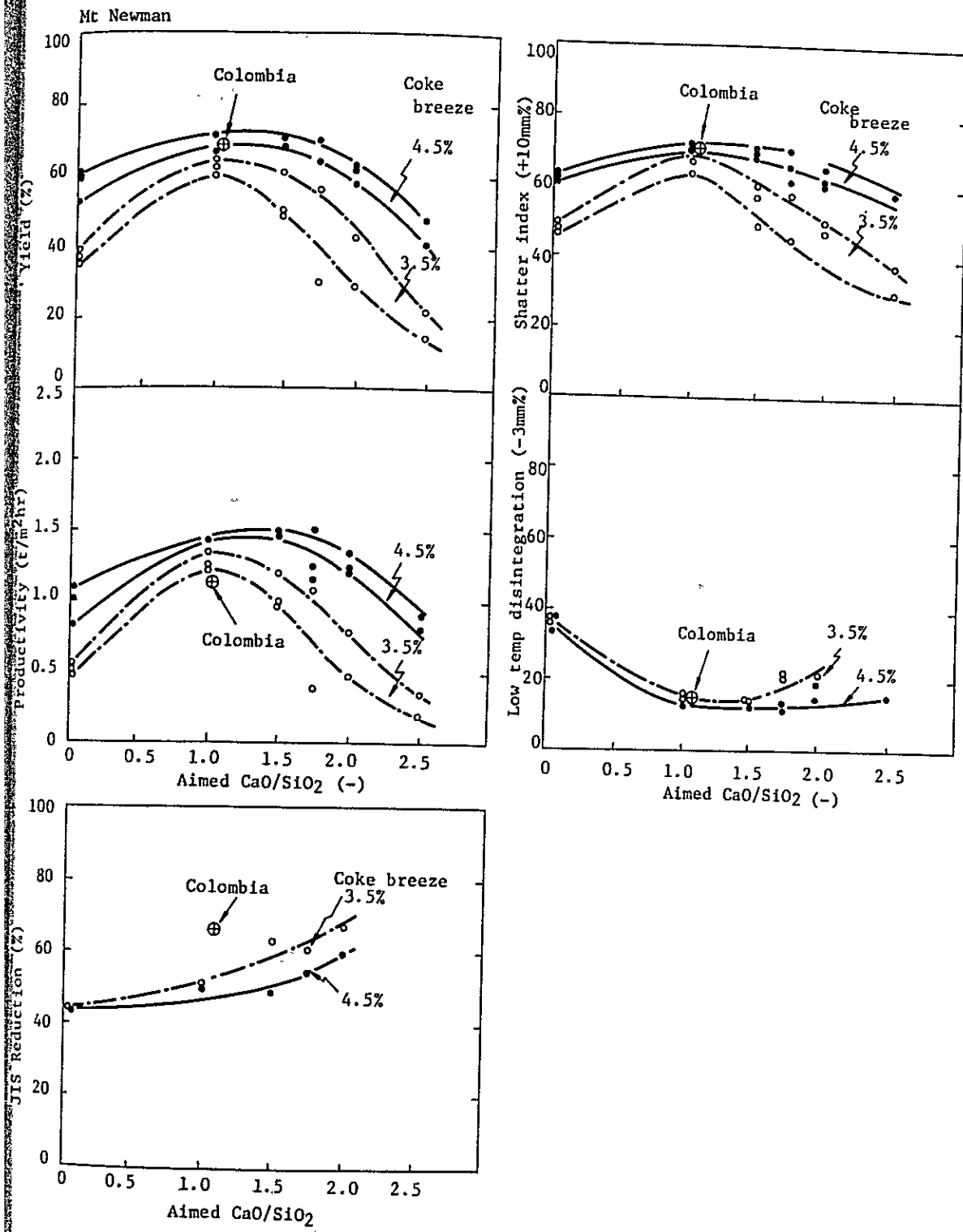


Fig. 2.4-6 Relationship between properties of Mt. Newman sinters and its basicity

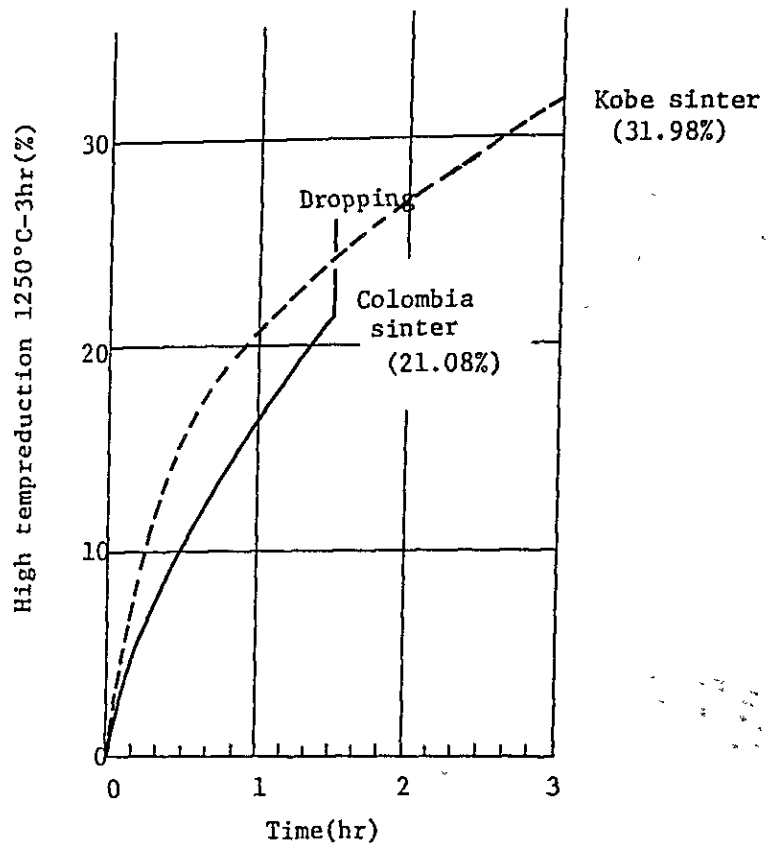


Fig. 2.4-7 High-temperature reduction curves of sinters

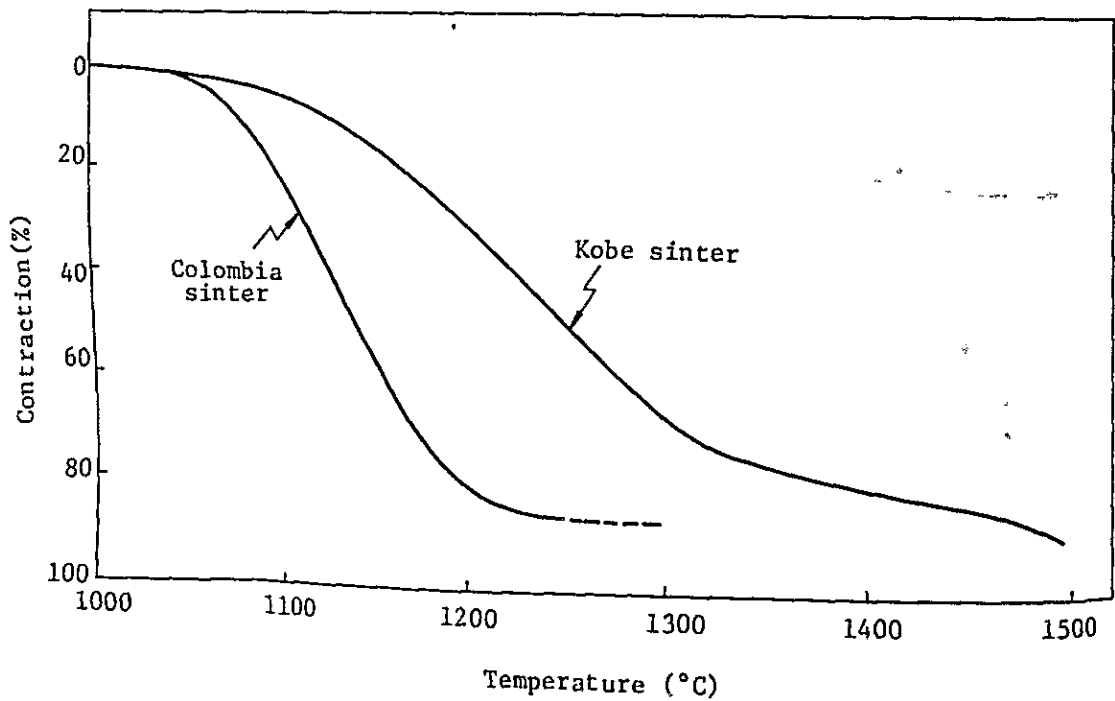


Fig. 2.4-8 High-temperature reduction under load curves of sinters

2.4.3 Direct reduction facilities

(1) Purpose

An objective of the direct reduction process is to achieve an increased pig iron output and a reduction in fuel consumption by making use of metallized materials chargeable into the blast furnace. The materials for the direct reduction process usually include lump ore, pellets, such solid reducing agents as coal, coke and char and such reducing gases as CO and H₂. In the case of iron making plant, use of fine ore and breeze which are hard to charge directly into the blast furnace is desirable.

In Japan, metallized material as a blast furnace charge, is said to increase the pig iron output by some 8% and reduce the fuel ratio by some 6% if it contains 10% of metal Fe.

(2) Current state of COLAR

At present, COLAR is trying to produce metallized material in a reducing kiln (1.15 mφ x 2.5 m long) by making use of fine ore (-1/4") and fine coke (-1/2").

(For the flow diagram and operating conditions, refer to Fig. 2.4-9)

It is expecting blast furnace gas as a preheating source. Namely, COLAR has an eye to making metallized material from excess fine ore and fine coke for the purpose of using it as a metal charge to increase the blast furnace productivity.

(3) Direct reduction facilities

The direct reduction facilities are classified into two types according to the type of reducing agent.

One counts on solid reducing agent like coke or coal, and the other on gaseous reducing agent like CO or H₂. Where coke is used as a solid reducing agent just as the case with COLAR, the rotary kiln process is no doubt the best.

The rotary kiln reduces lump ore or pellets using solid carbon as a reducing agent to metallized agglomeration and its operation is less restricted by the material and fuel to be used. However, it has a penalty of ring formation.

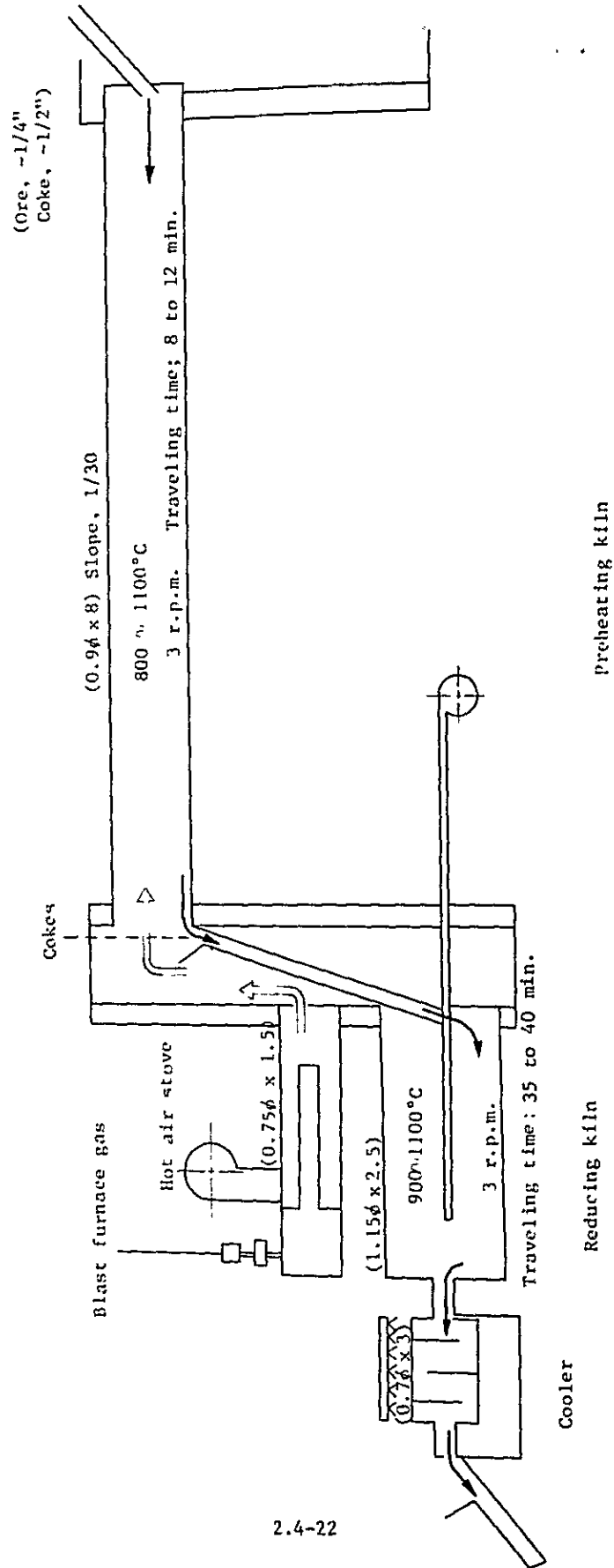
In the separate charging system employed by COLAR in which ore and reducing agent are charged separately, the reduction time becomes longer because of lower reduction speed as compared with encapsulated charging system in which reducing agent is occluded into the pellets. In the encapsulated charging system, the pellets become more porous as the reducing agent is consumed, and the product becomes fragile, developing dust to cause the ring. But the separate charging is susceptible to dust development to a lesser degree, and is escapable from ring troubles.

Anyway, COLAR's is an engineering prototype with which to establish operating technology. COLAR may well study a commercial-scale unit only when the problems shown in para. (4) are boiled down and solved through reseaches and studies by operation of the engineering prototype.

- (4) Problems left to future study
 - a) Establishment of operating technology
 - i) For the purpose of establishing the operating conditions that will make it possible to run the system for an extended period, the effects of charge grain size, reducing temperature, reducing time, and the content of reducing agent, etc. should be clarified.
 - ii) Establishment of a method for precise measurement of temperatures of intra-kiln charges
A system or method should be established in order to measure the charge temperature as accurately as possible.
 - b) Facilities
 - i) The equipment is deficient in the following measures against ring troubles.
 - ° Monitoring of ring developments.
 - ° Removal of rings.

- ii) The equipment must be able to run stably for an extended period.

In this respect, it is important to verify that the supports for the rotating bodies in the drying furnace and kiln are free of troubles.



2.4-22

2.4-22

Fig. 2.4-9 COLAR's direct reduction facilities

2.5 Studies of Blast Furnace Profile and Furnace Facilities in Order to Provide for the Next Remodelling

What is pressing the COLAR most is the overhaul of the Nelly in the time to come, and the blast furnace facilities are discussed here in this connection.

2.5.1 Problems involved in the present profile of the blast furnace

The problems concomitant of the Nelly as it is now include the following.

- i) Productivity in relation to profile.
- ii) Quality requirements of refractories for extending the furnace life, and selection of proper brands.
- iii) Structural design of wearing plate section.
- iv) Structural design of tuyere and tuyere cooler.
- v) Arrangement of shaft cooling box.
- vi) Structural design and installation level of cinder notch.
- vii) Lining for penstock and blowpipe.
- viii) Furnace douser, etc.

2.5.2 Blast furnace profile

One of the problems the Nelly's profile has is that the hearth diameter is smaller than the throat diameter.

This type of blast furnace was employed when the beneficiation was not so advanced as is today, that is, when the reduction efficiency was at a low level. Considering the growing technologies in iron industry, the Nelly is outmoded and will not be viable.

This type also leaves much to be desired in view of the behavior of furnace charges. The hearth diameter is closely related to the burning rate of coke.

As regards the relationship between the hearth diameter and coke burning rate, there are formulas proposed by Owen Rice, H. Schenk, Fukagawa and Tokunaga, etc.

Although these formulas cannot meet all the furnaces of different operating conditions, they are prized for their high degree of agreement.

Fukagawa and Tokunaga's formula, $F = 9.06 D^{2.32}$

where, F: coke burning rate, tons/day

D: hearth diameter, m

Fig. 2.5-1 shows the relationship between hearth diameter and fuel burning rate.

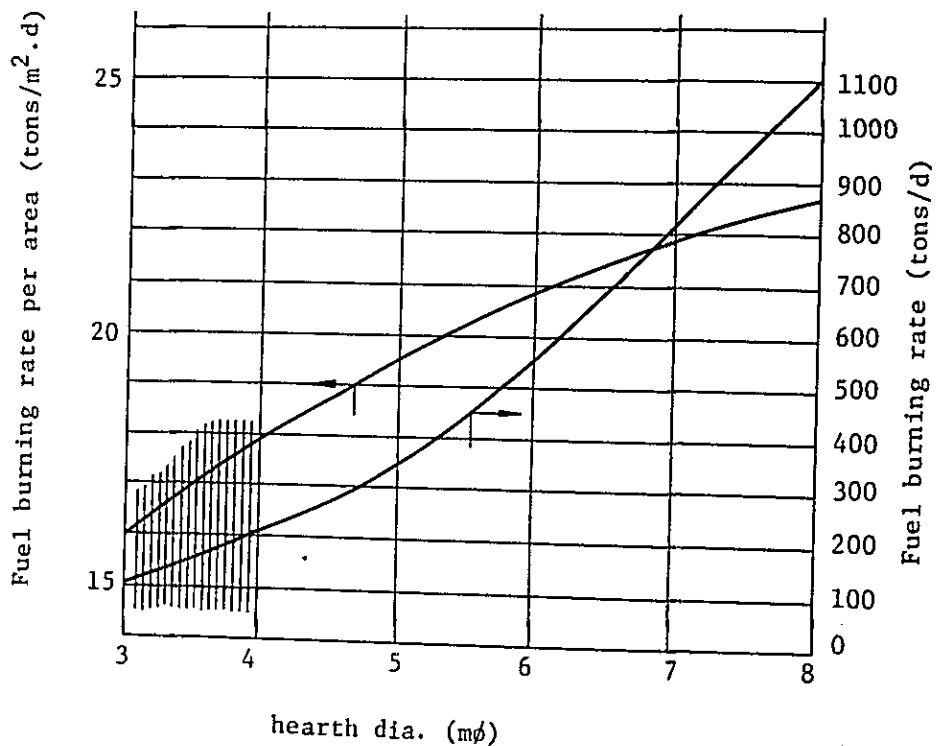


Fig. 2.5-1 Relationship between hearth diameter and fuel burning rate

Referring now to Fig. 2.5-1, let us assume that the coke burning rate per unit area of a furnace having a hearth diameter of 3.0 to 4.0 m is set at a conservative value of 15 tons/m².d. Then,

$$3.2 \text{ m}\phi \text{ furnace: coke burning rate} = 15 \times \pi (3.2/2)^2 = 120 \text{ tons coke/d.}$$

$$3.8 \text{ m}\phi \text{ furnace: coke burning rate} = 15 \times \pi (3.8/2)^2 = 170 \text{ tons coke/d.}$$

If the hearth diameter is increased from 3.2 mφ to 3.8 mφ, the coke burning rate will be increased by about 40%.

In order to increase the pig iron output, the following measures are necessary.

i) To reduce the fuel ratio

ii) To increase the fuel burning rate.

These are expressed by the following formula.

$$P = F/F_R$$

where, P : pig iron output (tons/day)

F_R : fuel rate

F : fuel consumption (tons/day)

The above formula shows that an increase in the fuel consumption rate can lead to an increase in pig iron output even when the fuel rate is held constant.

An increase in the hearth diameter leads to an increase in the annular active zone at the tuyere level, augmenting the fuel burning capacity.

Fig. 2.5-2 through -4 show the profiles of small blast furnaces in Japan in relation to the Nelly.

The singularities of the Nelly are as itemized below.

i) The shaft height is a little too much.

ii) The belly height is low.

iii) The sum of the shaft height and belly height is a bit too large.

iv) The bosh is too high.

v) The bosh angle is too small.

vi) $D_h/D > 1.0$; namely, the throat diameter is larger than the hearth diameter.

vii) D_b/D is too large.

In addition,

- viii) The distance between tuyere and cinder notch is short.
- ix) The distance between the tuyere and tap hole is short.
- x) The large bell stroke is rather too much.
- xi) The distance between the tuyere level and the bottom end of bosh is too much. (0.8 m → 0.6 m)

As discussed above, the reduction zone in which the solid phase and gaseous phase react upon each other can be improved for increased pig iron output by increasing the hearth diameter to harmonize the profile.

Fig. 2.5-5 shows a pattern of melting zone and an iron ore reduction state in relation to a blast furnace profile. Fig. 2.5-6 shows the reduction ratio in the $\text{Fe}_2\text{O}_3 \rightarrow \text{Fe}$ reduction process.

In Japan, the intra-blast furnace indirect reduction ratio is nearly in the range of 65 to 70%, and the direct reduction ratio in the range of 30 to 35%.

The reduction ratio as calculated from the cross sectional view of Fig. 2.5-5 is approximately 70%, which shows a good agreement with the indirect reduction ratio obtained from the gas analysis during blast furnace operation. The latter, however, shows a somewhat smaller value. This is because the apparent indirect reduction ratio is shifted in the arrow direction from (A) to (B) in Fig. 2.5-6 owing to the carbon solution loss reaction.

The left half of Fig. 2.5-5 is supposed of the present Nelly, and the right half refers to a case where the hearth diameter is increased with the throat diameter and belly diameter held intact. As already discussed, the increase in the hearth diameter leads to an increase in the fuel burning rate, increasing the reducing gas volume in the blast furnace.

Since the belly diameter is held intact, the increase in the reducing gas volume results in an increase in the speed of the gas passing through the belly, and in conjunction with the enlargement effect of hearth diameter, offers the following conditions in the blast furnace operation.

$$h_2 > h_1 \quad \text{and} \quad d_2 > d_1$$

Increasing the level of the melting zone results in an increase in the level of the dead core of the coke, which in turn works to increase the temperature of the molten liquid as it descends a long way through the dead core to the tuyere level.

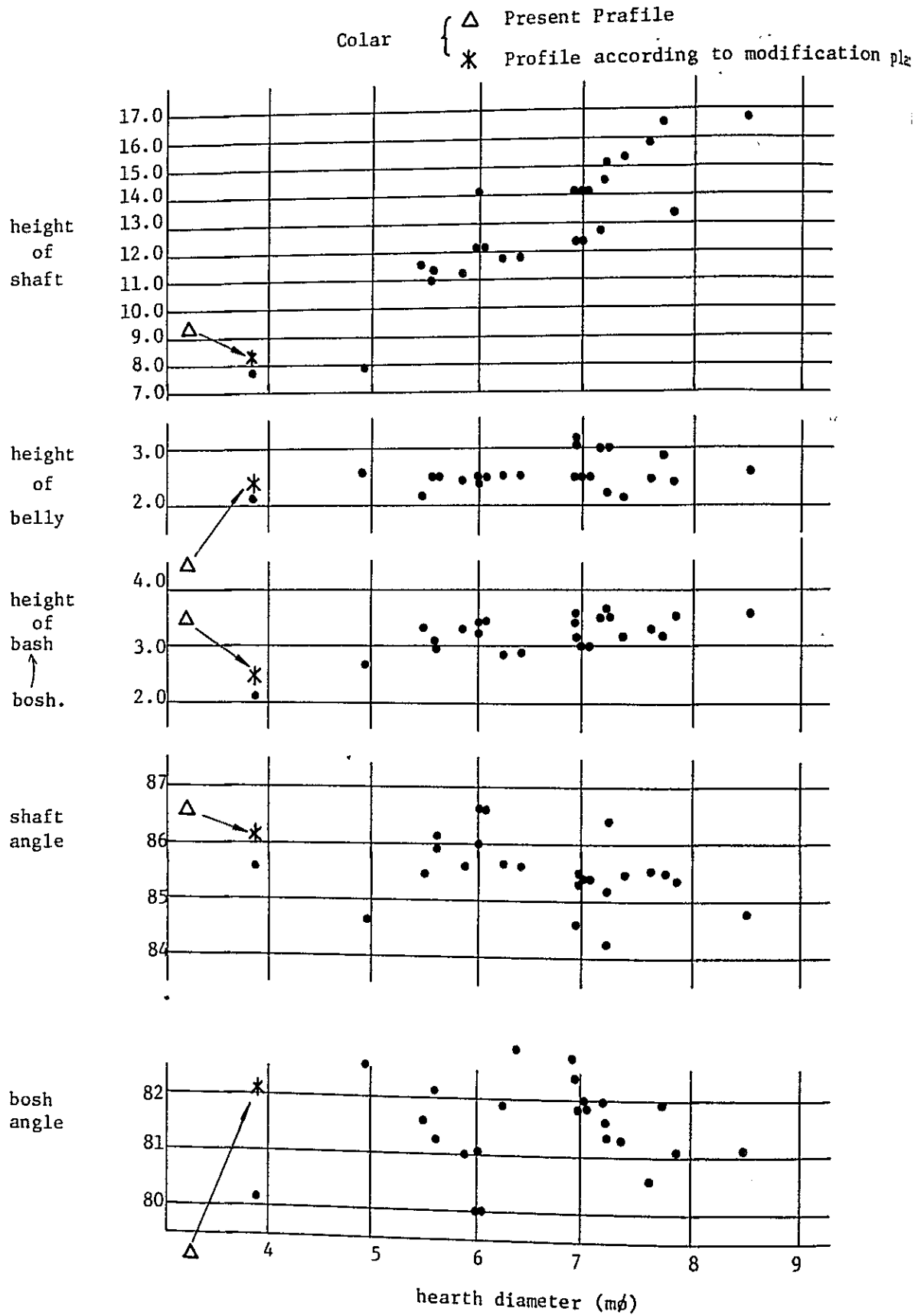
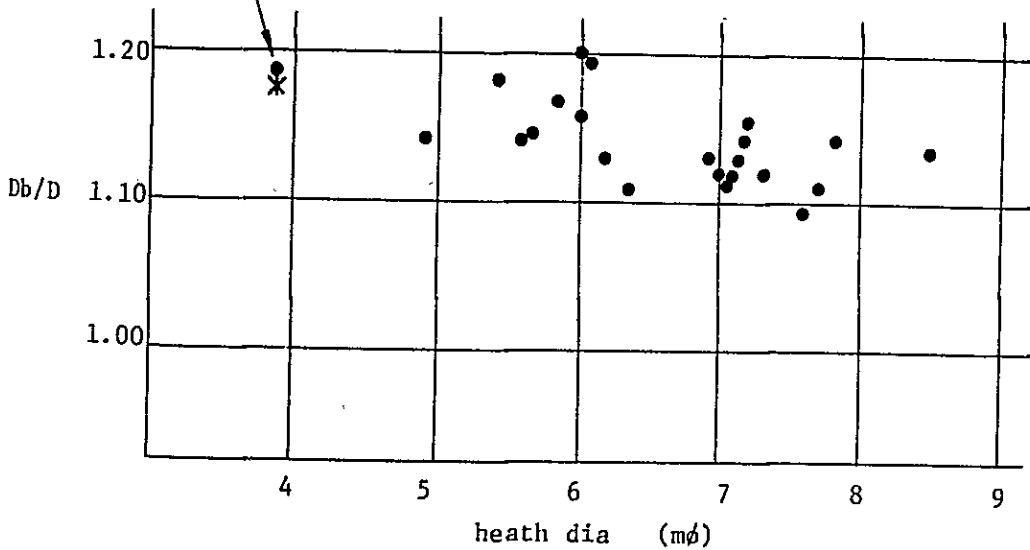
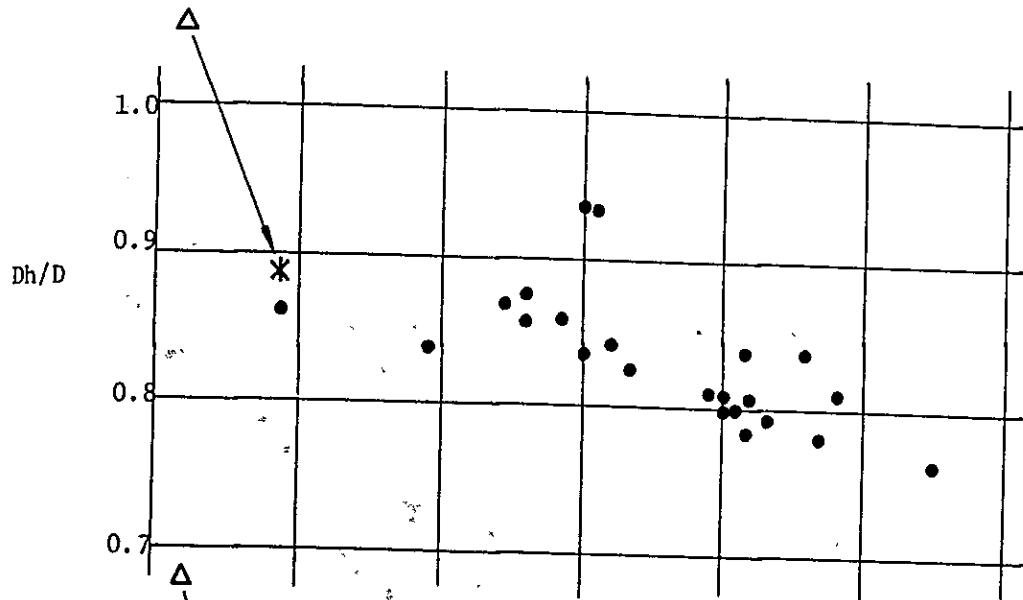


Fig. 2.5-2 Dimension of blast furnace for various hearth diameter 2.5-6



D : hearth dia.

Dh : throat dia.

Db : belly dia.

Fig. 2.5-3 On the diameter of throat and belly for various hearth diameters

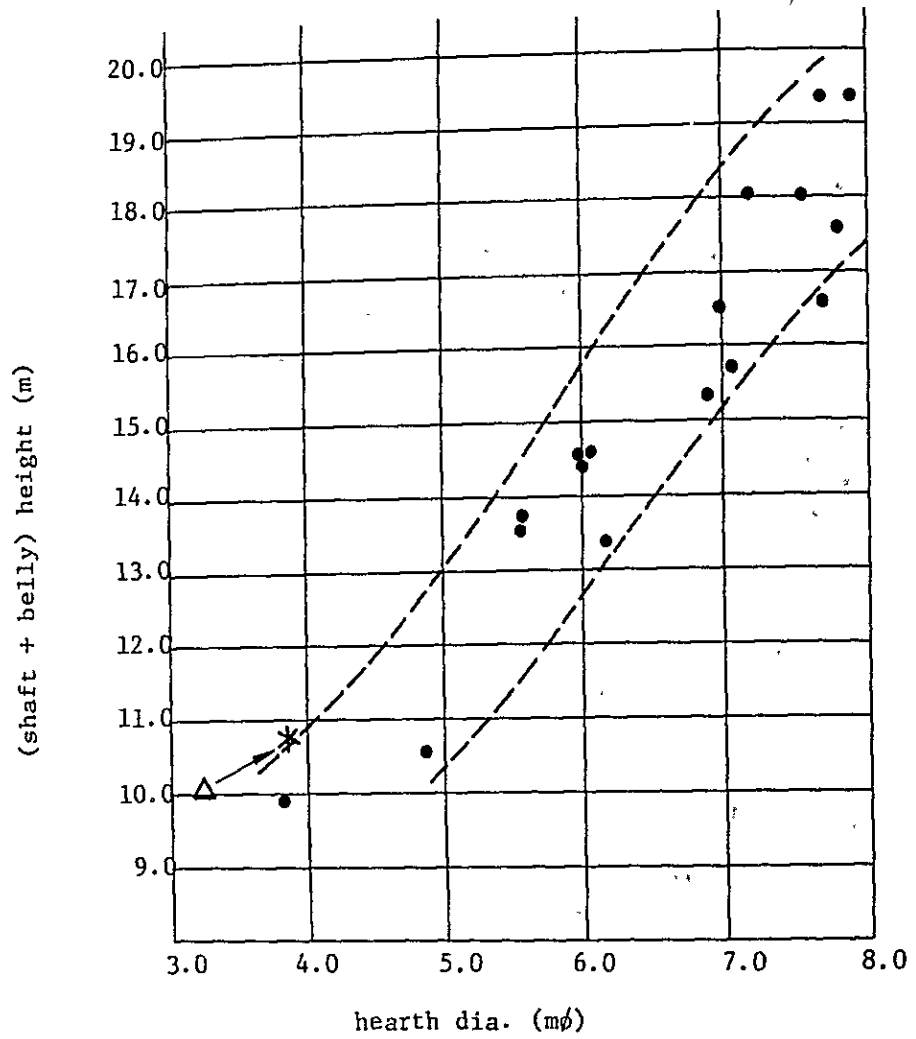


Fig. 2.5-4 Relationship between hearth diameter and the combined height of shaft and belly

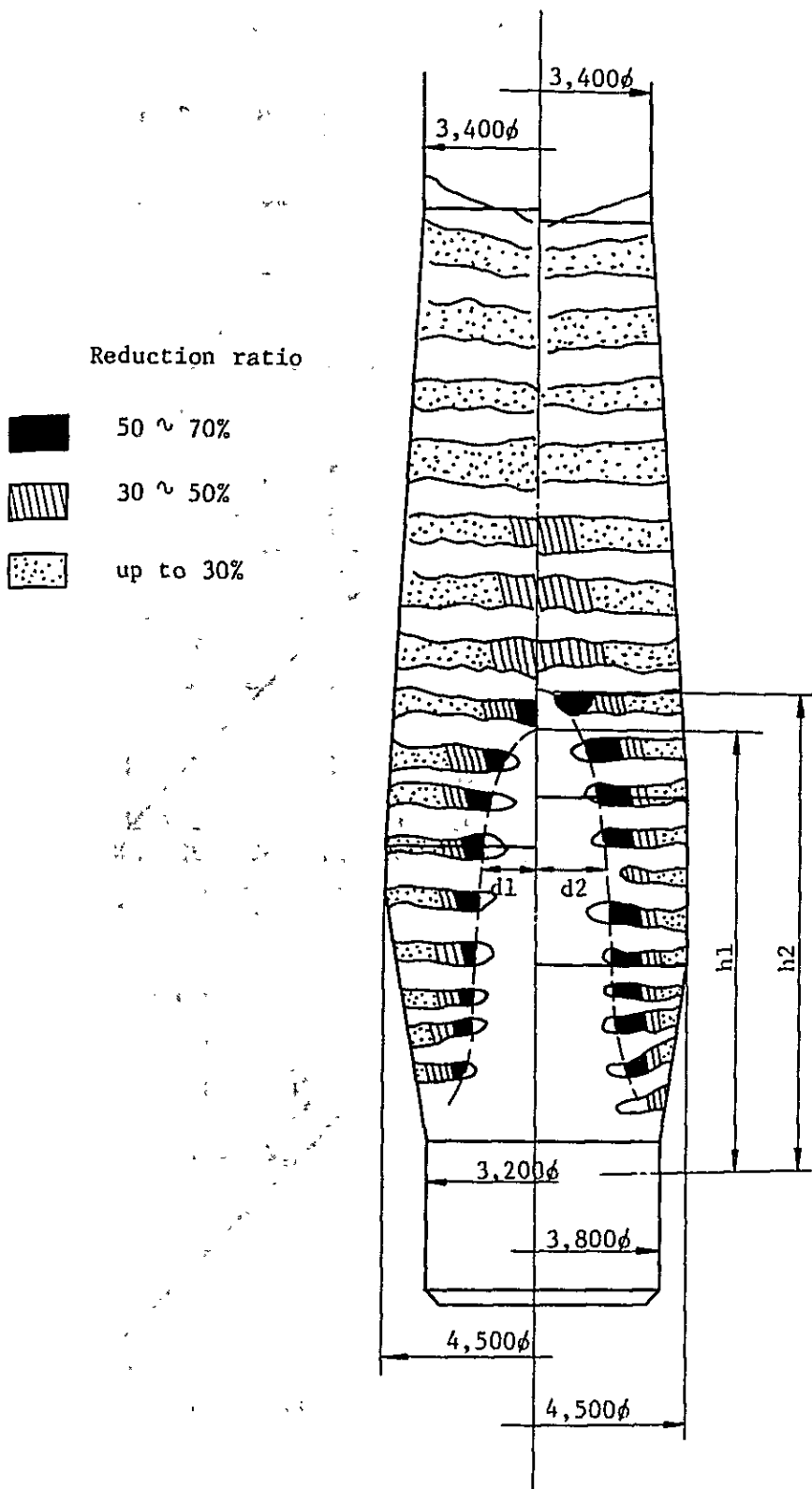


Fig. 2.5-5 Pattern of melting zone and reduction conditions according to blast furnace profile

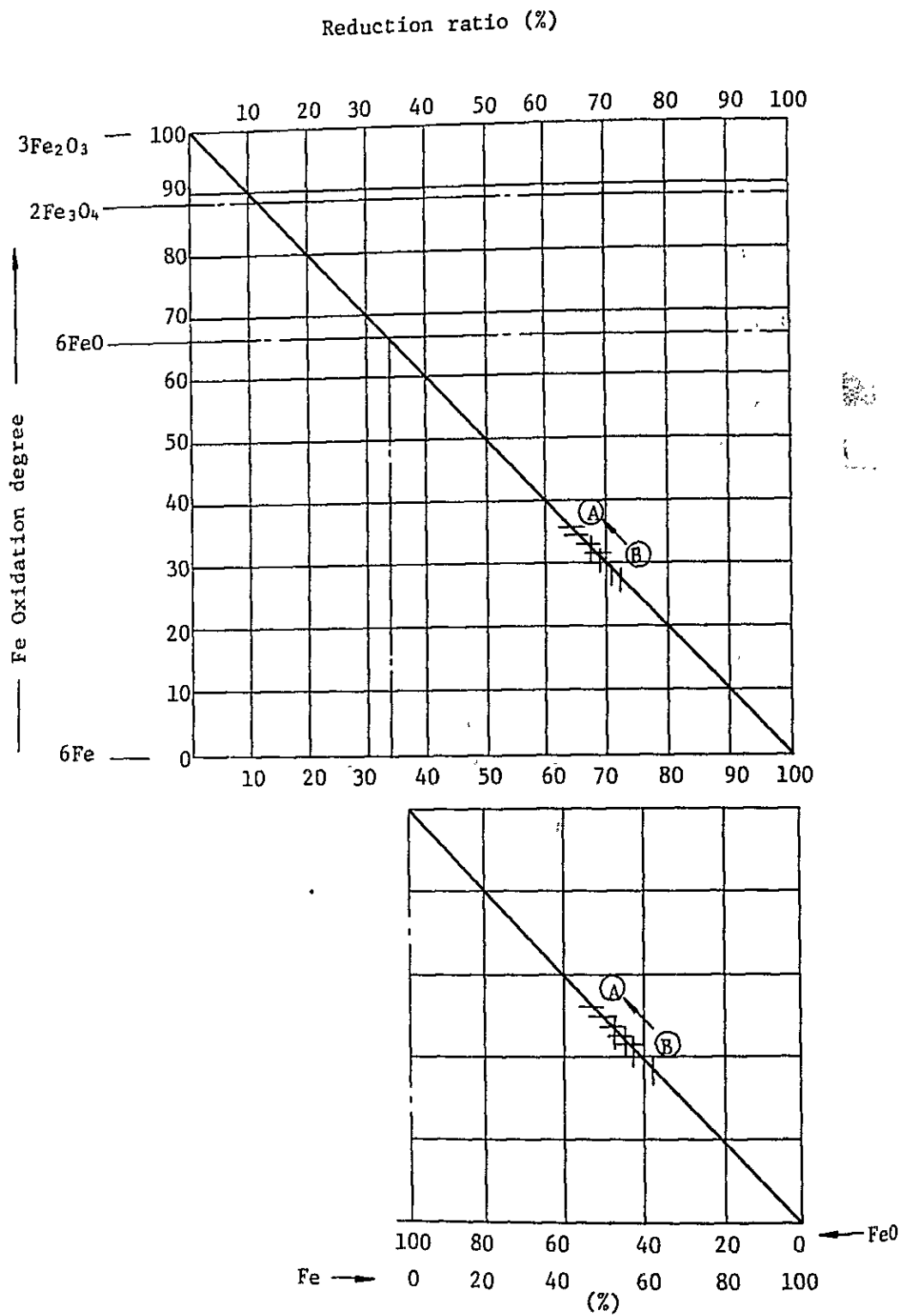


Fig. 2.5-6 Reduction ratio and iron oxidation degree in $\text{Fe}_2\text{O}_3 \rightarrow \text{Fe}$ reduction process

As illustrated in Fig. 2.5-5, the slope of the reduction ratio of the solid iron oxides enclosing the inverted-V melting zone is sharp. In a blast furnace in which the surface area of the inverted-V melting zone is small, volumes of charges of low reduction degree are supplied to the peripheral part, and then to the melting zone. As illustrated in Fig. 2.5-6, the iron oxides running into the melting zone are 50 to 60% by Fe and 40 to 50% by FeO. As soon as FeO is molten down, it reacts with solid carbon, and endothermic direct reduction takes place. Naturally, this kind of endothermic reaction should preferably take place at an elevated position of the blast furnace from the viewpoint of operations.

In the blast furnace operations, it is important to increase the reduction ratio in the solid state of iron ore in the reduction and melting processes.

If FeO plunges into a high-temperature zone, the melting temperature of the gangue in the ore will be reduced by the agent of FeO, slowing down the reduction by reducing gas, increasing the endothermic direct reduction, and thus sending up the fuel ratio.

From the explanations above, it is evident that the hearth diameter of the Nelly should be enlarged not only for increasing the pig iron output, but also for cutting down on fuel rate.

It should be added by the way that the characteristics of the charges must be improved to meet the blast furnace operating speed. For the purpose of improving the Nelly's profile, the following conditions are set.

a) Restraints

- i) The furnace height, belly diameter and throat diameter are to be held intact.
- ii) The tuyere level is to be held unchanged in consideration of its relation to the bustle pipe, though desirable to be increased some 200 mm if at all possible.
- iii) The iron notch level is to be held as it was in view of its dimensional relationship with the cast house

b) Profile improving conditions

- i) Bosh angle to be set at nearly 82°.
- ii) (Belly diameter/Hearth diameter) to be set at 1.1 to 1.2.
- iii) Bosh height to be 2.0 to 3.0 m.
- iv) Belly height to be 2.4 m in view of cooling box spacing.
- v) The length of wearing plate to be extended 200 mm downward as the present charging level is at the bottom end of the wearing plate.

The studies were made according to the conditions given above, and an improved profile was achieved as illustrated in Fig. 2.5-7.

With reference to Fig. 2.5-7, the left hand is the existing profile, and the right hand the improved one.

Blast furnace inner volume

	<u>Existing</u>	<u>Improved</u>
Total Tap hole bottom to 1,000 mm volume : below bell opening	180.08 m ³	202.96 m ³
Working Tuyere center to 1,000 mm volume : below bell opening	168.22 m ³	186.23 m ³

Left : existing profile

Right: improved profile

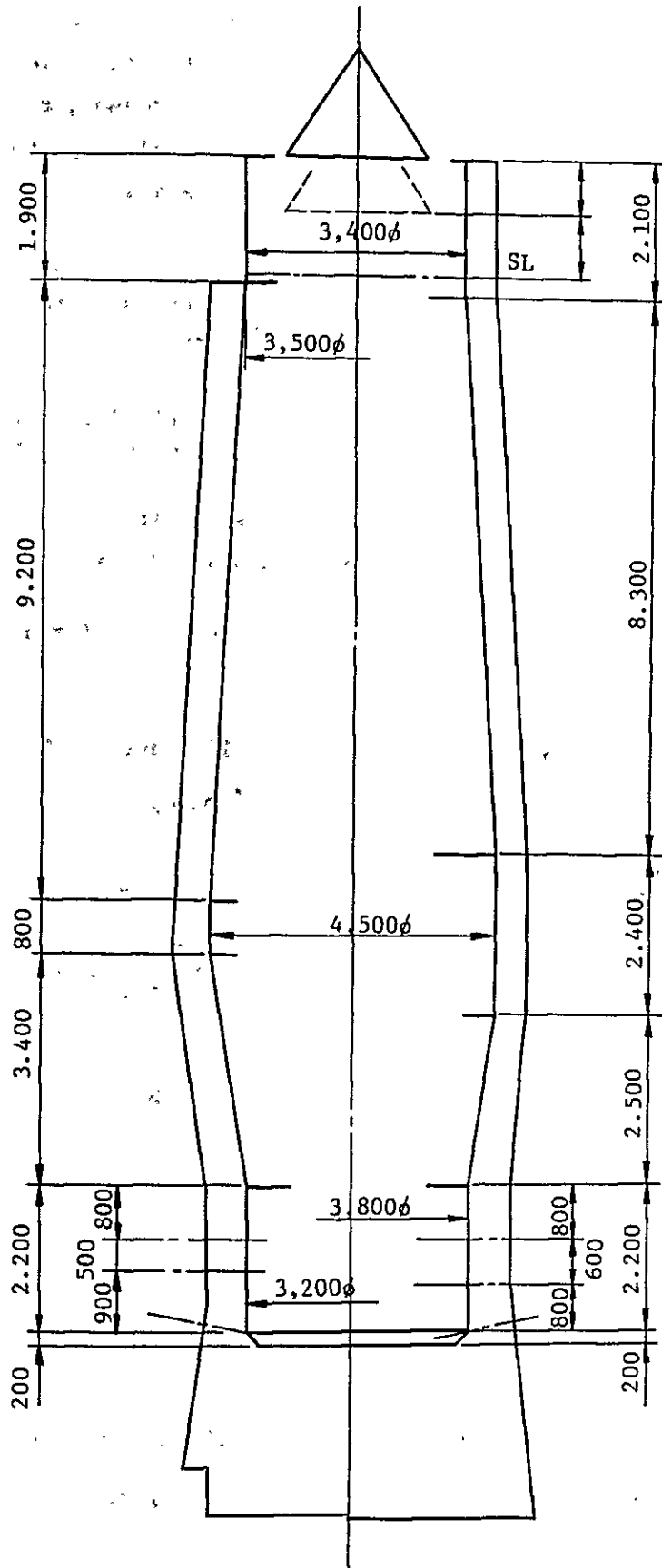


Fig. 2.5-7 Improvements in blast furnace profile
2.5-13

In the case of the COLAR, the slag ratio is high, so that the slag flushing volume from the cinder notch should be increased. If a great quantity of slag is discharged from the tap hole, the tap hole lining will be damaged seriously. For this reason, the cinder notch is lowered 100 mm from the existing level. Although this reduce the capacity of the basin, the following capacity still exists.

$$S = 6.8 \pi (D/2)^2 h \alpha$$

where, h: depth of basin, 0.9 m (increased from the present 0.8 m by adjusting the tap hole clay material)

D: hearth diameter, 3.8 m

α : volume factor, 0.40 (a little larger value taken to allow for the sidewall effect due to small size of blast furnace)

S: storage capacity, tons-pig iron

$$S = 6.8 \times \pi \times (3.8/2)^2 \times 0.9 \times 0.4 = 28 \text{ tons-pig iron}$$

Now let us examine the gas velocity in the blast furnace.

Given:

- | | | | |
|-------|---|---|---|
| 1) | Coke consumption | : | 150 tons - coke/day |
| ii) | Coke rate | : | 900 kg/ton-iron |
| iii) | Solid carbon available from coke | : | 84% |
| iv) | Composition of blast air (dry) | : | 21% O ₂ , 79% N ₂ |
| v) | Oxygen reduced from iron ore to produce a ton of pig iron | : | 425 kg |
| vi) | Direct reduction ratio | : | 33% |
| vii) | Carbon content of pig iron | : | 4.0% |
| viii) | Coke runoff as a dust | : | 10 kg/ton-iron |
| ix) | Furnace top gas temperature | : | 150°C |
| x) | Hot blast temperature | : | 600°C |
| xi) | Limestone consumption | : | 100 kg/ton-iron |
| xii) | Blast pressure | : | 0.4 kg/cm ² |

- xiii) Furnace top gas pressure : 1,500 mm Aq.
- xiv) Atmospheric pressure : 580 mm Hg
- xv) Mean voids in the furnace : 0.55

According to the suppositions above, the gas velocity in the furnace and at the throat is calculated as follows.

- (1) Pig iron output: $150 \div 0.9 = 166.6$ tons - pig iron/day
- (2) Carbon consumed for direct reduction:
 $425 \times 0.33 \times 12/16 = 105$ kg -C/ton-iron
- (3) Carbon runoff as dust: $10 \times 0.84 = 8.4$ kg - C/ton-iron
- (4) Carbon taken into pig iron: $1,000 \times 0.04 = 40$ kg -C/ton-iron
- (5) Carbon burnt at the tuyere:
 $900 \times 0.84 = ((2) + (3) + (4)) = 602.6$ kg - C/ton-iron
- (6) Wind rate required: $602.6 \times 16/12 \times 22.4/32 \div 0.21 =$
 $2,678$ m² air/ton-iron
- (7) Lime-dissociated gas: $100 \times 0.52 \times 12/(40.08 + 12 + 48)$
 $\times 22.4/12 = 13.8$ m³ CO₂/ton-iron
- (8) Pig iron production rate: $166.6 \div 24 \div 60 \div 60 =$
 0.001928 ton-iron/sec.
- (9) Furnace gas developing rate: $(2,678 \times 0.79 + 2,678 \times$
 $0.21 \times 2 + 105 \times 22.4/12 + 13.85) \times 0.001928$
 $= 6.652$ m³-gas/sec.
- (10) Blasting pressure (abs.): $1,033/2 \times 580/760 + 400$
 $= 1,188.5$ g/cm²
- (11) Furnace gas top pressure (abs.): $(1,500/10,332 + 0.788) \times$
 $1,000 = 933.7$ g/cm²
- (12) Mean cross-sectional area between stock line and tuyere:
 $(3.8 \times 0.8 + 4.15 \times 2.5 + 4.5 \times 2.4 + 3.95 \times 8.3)/$
 $(0.8 + 2.5 + 2.4 + 8.3) = 4.071$ m ϕ
 $(4.071/2)^2 \pi = 13.02$ m²

(13) Theoretical combustion temperature at the tuyere:

$$0.834 \times 600 + 60.79 \times 21 + 288.3 = 2,065.3^{\circ}\text{C}$$

(14) Mean gas velocity in the charges:

$$v_s \doteq G \times \frac{\frac{T_1 + T_2}{2} + 273}{273} \times \frac{1,033}{\frac{P_1 + P_2}{2}} \times \frac{1}{A} \times \frac{1}{0.55}$$

where, v_s : mean gas velocity in the furnace, m/sec.

T_1 : theoretical combustion temperature at tuyere, $^{\circ}\text{C}$

T_2 : furnace gas temperature, $^{\circ}\text{C}$

P_1 : blast pressure (abs.), g/cm^2

P_2 : furnace top gas pressure (abs.), g/cm^2

A : mean cross-sectional area between stock line and tuyere, m^2

0.55: mean voids in the furnace

G : furnace gas generating rate, m^3/sec .

$$v_s = 6.652 \times \frac{\frac{2,065.3 + 150}{2} + 273}{273} \times \frac{1,033}{\frac{1,188.5 + 933.7}{2}} \times \frac{1}{13.02} \times \frac{1}{0.55}$$

$$= 4.573 \text{ m/sec.}$$

(15) Throat gas velocity: v_t

$$v_t = 6.652 \times \frac{273 + 150}{273} \times \frac{1033}{933.7} \times \frac{1}{\pi(3.4/2)^2} = 1.2558 \text{ m/sec.}$$

(16) Furnace gas composition

$$\text{CO}_2 \text{ content : } 425 \times 0.67 \times 22.4/16 + 13.85 = \\ 412.5 \text{ m}^3\text{-CO}_2/\text{ton-iron}$$

$$\text{CO content : } (602.6 + 105) \times 22.4/12 - 425 \times 0.67 \times \\ 22.4/16 = 922.2 \text{ m}^3\text{-CO/ton-iron}$$

$$\text{N}_2 \text{ content : } 2,678 \times 0.79 = 2,115.6 \text{ m}^3\text{-N}_2/\text{ton-iron}$$

$$\text{Furnace gas volume : } 412.5 + 922.2 + 2,115.6 = \\ 3,450 \text{ m}^3\text{-gas/ton-iron}$$

CO₂ : 412.5/3,450 = 11.95%
 CO : 922.2/3,450 = 26.73%
 N₂ : 2,115.6/3,450 = 61.32%

(17) Furnace charge fluidization start velocity

In the blast furnace operation, it is required to let coke and ore fall stably as against the ascending flow of furnace gas.

Here, studies are made as to whether the ore and coke may succumb to fluidization under the influence of ascending gas flow.

In order to determine the fluidization start velocity, the following formula, a modification of Carman's theoretical formula, is employed.

$$U_{mf}^{1.9} = (g/2.9) \times (\rho_s - \rho_f) / (\rho_f \cdot \mu_f^{0.1}) \times \epsilon_m^3 / (1 - \epsilon_m)^{0.1} \times (D_p \cdot \phi)^{1.1}$$

Where, U_{mf}: fluidization start velocity, m/sec.

D_p : particle diameter, m

ρ_s : particle density, kg/m³

ρ_f : gas density, kg/m³

μ_f : gas viscosity, kg/m.sec.

φ : particle form coefficient

ε_m : max. percentage of voids

g : gravitational acceleration, m/sec.²

Here, the physical properties of coke and ore are set as follows.

	Coke	Ore
D _p (m)	0.05	0.03
ρ _s (kg/m ³)	1,000	3,600
φ	0.7	0.8
ε _m	0.47	0.47

a) Gas density: ρ_f

Composition: 11.95% CO₂, 26.73% CO, 61.32% N₂

Furnace gas temperature: 150°C

Furnace top gas pressure: 0.9337 kg/cm²

$$\begin{aligned} \text{Then, } \rho_f &= (44.0 \times 0.1195 + 28 \times 0.2673 + 28 \times 0.6132) / \\ & 22.4 \times 273 / (273 + 150) \times 0.9337 / 1.033 \\ & = 0.770 \text{ kg/m}^3 \end{aligned}$$

b) Gas viscosity: μ_f

From Wilke's formula, the viscosity of pure gas at 1 atm., 150°C, is given as follows.

$$\text{CO}_2 : 208 \times 10^{-6} \text{ P}$$

$$\text{CO, N}_2 : 227 \times 10^{-6} \text{ P}$$

$$\begin{aligned} \mu_f &= 208 \times 10^{-6} / \{1 + (26.73/11.95)\phi_{\text{CO}_2-\text{CO}} + \\ & (61.32/11.95)\phi_{\text{CO}_2-\text{N}_2}\} \\ & + 22.7 \times 10^{-6} / \{1 + (11.95/26.73)\phi_{\text{CO}-\text{CO}_2} + \\ & (61.32/26.73)\phi_{\text{CO}-\text{N}_2}\} \\ & + 227 \times 10^{-6} / \{1 + (11.95/61.32)\phi_{\text{N}_2-\text{CO}_2} + \\ & (26.73/61.32)\phi_{\text{N}_2-\text{CO}_2}\} = 223 \times 10^{-6} \text{ P} \\ & = 223 \times 10^{-7} \text{ (kg/m.sec.)} \end{aligned}$$

Hence, U_{mf} is given as follows.

$$\begin{aligned} \text{Coke } U_{mf}^{1.9} &= (9.80/2.9) \times (1,000 - 0.77) / ((0.77 \times \\ & (223 \times 10^{-7})^{0.1}) \times 0.47^3 / (1 - 0.47)^{0.1} \\ & \times (0.05 \times 0.7)^{1.1} \\ & = 6.4 \text{ m/sec.} \end{aligned}$$

$$\begin{aligned} \text{Ore } U_{mf}^{1.9} &= (9.80/2.9) \times (3,600 - 0.79) / ((0.77 \times \\ & (223 \times 10^{-7})^{0.1}) \times 0.47^3 / (1 - 0.47)^{0.1} \\ & \times (0.03 \times 0.8)^{1.1} \\ & = 10.1 \text{ m/sec.} \end{aligned}$$

So far as the mean gas velocity is concerned, neither coke nor ore will be fluidized at throat or in the shaft.

Since the intra-furnace gas pressure and atmospheric pressure are low, the gas volume will inflate to increase the gas velocity a little higher as compared with the blast furnaces of ordinary pressure in Japan.

Usually, the gas velocities within a cross section show a large difference. An actual example of gas speed distribution as measured at the throat of No.2 blast furnace at Kobe Steel Amagasaki Works is shown in Fig. 2.5-8.

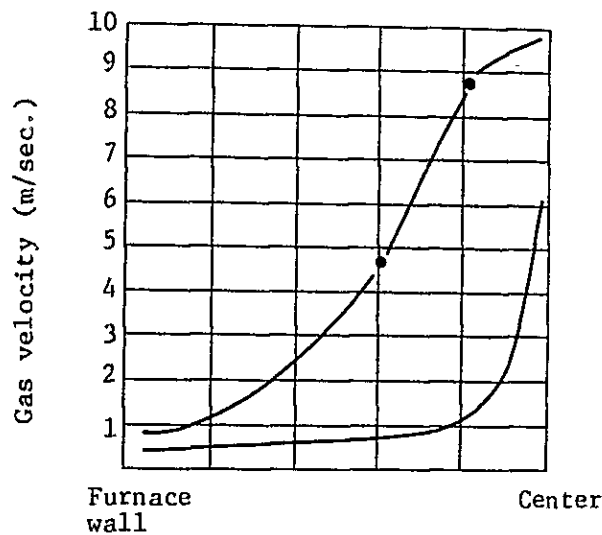


Fig. 2.5-8 Gas velocity distribution at the throat, Kobe Steel, Amagasaki Works

As illustrated in Fig. 2.5-8, the gas velocity is usually the highest at the furnace center. For this reason, the charges at the furnace center develop a fluidization, and are liable to develop a disturbance in stratification and cause a mixed layer of coke and ore. Even with the improved profile, some degree of disturbance at the furnace center will unavoidably be developed. Since this disturbance will take place within a narrow limited area at the center, it will never affect the furnace operations seriously.

2.5.3 Structural design of wearing plate

The soundness of the wearing plate has a great bearing on the distribution of charges. The following measures are required for the purpose of extending the service life of the wearing plate.

- i) To give high resistivity to heat and abrasion.
- ii) To divide into segments for the purpose of reducing thermal deformation.
- iii) To provide an ample measure for the prevention of slumping.

The material of which the wearing plate is to be made should be selected from among low-Mn, Cr cast steel, ductile cast iron, etc.

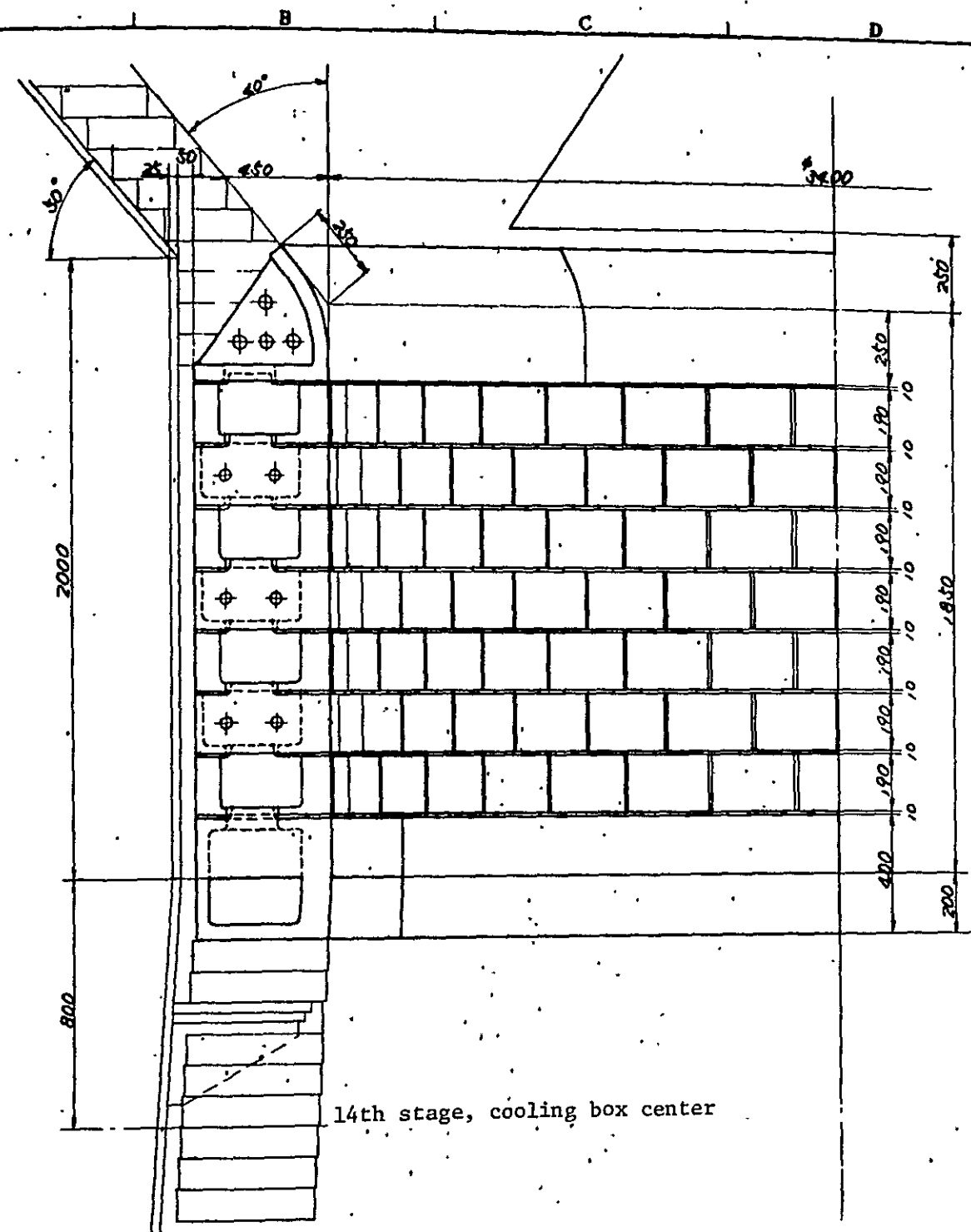
An example of chemical composition of wearing plate, %

C	Mn	Cr	Si	P	S
0.3~0.4	1.0~1.2	1.0~1.5	0.3~0.5	<0.06	<0.06

The present Nelly uses a wearing plate common to the furnace mantle. Namely, the wearing plate is made of a steel iron plate. Accordingly, its thermal deformation reduces the life of the mantle. To avoid this trouble, the wearing plate designed as illustrated in Fig. 2.5-9 is recommended.

The straight part of the recommended wearing plate is 200 mm longer than the existing wearing plate.

This is because with the existing wearing plate length, the position at which the charges collide with the wearing plate is too close to the stack brick lining.



14th stage, cooling box center

Chemical composition						hardness
C	Mn	Cr	Si	P	S	Shore Hs
0.3~0.6	1.0~1.2	10~15	0.3~0.5	>0.06	>0.06	30~40

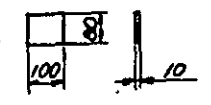
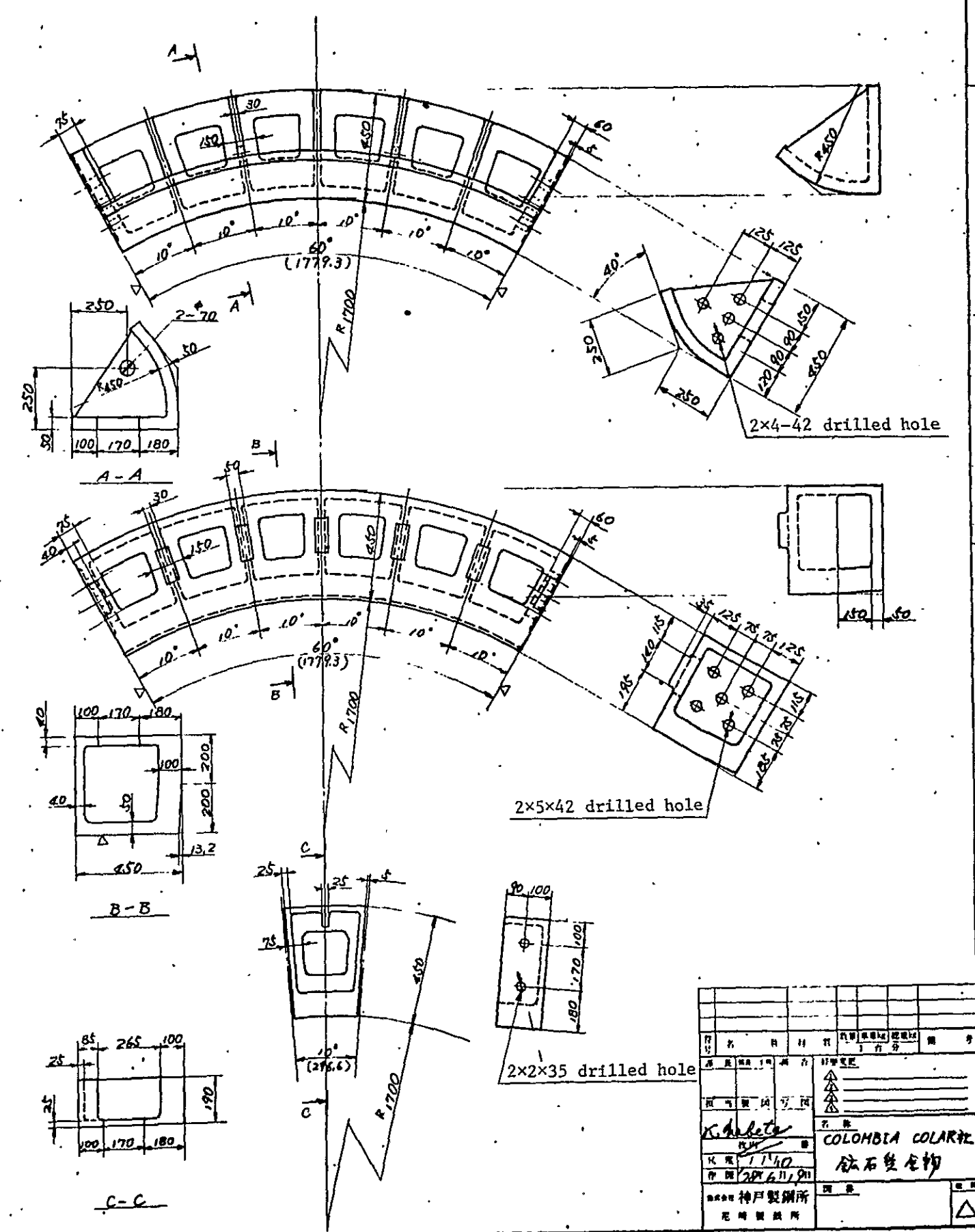


Fig. 2.5-9 Structural design of wearing plate.



2x4-42 drilled hole

2x5x42 drilled hole

2x2x35 drilled hole

材料	COLOMBIA COLARTE
名称	磁石垫龙物
规格	1140
数量	200, 611, 911
产地	神戸製鋼所

2000

2001

2002

Estimated falling locus of charges

The falling locus of the furnace charges currently in use is estimated.

Charge : 1,700 kg- coke, 3,400 kg -ore, 1,400 kg- limestone

Specific volume of charge : Coke, 2.1 m³/ton; ore, 0.45 m³/ton; limestone, 0.6 m³/ton

Dimensions : Large bell, diameter ... 2,200 mmφ
Large bell stroke 800 mm
Throat diameter 3,400 mmφ
Bell lowering speed In absence of the data about bell lowering speed, the following three values are considered.

i) 39 mm/sec.

ii) 30 mm/sec.

iii) 21 mm/sec.

Falling locus reckoning formula

$$y = x \cdot \tan \alpha + g \cdot x^2 / 2 \left((v_0^2 + 2sg (\sin \alpha - \mu \cos \alpha)) \cos^2 \alpha \right)$$

Where, g : gravitational acceleration, 9.8 m/sec.²

S : distance from the bottom of the large bell hopper to the bottom margin of the large bell along the bell surface with the large bell closed, m

v_c : critical discharge velocity from large bell hopper, m/sec.²

v₀ : initial discharging speed from the hopper, m/sec.
(0 ≤ v₀ ≤ v_c)

α : large bell angle. deg.

μ : friction coefficient between charge and bell surface

x : horizontal flying distance of particle, m

y : vertical falling distance of particle, m

In the case of the Nelly

$g : 9.8 \text{ m/sec.}^2$

$s : 0.65 \text{ m}$

$v_0 : 0 - 3 \text{ m/sec.}$

{ 0: the moment when the large bell is opened;
3: when the large bell is fully opened

$\alpha : 55^\circ 30'$

$\mu_{\text{coke}} : 0.31 \quad \mu_{\text{ore}} : 0.43$

a) Falling locus of coke:-

If $v_0 = 0$: $y = 1.455x + 1.849x^2$

If $v_0 = 3$: $y = 1.455x + 0.8848x^2$

b) Falling locus of ore:-

If $V_0 = 0$: $y = 1.455x + 2.065x^2$

If $V_0 = 3$: $y = 1.455x + 0.9316x^2$

Fig. 2.5-10 shows a falling locus in the Nelly.

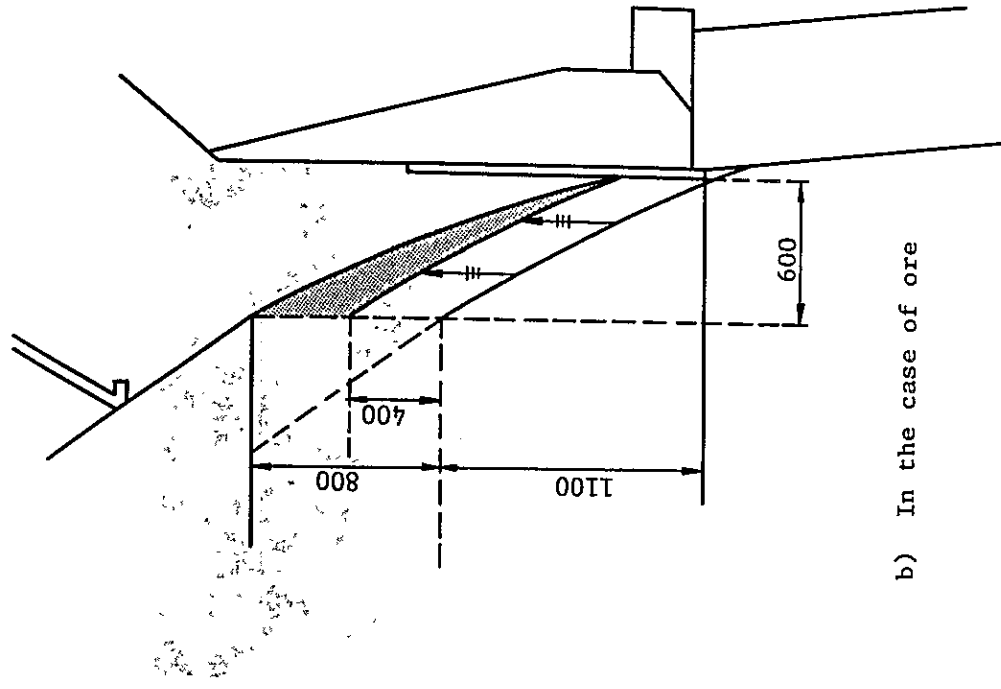
The charge on the bell of the Nelly is expected to be dislodged totally when the bell opening stroke is at 400 mm. According to our experiments, the falling locus showed little change within the range of said three levels of bell lowering speed. For this reason, the falling locus when the bell is totally open is determined by translating 400 mm below from the bell closed state. As is clear from the figure, both coke and ore show a unique projectile curve which eventually converges at a point on the wearing plate.

The hitting position is:

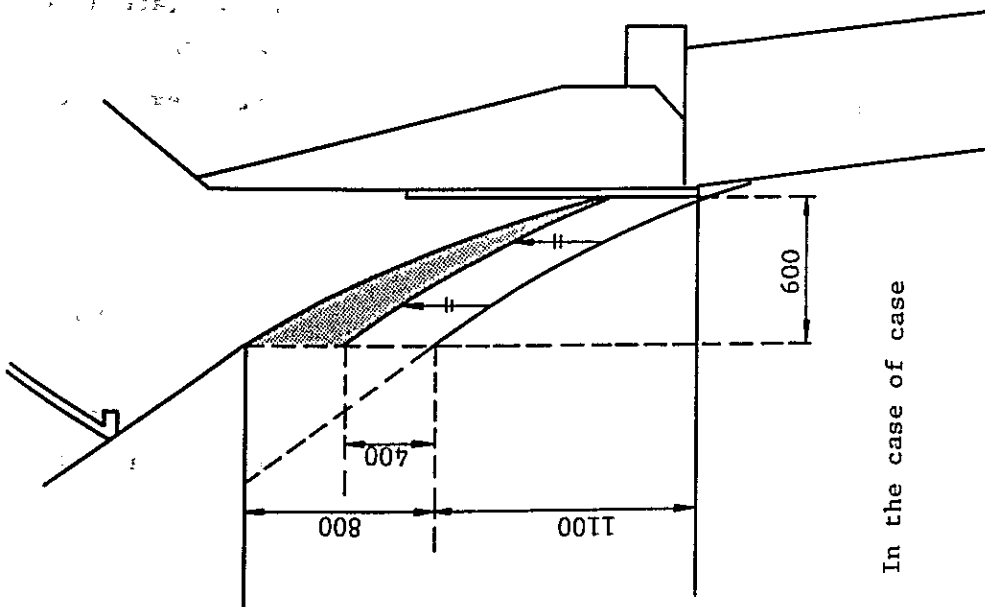
In the case of coke: $1,900 - (1,455 \times 600 + 1,849 \times 600^2) = 361 \text{ mm}$
from the bottom of the wearing plate

In the case of ore : $1,900 - (1,455 \times 600 + 2,065 \times 600^2) = 283 \text{ mm}$
from the bottom of the wearing plate

These are too close to the bottom margin of the wearing plate, and agree with the position shown on Photo 2.5-1, demonstrating the justifiability of the calculated results.

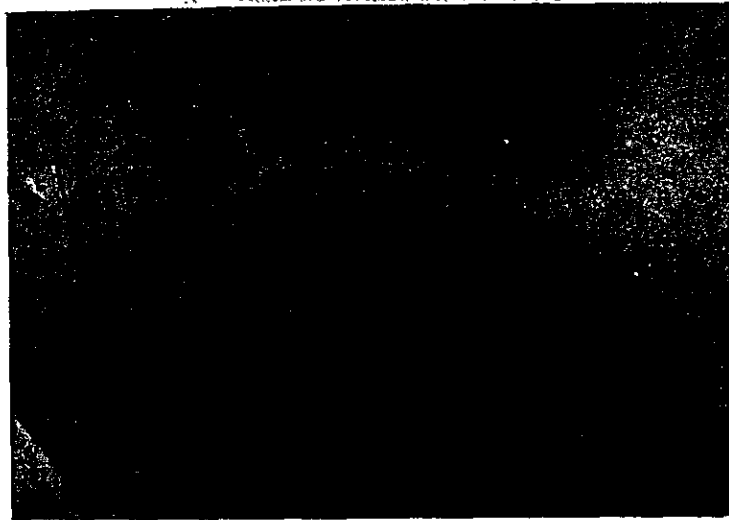


b) In the case of ore



a) In the case of case

Photo 2.5-1 Position of sideswipe on the wearing plate



If, however, the dislodging of the charges from the bell is carried out with the bell at the downmost position, the place of collision will be shifted below the bottom end of the wearing plate as illustrated in Fig. 2.5-10, breaking the shaft brick lining.

In order to avoid this trouble, it is recommended to extend the skirt length of the wearing plate 200 mm downward.

2.5.4 Quality and brand of refractories

This is one of the most important questions asked by the COLAR, and will be discussed in detail in 2.6.

The arrangement of refractories by quality is shown in Figs. 2.5-23 and 2.6-22. The block refractories are carbon bricks, and castings are chamotte.

2.5.5 Structural design tuyere and tuyere cooler

Fig. 2.5-11 is a sketch showing the construction of the tuyere and tuyere cooler of the present Nelly.

As is clear from the figure, the following problems exist in the construction.

- i) The tuyere is consumable. If it is too heavy in weight, it will cost the COLAR much in investment and in replacement work.
- ii) Excessive area of tuyere tip will permit easy attack by molten pig iron, and also will reduce the cooling efficiency in the tuyere.
- iii) The tuyere is liable to be attacked by molten iron because of its insertion angle and tip shape.
- iv) As the penetrated length of tuyere into the furnace is too short, the lining right above the tuyere is liable to be damaged under the attack of tuyere gas, and also the lining around and right under the tuyere is corroded by fused materials.
- v) The tuyere is mated over a short lapping with the tuyere cooler fixed to the furnace body. Its bond to the furnace is therefore insufficient. Nevertheless, the tuyere experiences a heavy load of refractoriés from above and an expansion force from below. As a result, the brick joints may get loose. The tuyere should be free from the furnace lining.
- vi) The location of the port of the drain pipe is not proper. As illustrated in Fig. 2.5-4, the port of drain pipe should be placed above the tuyere and tuyere cooler. This scheme should be employed in case the tuyere and tuyere cooler should be emptied of water owing to siphon phenomenon at the time of water service interruption due to power failure or others.

In order to solve all these problems, the facilities are modified as illustrated in Figs. 2.5-12 through -14.

In more details, the following provisions are made.

- i) The penetration length of tuyere cooler is made almost the same as the lining thickness at that part, and the lining is fixed with the tuyere cooler and the lining set together.

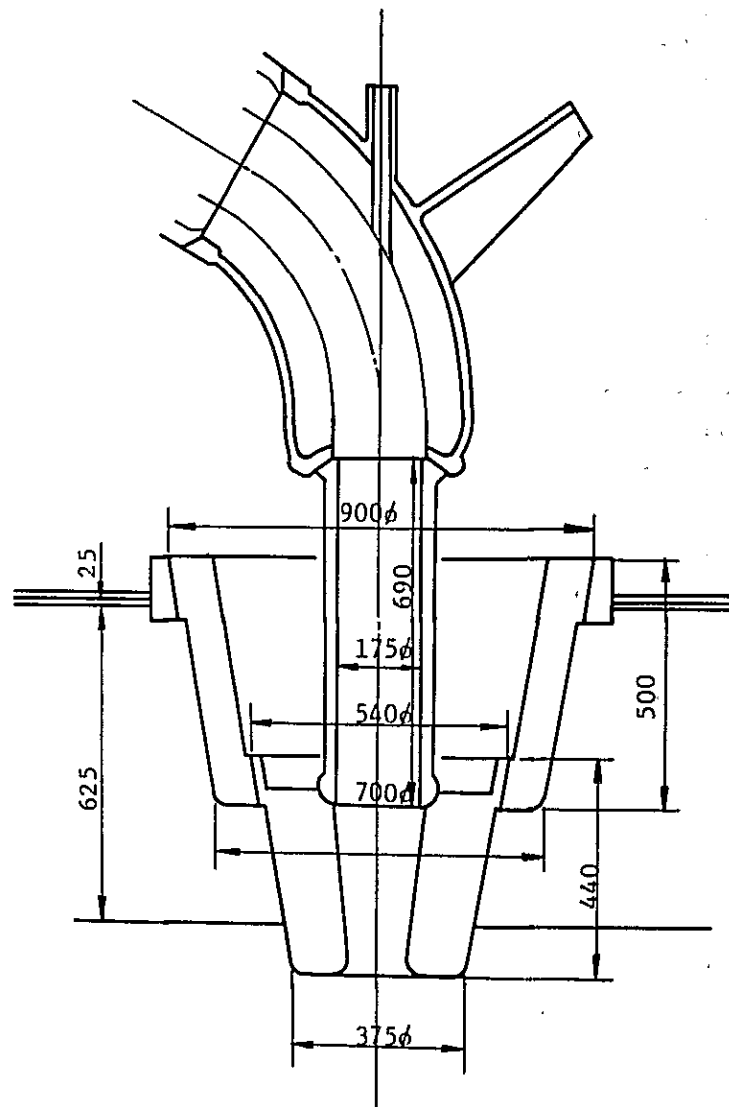


Fig. 2.5-11 A sketch of the present tuyere

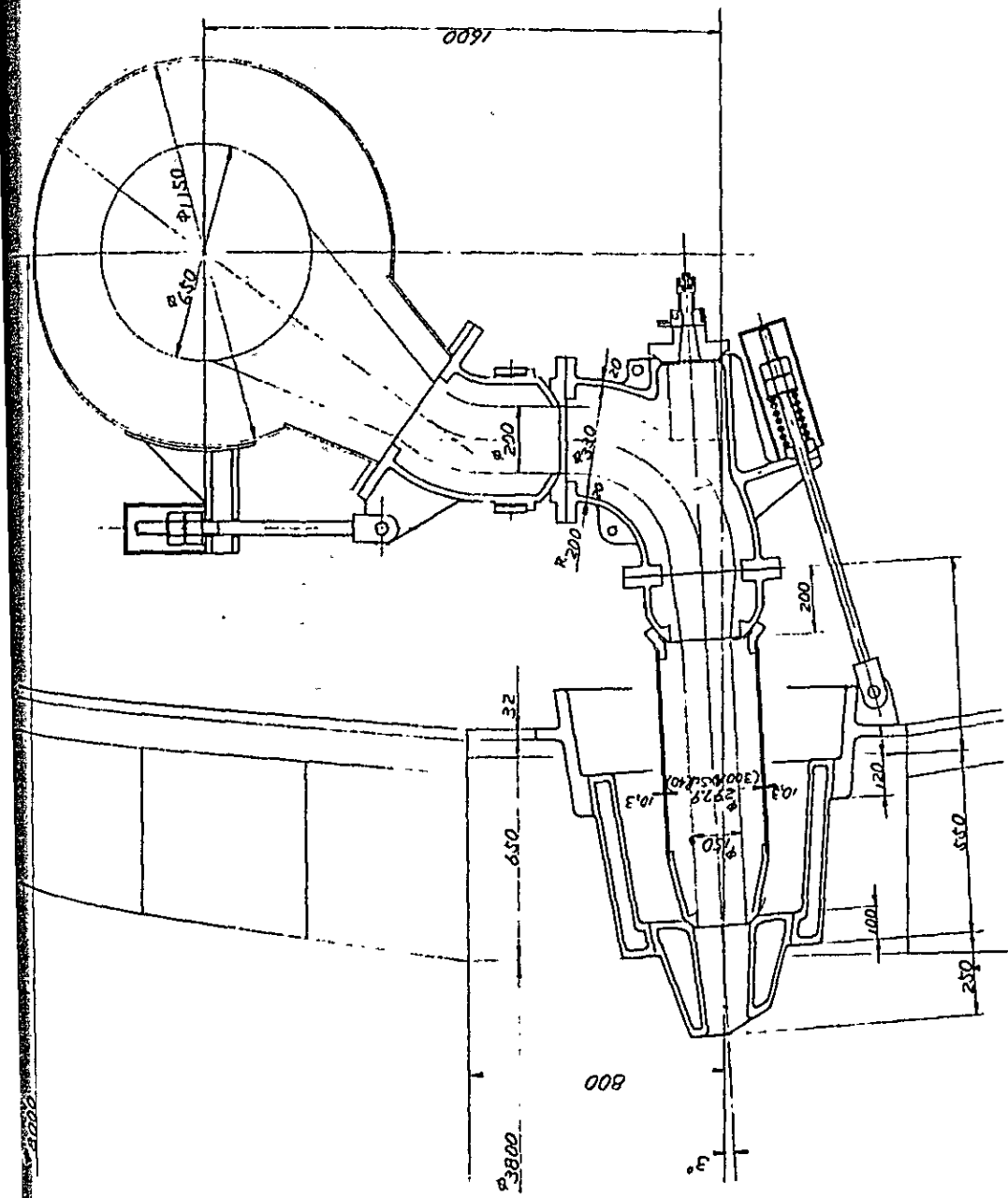


Fig. 2.5-12 Construction of tuyere and tuyere cooler

f

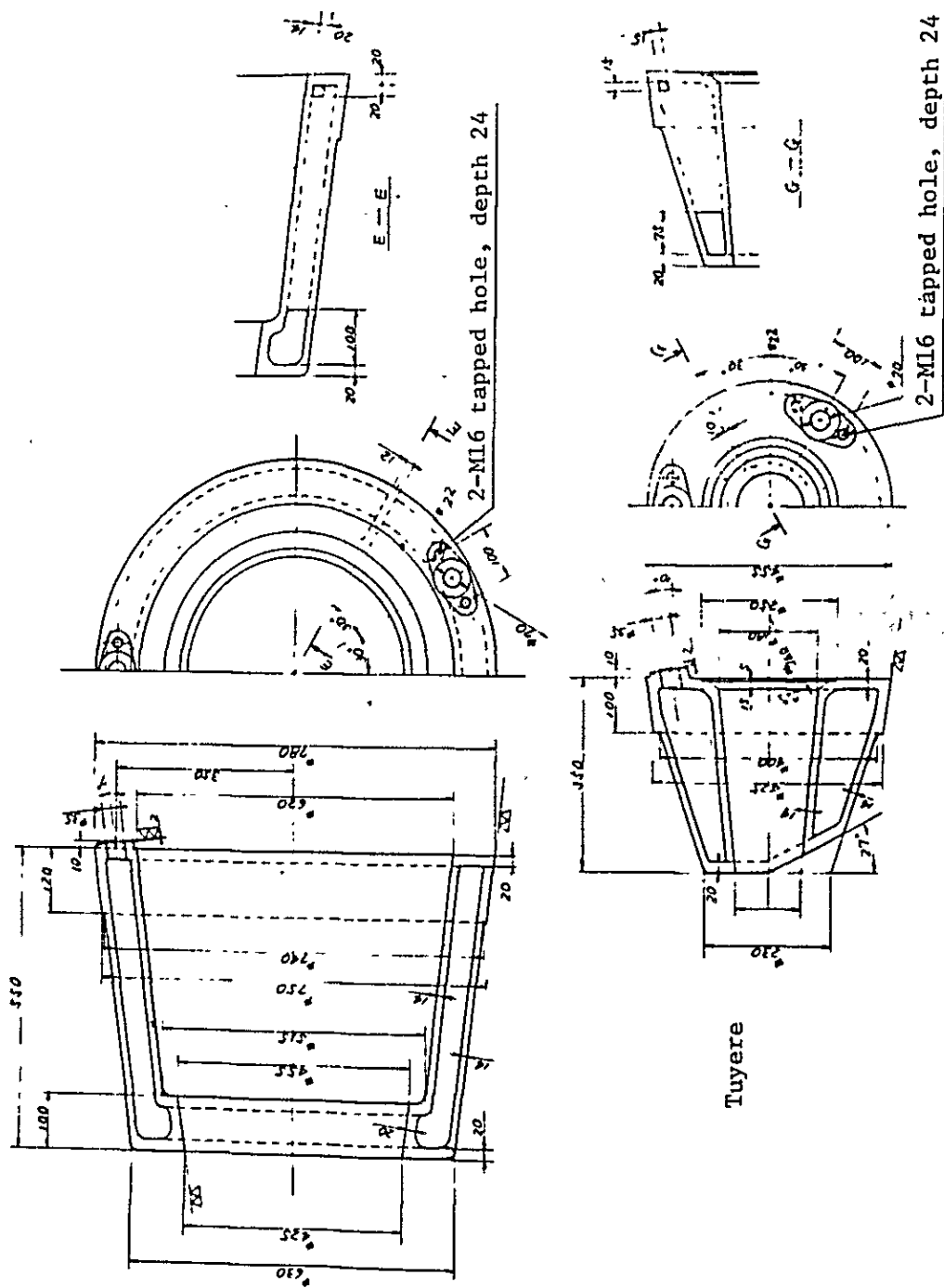


Fig. 2.5-13 Tuyere and tuyere cooler

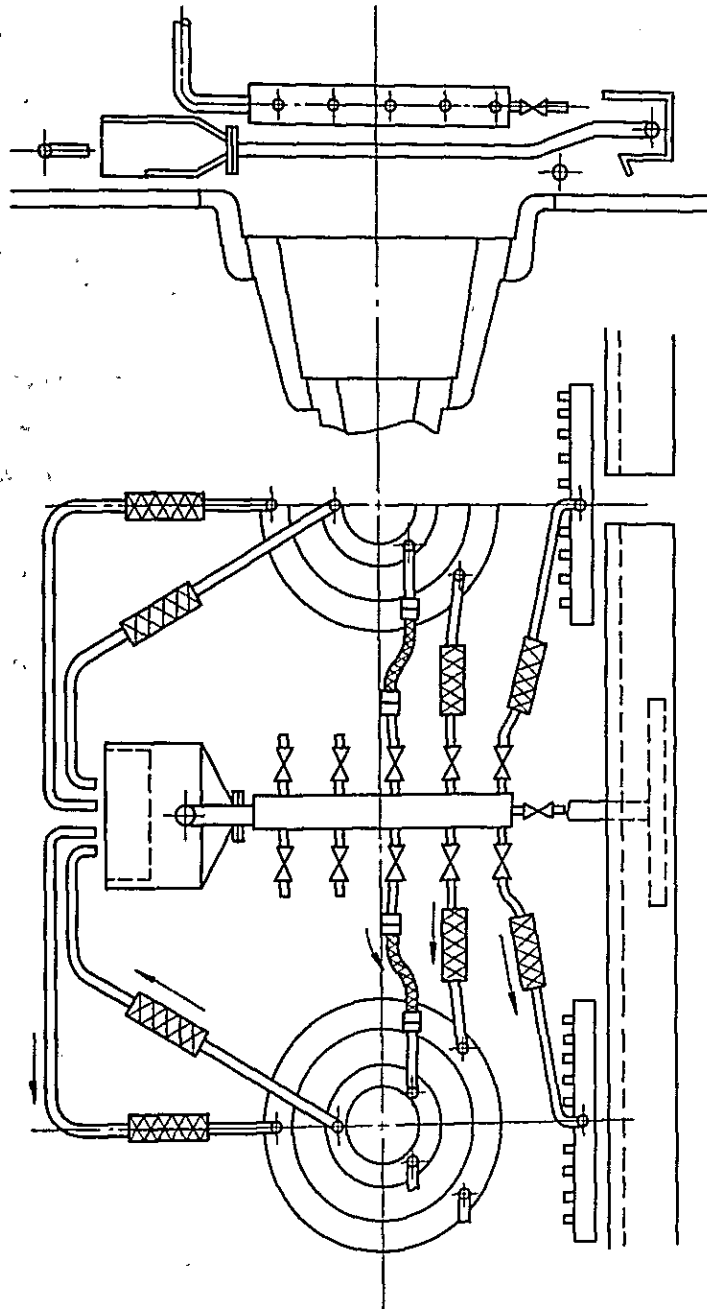


Fig. 2.5-14 Modified plan for the arrangement of tuyere cooling water drain ports

- ii) The tuyere is arranged in line with the penstock and blowpipe for the purpose of minimizing the turbulence in blast air flow, and its angle from the level plane is set 3° downward toward the furnace center.

The reasons are as follows.

- a) To blow in tuyere gas into the lower furnace center to increase heat input there.
- b) To prevent the burnout of the tuyere by turning it downward.
- c) To provide an allowance that will ensure that the tuyere will not turn upward when the furnace lining has expanded to rise upwards.

Fig. 2.5-15 shows the tuyere burnout failure frequency of Kobe Steel Amagasaki No. 2 blast furnace with respect a case where the tuyere was turned 2° to 4° upwards under an anomalous upward expansion of the wall bricks below (repairs were made without waiting a long-time campaign) and a case where the tuyere angle was normal before and after that trouble.

As is evident from Fig. 2.5-15, the upward turn of the tuyere increases the frequency of tuyere burnout failure.

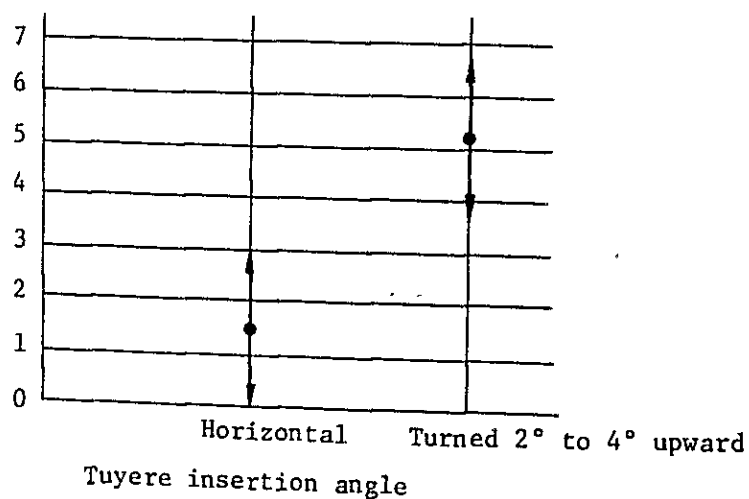


Fig. 2.5-15 Relationship between tuyere setting angle and frequency of burnout failure

(Total number of tuyeres: 16)

iii) That part of the tuyere which is projected from the furnace wall is set at 250 mm for the purpose of protecting the furnace wall lining.

iv) The unit weight of the tuyere is reduced as follows with a view to increasing the efficiency of tuyere replacement work and also reducing the unit cost of tuyere.

650 kg → 110 kg (in case of 120 mmφ tuyere)

v) The outside diameter of the tip of the tuyere is reduced.

Outside diameter: 375 mmφ → 230 mmφ

Area of the vertical cross section of tuyere tip
(in case of 120 mmφ tuyere):-

Existing: $(0.375/2)^2\pi - (0.12/2)^2\pi = 0.099 \text{ m}^2/\text{tuyere}$

Improved: $(0.23/2)^2\pi - (0.12/2)^2\pi = 0.030 \text{ m}^2/\text{tuyere}$

This reduction in tuyere diameter can reduce the tuyere burn-out failure for reasons explained below.

a) Reduction in the area of tuyere to be attacked by molten iron leads to the reduction in burnout failure of tuyere.

b) The cooling water flow speed can be increased on a same supply rate basis, and not only the area exposed to heat, but the amount of heat to be received can be reduced to check the rise of cooling water temperature.

The tip of the tuyere projected into the furnace is exposed unprotected with slag unlike the circumferential parts.

Namely, the tip always bears the brunt of a high heat flux. For example, the tip of the tuyere of Amagasaki No. 2 blast furnace operating at a hot blast temperature of 1,100°C while blowing in 50 kg oil is calculated to receive the heat flux as follows.

$$\begin{aligned} \text{Heat flux: } Q &= k(Q_C - T + Q_G - T) \quad (\text{kcal/m}^2.\text{h}) \\ &= k((441,200 + 2.06(T_T/100)^4)) \quad (\text{kcal/m}^2.\text{h}) \end{aligned}$$

Where, k : the sum of convection heat transfer ratio and radiant heat transfer ratio with radiant heat transfer taken as 1

$Q_{C - T}$: radiant heat from coke to tuyere (kcal/m².h)

$Q_{G - T}$: radiant heat transfer from gas to tuyere (kcal/m².h)

T_T : temperature of tuyere tip exposed to furnace atmosphere (°K)

The tuyere tip is exposed to a high-temperature furnace atmosphere. It is water cooled, and its temperature is comparatively low (150° to 200°C). Hence, the second term in the above equation can be omitted, and we obtain the following approximate formula.

$$Q = 441,200 k \text{ (kcal/m}^2\text{.h)}$$

Calculated in Fig. 2.5-16 from the formula is the relationship between the heat flux and the k -value governing the heat transfer from the furnace atmosphere to the tip of the tuyere. Although the formula is based on assumptions, it shows a good agreement with the actual measurements. The mean heat flux the tip of the tuyere receives is estimated at about 6×10^5 kcal/m².h. Tuyere gas flow is higher the more it goes upward in the tuyere opening. Thus, the k -value is larger in the upper rather than the lower part.

The parts of the tuyere tip experience more heat flux the nearer they go to the upper margin. In order to protect the tuyere from burnout due to the attack by the flow of molten iron, the following measures are needed.

- a) To reduce the cooling water temperature, and to minimize the temperature rise of cooling water due to heat flux incident upon the tuyere tip. (Reduction of surface area of tuyere)
- b) To increase the cooling water velocity.
- c) To increase the cooling water pressure in order to increase the saturation temperature of cooling water.
- d) To make the water passages in the tuyere smooth.

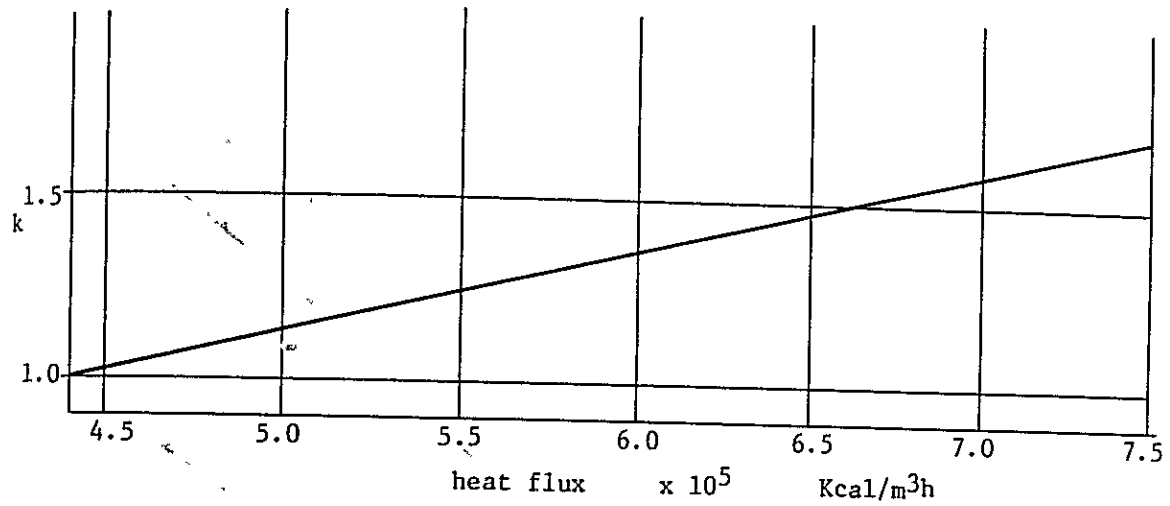


Fig. 2.5-16 Heat flux vs. k-value at the tip of tuyere

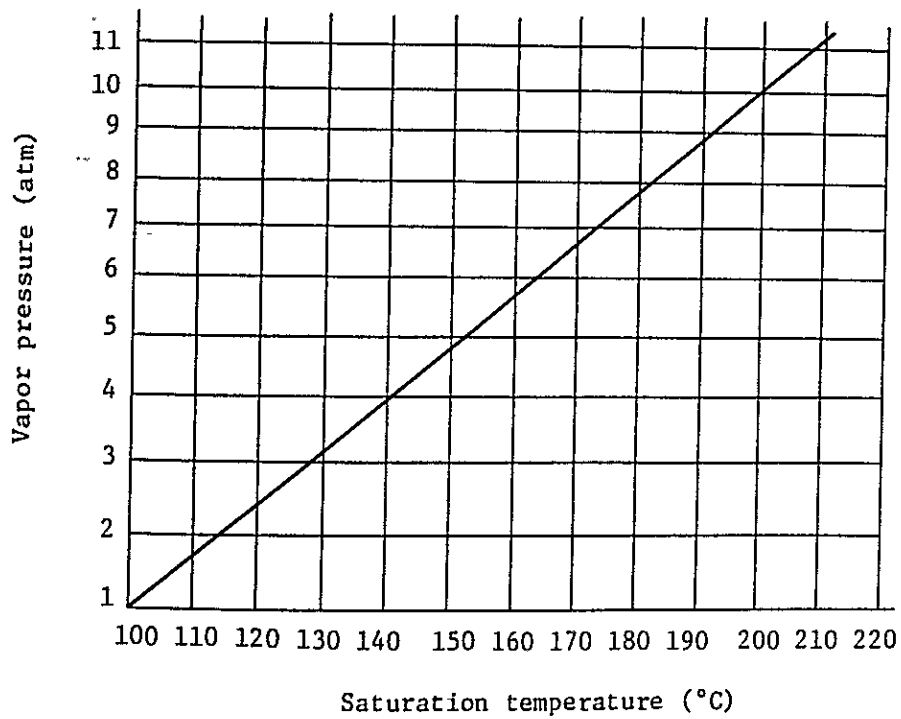


Fig. 2.5-17 Saturation temperature and vapor pressure of water

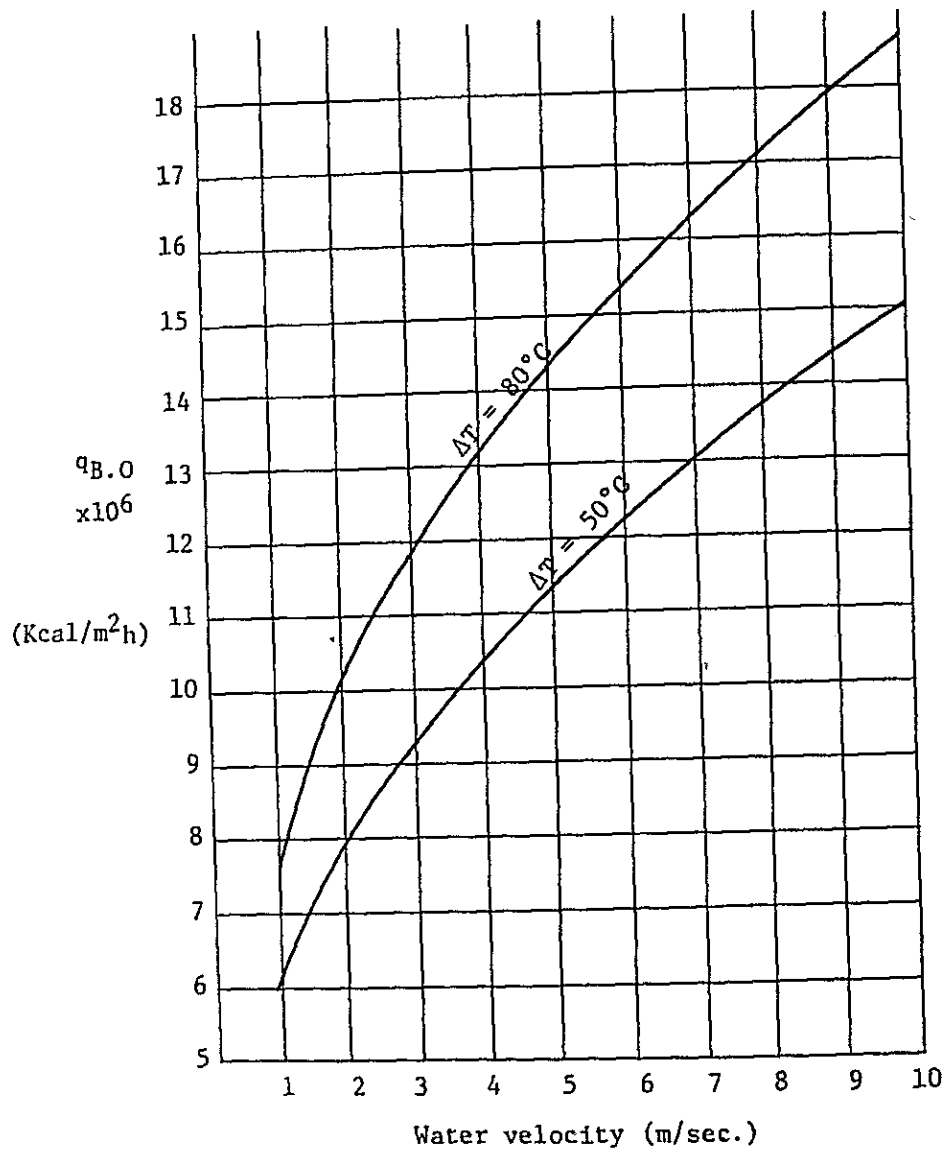


Fig. 2.5-18 Water velocity vs. $q_{B.O}$

In recent years, a double water-cooled tuyere whose tip is put to forced water cooling through a special cooling water passage has come into popular use.

The cooling water pressure used seems to rise more and more. With reference to the tuyere burnout failure, the water velocity, subcooling temperature and critical heat flux hold the relationships given by the following formula.

$$q_{B,0} = (3.5 \times 10^6 + 5.0 \times 10^4 \Delta T)v^{0.4} \quad (\text{kcal/m}^2 \cdot \text{h})$$

Where, ΔT : subcooling temperature (= $T_s - T_l$) ($^{\circ}\text{C}$)

T_l : cooling water temperature ($^{\circ}\text{C}$)

T_s : saturation temperature of cooling water ($^{\circ}\text{C}$)

(For the T_s vs. vapor pressure relationship, refer to Fig. 2.5-17).

v : water velocity (m/sec.)

The relationship between $q_{O,B}$, ΔT and v is given in Fig. 2.5-18. Fig. 2.5-18 demonstrates that increasing ΔT and v is of critical importance in the prevention of tuyere burnout. So far as the present conditions of operation by the COLAR stand, the load on the tuyere is extremely light. But the expected future increase in the blast furnace operating efficiency will also increase the frequency of tuyere trouble.

How to extend the service life of tuyere will therefore become an important issue in the future.

2.5.6 Structural design of cinder notch

As already discussed, the COLAR's slag ratio is extremely high. Discharging quantities of slag from the tap hole will make it hard to carry out the tapping and also will erode the tap hole clay seriously.

The slag should be flushed off through the cinder notch so far as the circumstances permit. As shown in the recommended plan for blast furnace profile in Fig. 2.5-7, the cinder notch level is lowered by 100 mm in order to guide as much slag as possible into the cinder notch.

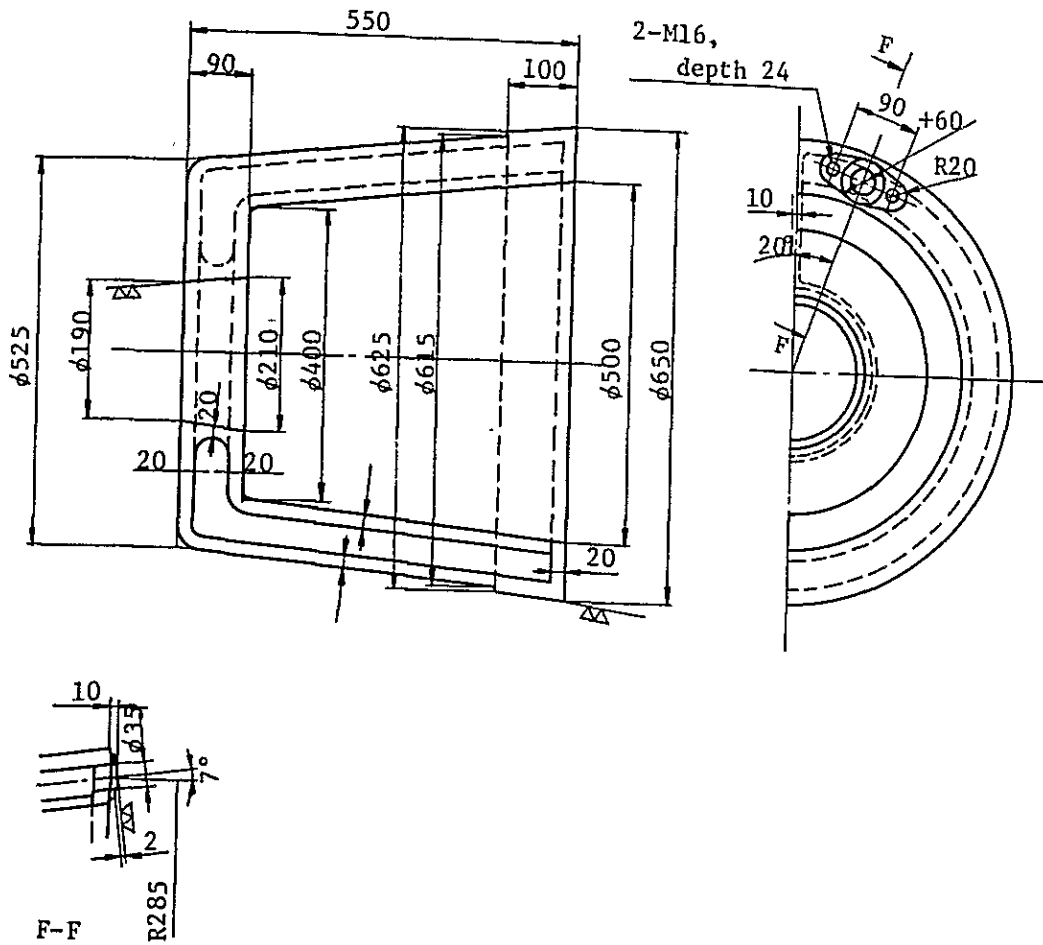
The slag passage in the cinder notch cooler is lined with a stamping material as illustrated in Fig. 2.5-20 for the purpose of protecting the cinder notch cooler from burnout failure by molten iron which sometimes leads to a serious plant fault. The cavity diameter of the existing cooler is too small, and is increased to 400 mm ϕ at the tip (see Fig. 2.5-19) so that the stamping may be feasible.

2.5.7 Furnace cooling

(1) Reinforcement of tap hole with a cooling box

The lining of the tap hole is damaged seriously by every tapping operation. Its cooling should therefore be more intensified than any other parts for the purpose of extending the lining service life. The COLAR should not miss inserting the cooling boxes on the occasion of the next repair. The cooling box is of a totally enclosed type made of copper. The dimensions of the cooling box are shown in Fig. 2.5-21, and the layout in Fig. 2.5-22.

a) Cinder notch cooler



b) Cinder notch tuyere

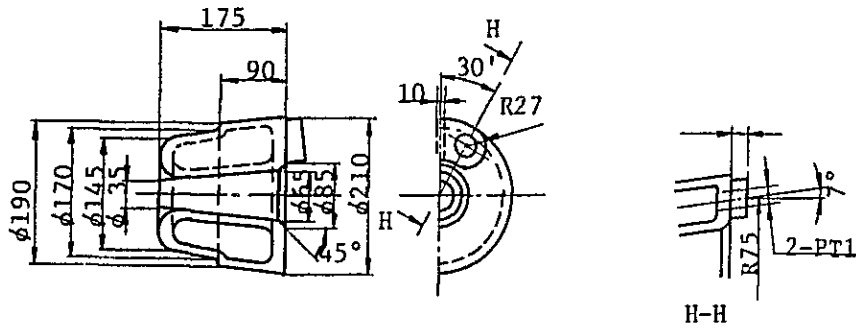


Fig. 2.5-19 Cinder notch tuyere and cooler

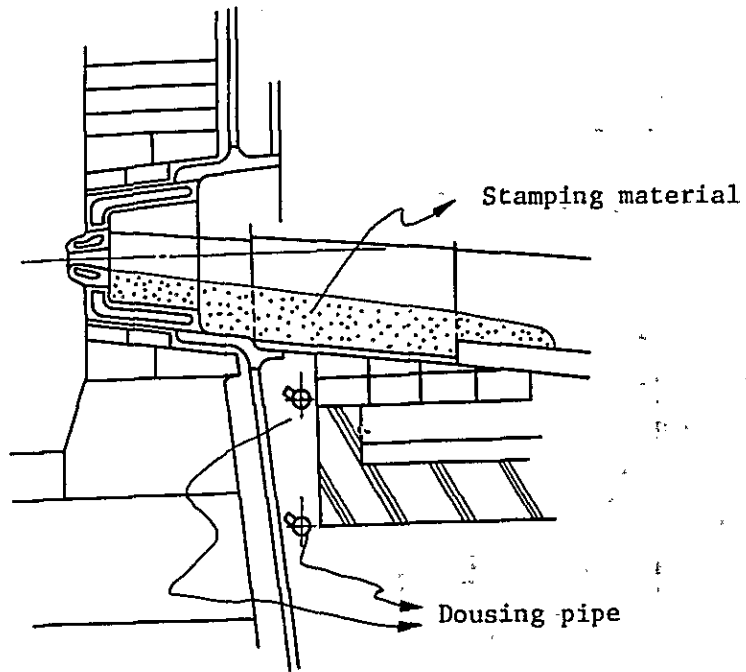
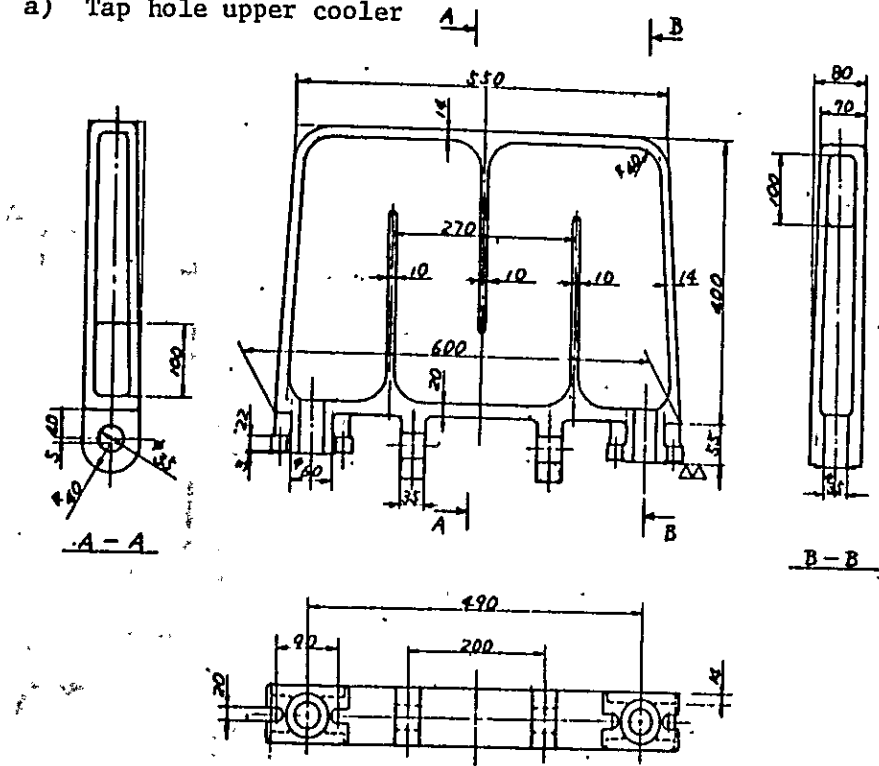


Fig. 2.5-20 Cinder notch and its surroundings

a) Tap hole upper cooler



b) Tap hole side cooler

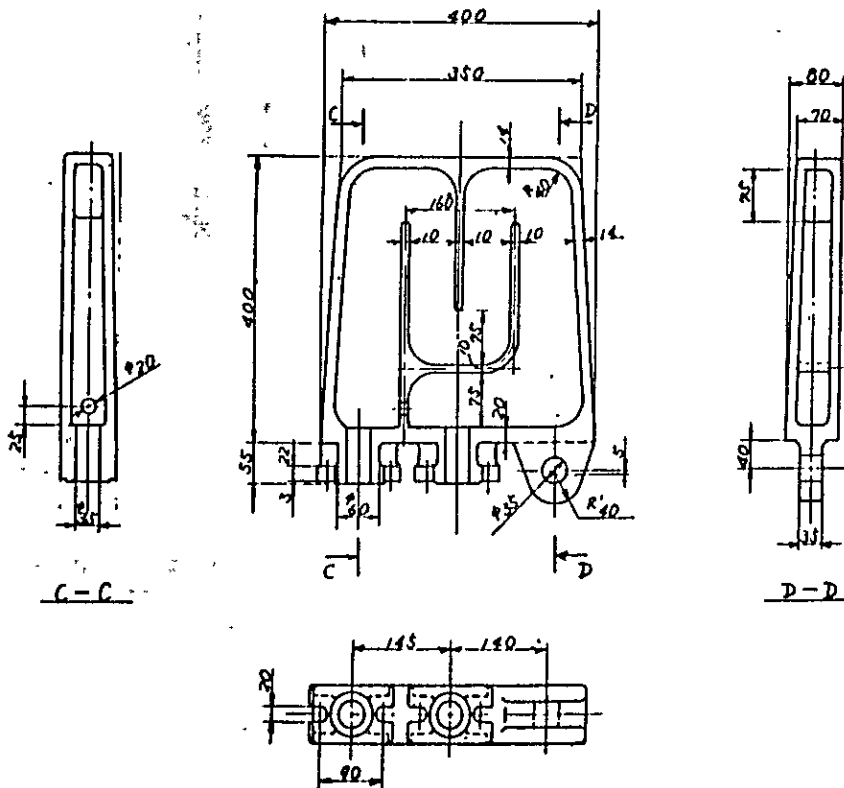


Fig. 2.5-21 Tap hole cooler

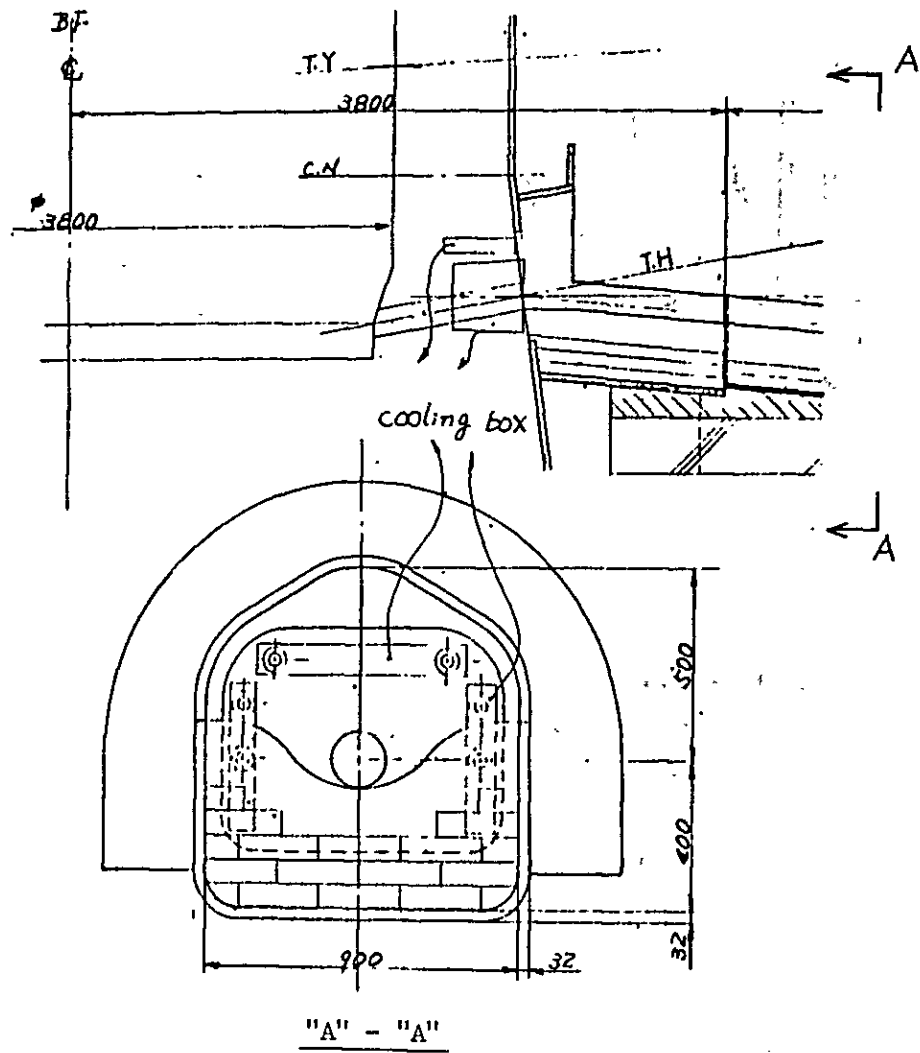


Fig. 2.5-22 Layout of cooling boxes around the tap hole



(2) Cooling for the linings of bosh, belly and shaft

The steel cooling box is unreliable as it is subject to corrosion and water leakage at the welds, and to thermal deformation and oxidation, and therefore is superseded by a cast iron one. Major improvements incorporated in the design this time are as follows.

- i) The cooling box insertion level is lowered by 300 mm in order to protect that part above the bosh which has a large thermal load.
- ii) The number of circumferential cooling boxes is increased from the present 16 to 20 for that part below the belly which has a high thermal load.
- iii) Cooling boxes are set in the upper and middle zones of the shaft for the purpose of cooling the lining and at the same time preventing the slumping of lining bricks. The number of cooling boxes per unit area is less the higher they go up. This is for the purpose of preventing the formation of encrustations due to intensified cooling.
- iv) As illustrated in Fig. 2.5-23, a packing is set between the furnace mantle and cooling box in order to prevent gas leakage.

(3) Intensified dousing on the shell

- i) Intensified dousing on the tap hole and below the cinder notch.
- ii) Intensified dousing on the bosh.
- iii) Intensified dousing on the hearth mantle.

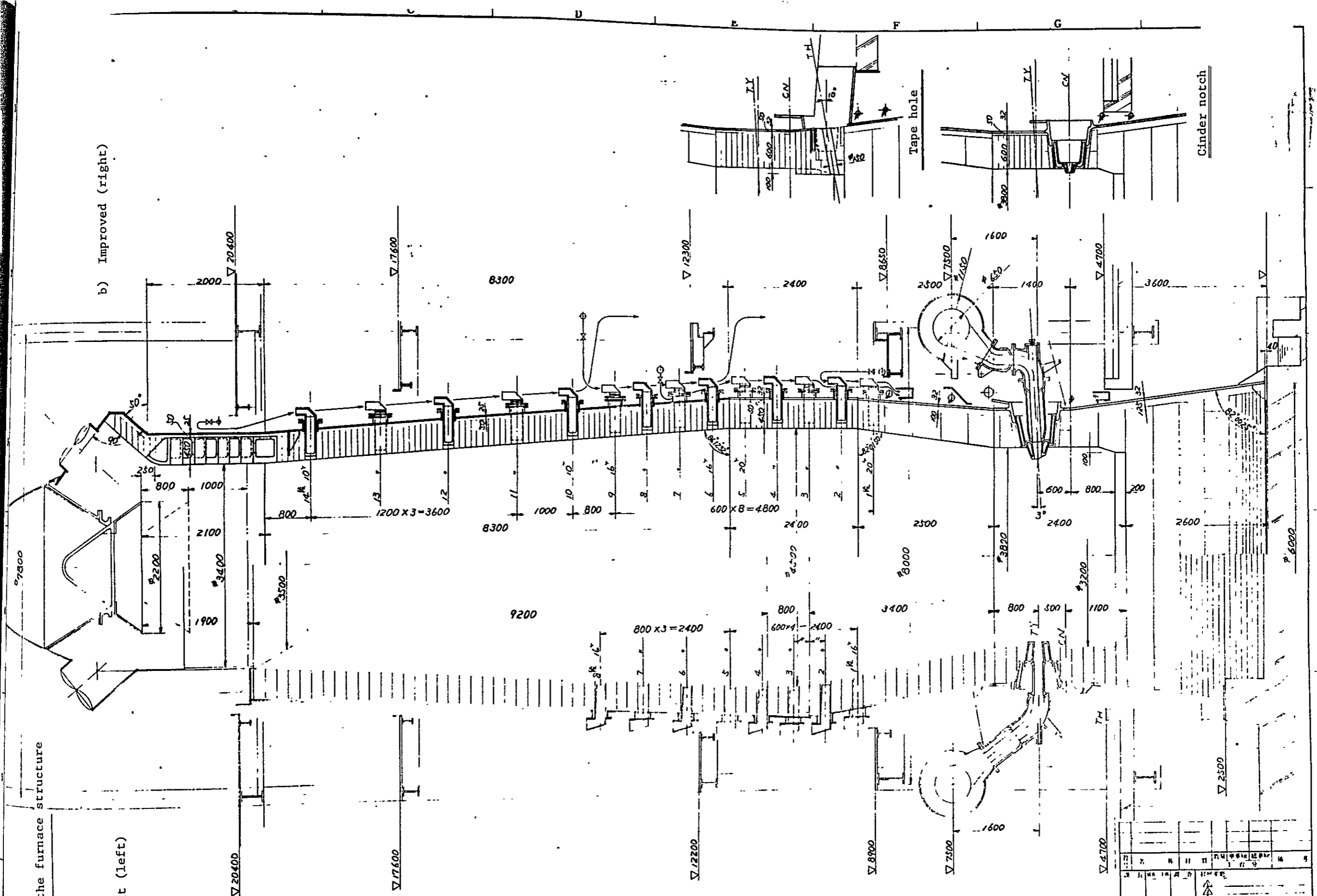
[Note] See Figs. 2.5-20, -22 and -23.

Fig. 2.5-24

Overall view of the furnace structure

b) Improved (right)

a) Present (left)



设计	审核	校对	制图	日期	比例
设计	审核	校对	制图	日期	比例
设计者: <i>K. Kobayashi</i> 审核者: <i>Y. Yamamoto</i> 日期: 1961. 11. 11 比例: 1:1			设计单位: COLOMBIA COLAK 社 设计项目: BF 全体检讨图		
1 04367					设计所: 神户製鋼所 设计者: 尾崎 隆夫



2.6 Blast Furnace Wall Refractories

2.6.1 The mechanism that erodes the furnace wall refractories

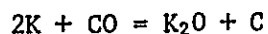
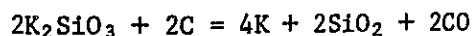
The blast furnace is a vessel in which spectra of temperatures, gas compositions (incl. volatiles), gas pressure, loads and reactives are seen both vertically and horizontally to demonstrate a microcosm of thermodynamics and chemistry.

Table 2.6-1 lists the major causes of refractory damage and the requirements of refractories to overcome them. The refractories should be selected to meet specific conditions which exist where they are used. The furnace wall erosions are most noticeable in the middle and bottom zones of the shaft and in the upper zone of the bosh. Particularly, the lower part of the shaft and the belly are vulnerable to wear.

The temperature of the gases flowing over their inner walls is lower than 1,000°C and not so high, but alkali and zinc vapor react with each other to corrode the lining.

Alkali sources entering the blast furnace include iron ore and coke. Fig. 2.6-1 shows the contents of Na₂O and K₂O in the iron ore and coke. Generally speaking, the iron ore contains more K₂O than Na₂O as shown in Fig. 2.6-1. This holds true of the coke.

Alkalies in the charges exist in the form of alkali silicates. By reduction, they are transformed into alkali vapor, which is then oxidized by CO into alkali carbonates, alkali silicates or alkali aluminates.



There is not so large a difference in quantity between Na₂O and K₂O to be charged into the furnace.

But, thermodynamically, the potassium is more unstable and liable to be vaporized and transformed into recirculatory alkalies than Na₂O. Naturally, the furnace tends to have more of potassium.

On the other hand, Na₂O is liable to be trapped in the form of glass phase under the influence of CaO and MgO, and is discharged together with slag. Fig. 2.6-2 shows an alkali distribution in the blast furnace.

Table 2.6-1 Major causes of damage on the blast furnace refractories, and the requirements of refractories to provide against them

Section	Major causes	Requirements of refractories
Below wearing plate	<ul style="list-style-type: none"> ◦ Collision with falling charges; abrasion due to upward flow of dust-laden gases 	<ul style="list-style-type: none"> ◦ High abrasion resistance ◦ Low porosity, high strength ◦ High thermal shock resistance
Upper and middle zones of shaft	<ul style="list-style-type: none"> ◦ Abrasion and damage due to falling charges ◦ Deposition of carbon dissociated from CO₂ gas ◦ Deposition of zinc 	<ul style="list-style-type: none"> ◦ High abrasion resistance ◦ Low porosity, high strength ◦ High resistance to CO₂ gas ◦ High thermal shock resistance
Lower shaft; belly; bosh	<ul style="list-style-type: none"> ◦ Deposition of carbon dissociated from CO₂ gas ◦ Alkali reactions in gaseous and liquid phases ◦ Erosion due to slag and molten iron ◦ Deposition of zinc 	<ul style="list-style-type: none"> ◦ Low porosity, low permeability ◦ High alkali resistance ◦ High corrosion resistance ◦ High thermal conductivity ◦ High resistance to CO₂ gas
Around tuyere; at tap hole	<ul style="list-style-type: none"> ◦ Erosion due to slag and molten iron ◦ Gas leakage ◦ Spalling due to expansion and contraction 	<ul style="list-style-type: none"> ◦ High erosion resistance ◦ High thermal shock resistance ◦ High structural stability
Furnace bottom	<ul style="list-style-type: none"> ◦ Erosion due to slag and molten iron ◦ Slackening of bricks ◦ Damage on joints 	<ul style="list-style-type: none"> ◦ High erosion resistance ◦ High volumetric stability under hot conditions ◦ Low porosity and low permeability

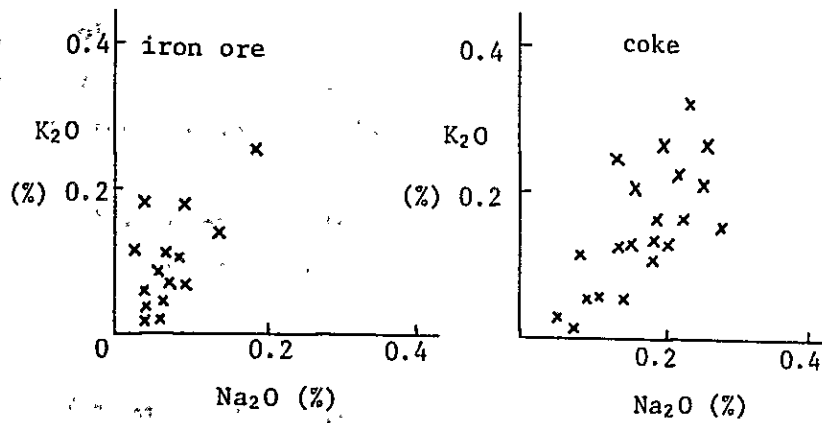


Fig. 2.6-1 Contents of Na₂O and K₂O in iron ore and coke

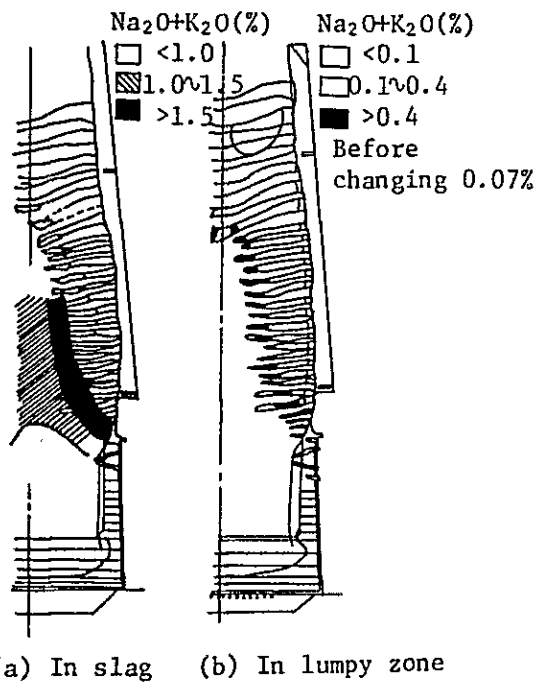


Fig. 2.6-2 Distribution of alkali in blast furnace, Nippon Steel, Hirohata Works, No.1 B/F [from Tetsu to Hagane, 62 (1976), p.94]

The furnace charges adsorb alkali while descending through the furnace, and when having reached a high temperature zone in the lower part, release alkali because of reduction and gasification. In this way, alkali circulates within the furnace. However, at the time of tapping and slag flushing, the alkali nearly equal to that charged is discharged.

The alkali is adsorbed into the furnace wall bricks as illustrated in Fig. 2.6-3 as it circulates through the blast furnace.

When $Al_2O_3-SiO_2$ refractories are turned into silicates upon reaction with alkali, they expand and crack.

This is because mullite ($3Al_2O_3-2SiO_2$), Al_2O_3 , and other minerals of which the refractories are composed are turned into K_2O -base minerals of low specific gravity.

Table 2.6-2 Volumetric change due to conversion into alkali silicates

	Specific gravity	Volumetric change	
Mullite ($3Al_2O_3 \cdot 2SiO_2$)	3.03	Mullite → $K_2O \cdot Al_2O_3 \cdot 2SiO_2$	16.9%
Corundum ($\alpha-Al_2O_3$)	4.00	Mullite → $K_2O \cdot Al_2O_3 \cdot 4SiO_2$	22.6%
Quartz (SiO_2)	2.65	Mullite → $K_2O \cdot Al_2O_3 \cdot 6SiO_2$	10.2%
Cristobalite (SiO_2)	2.33	Corundum → $K_2O \cdot 11Al_2O_3$	17.2%
Kalsilite ($K_2O \cdot Al_2O_3 \cdot 2SiO_2$)	2.59	Quartz → K_2O-SiO_2 family glass	20.4%
Leucite ($K_2O \cdot Al_2O_3 \cdot 4SiO_2$)	2.47	Cristobalite → K_2O-SiO_2 family glass	5.9%
Sanidine ($K_2O \cdot Al_2O_3 \cdot 6SiO_2$)	2.75	Volumetric change, % = $(1/dA - 1/dB) / (1/dA) \times 100$ Where, dA: specific gravity of mineral before transmutation dB: specific gravity of mineral after transmutation	
β -Alumina ($K_2O \cdot 11Al_2O_3$)	3.31		
K_2O-SiO_2 family glass	2.20		
K_2O-SiO_2			

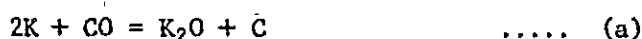
The siliceous bricks having a high $\text{SiO}_2/\text{Al}_2\text{O}_3$ ratio show a fair strength against alkali, while high-alumina bricks and clay bricks are susceptible to swelling and crumbling under the attack of alkali. As against Na_2O , high- Al_2O_3 bricks are sturdy against burnout failure. On the other hand, clay bricks which has a comparatively high content of SiO_2 are vitrified when attacked by Na_2O , and check penetration of Na_2O , but are highly vulnerable to fusion loss as nepheline and carnegieite are produced.

To sum up, high-alumina brick of low porosity burned at high temperatures is preferable for reducing the brick trouble due to Alkali attack.

As compared with clay brick, it is excellent in corrosion resistance by nature and also in that the penetration of alkali can be limited to around exposed pores.

Silicon carbide brick is a little better in anti-alkali property than high-alumina brick. The blast furnace gas contains CO by 30 to 40%, and carbon liberated from CO is also considered as an active contaminant destroying furnace refractories.

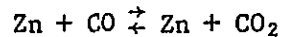
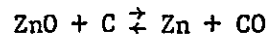
The cracking reaction of CO gas is as follows.



The reaction represented by the formula (b) takes place at as low a temperature as around 500°C because of a catalytic effect of iron oxides.

The reaction (b) is invigorated with increase in temperature from 600°C to $1,000^\circ\text{C}$, liberating quantities of carbon. As shown in Fig. 2.6-3, the circumstances will be well understood from the correlation between K_2O distribution and C distribution. The bricks contain iron oxides, little though they are. These iron oxides are inactivated by burning in the brick-making process. However, when attacked by alkali, they are again activated, and the reaction (b) takes place in lateral sections where the temperature is around 500°C . The free carbon grows around catalytic particles, exerts a high segregation pressure which causes local rupture and cracking.

Zinc also exists in the furnace charges in the form of oxides though its content is very small. When getting in contact with CO gas in the temperature range of 1,000°C to 1,200°C, zinc is reduced and vaporized. The reaction is as follows.



The metallic zinc ascends together with furnace gas, and is oxidized in the low-temperature zones and fall together with furnace charges. In this way, zinc moves up and down in the blast furnace just as alkali does. Fig. 2.6-4 illustrates a distribution of Zn in the furnace.

In the circulating process, part of zinc is fixed into the joints or body of the brick, and starts liberating carbon to a less degree than alkali. The zinc itself also expands and wedges its way into the brick. Figs. 2.6-5 and 6 show the relationships between K_2O , ZnO , and liberated carbon.

The contact between furnace walls and slag takes place in the high-temperature zones below the bosh.

Because molten slag contains alkali less, the alkali corrosion is scarcely. But the refractories in such zones necessitate a high resistance against erosion due to molten slag. The major causes of damage on the refractories in the bosh and around tuyeres are abrasion due to charges and blast, erosion due to slag, thermal shocks and vibration. The rate of the loss of the refractories in the bosh is particularly high as shown in Fig. 2.6-7.

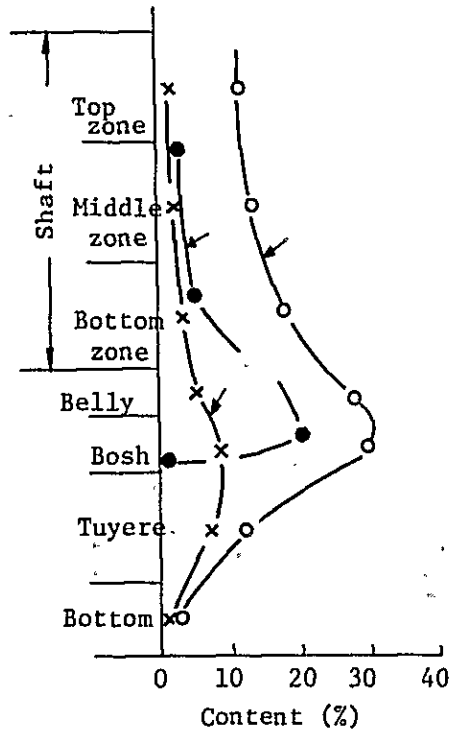


Fig. 2.6-3 A distribution of alkali and carbon in the surface layer of bricks after use

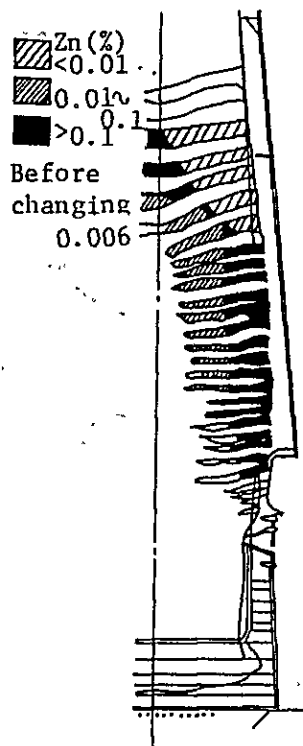


Fig. 2.6-4 Distribution of zinc in the blast furnace (Hirohata No.1 blast furnace) (from Tetsu to Hagane, 62 (1976), p95)

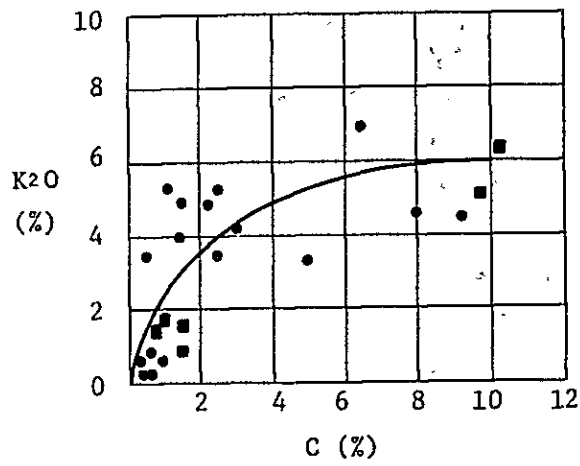
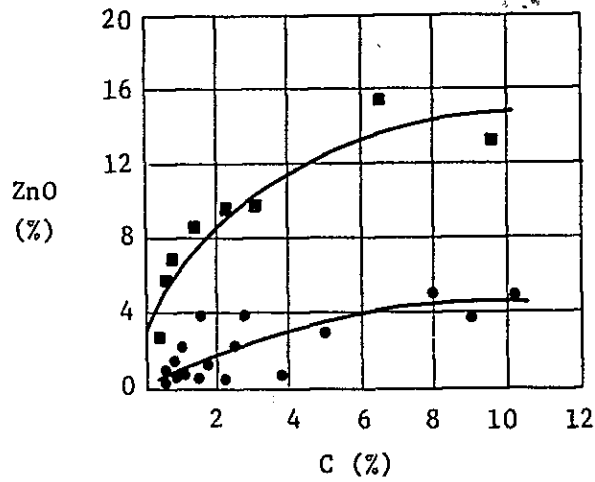


Fig. 2.6-5 Relationship between carbon and K₂O in the bricks of denaturalized blast furnace



- Layer exposed to heat.
- Denaturalized layer at the back

Fig. 2.6-6 Relationship between carbon and ZnO in the bricks of denaturalized blast furnace
2.6-8

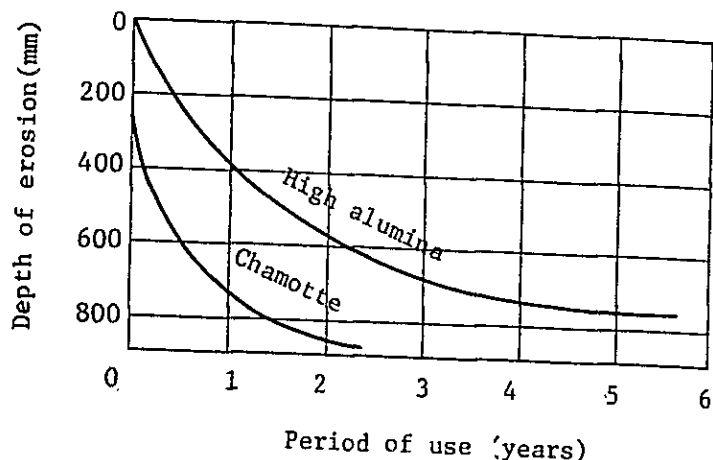


Fig. 2.6-7 Erosion speed of the bricks in the bosh (calculated example)

The major causes of damage on the refractories in the furnace bottom include the penetration of molten iron into the brick joints, the coming-afloat of bricks due to contraction and cracking, and erosion due to slag and molten iron.

2.6.2 Evaluation of the present Nelly from the viewpoint of lining

The causes for the slumping of shaft lining cannot be identified clearly for want of data, including a time record of shaft temperature until slumping, initial quality of bricks, and samples showing the erosion of bricks.

So far as the thermal deformation of shell stands, it is unlikely that an extremely exacting overheat has taken place in the furnace walls. It is also surmised from the deformation in the upper part of the shaft shell that the lining may have not been subjected to an abnormal expansion.

While the causes of the trouble remain unidentified, the insertion of cooling boxes on the occasion of next repair as discussed in the foregoing paragraphs will prevent the slumping of bricks mechanically and at the same time will go a long way toward checking the bricks from denaturalization.

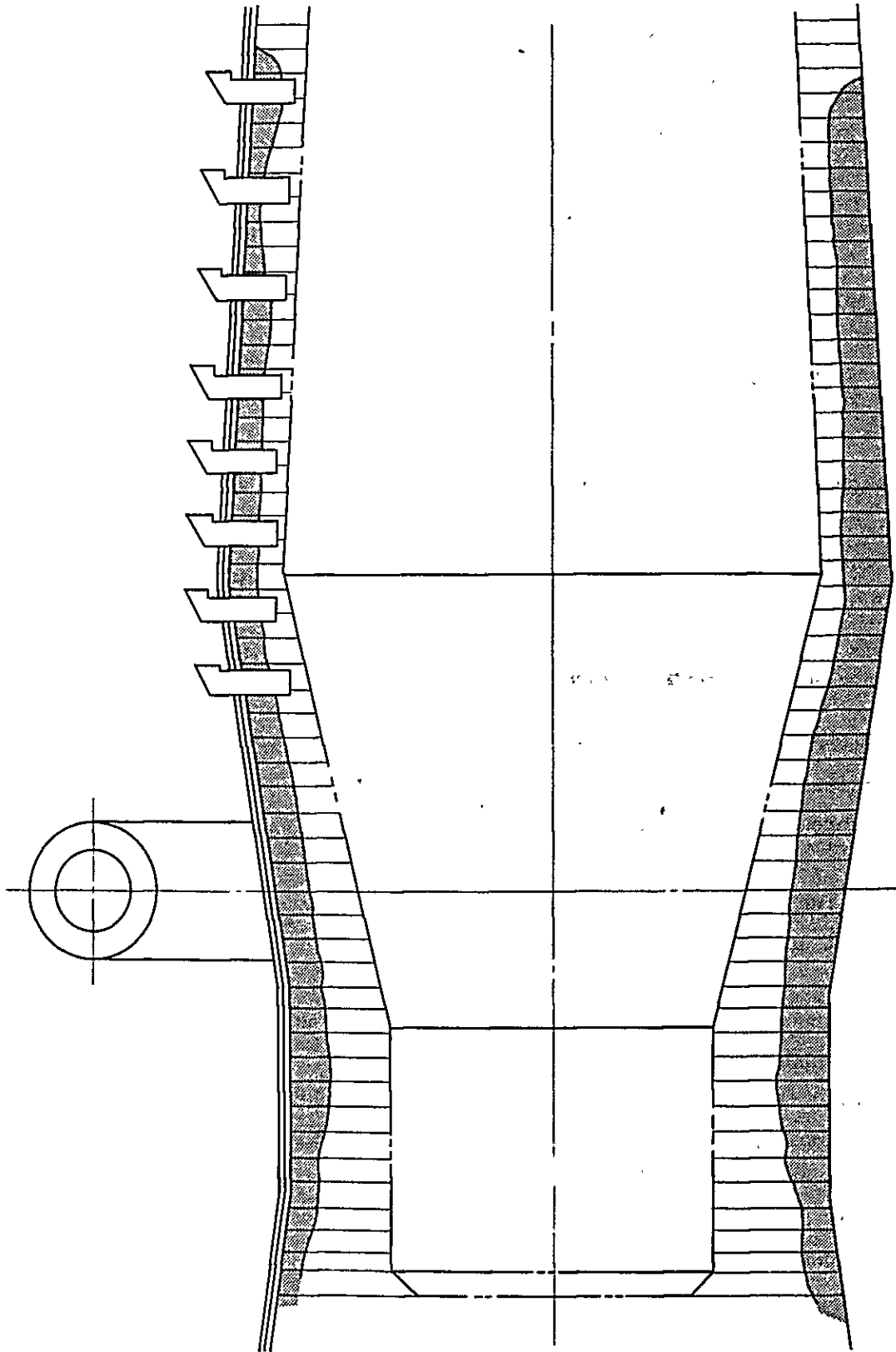


Fig. 2.6-8 A sketch showing the brick walls remaining in the Nelly

As regards the loss of the linings in the shaft, belly and bosh which are subject most to erosion and corrosion, the Nelly is surprisingly in shape for its five and odd years of operation. This may be due to the fact that the hearth diameter is smaller as compared with the belly diameter as discussed in Sec. 2.5 and that the production rate has been low.

The life expectancy of these parts will be considerably long. However, the hearth wall lining has been damaged seriously to an almost dangerous degree, and the following should be studied, accordingly.

- i) Was the brick property proper?
- ii) Was the dousing on the hearth mantle enough?
- iii) Was the material used in blocking the tap hole proper?
(Tap hole and its surroundings are worn out seriously.)

2.6.3 Forecast of furnace life after emergency repairs, and the measures to be taken in the future

The emergency repairs this time are significant as:

- i) the slumping of the shaft lining from below the wearing plate will affect the furnace productivity;
- ii) the loss of lining from the bottom will govern the furnace campaign.

What the COLAR must set store by after recommissioning will be the protection of the hearth sidewall lining.

Fig. 2.6-9 shows the repaired lining in the furnace bottom.

Kobe Steel has no experience in this kind of repair, and cannot foretell the furnace life either.

For the purpose of obviating emergency shutdown, the COLAR should make all possible preparations for the major repairs in good time.

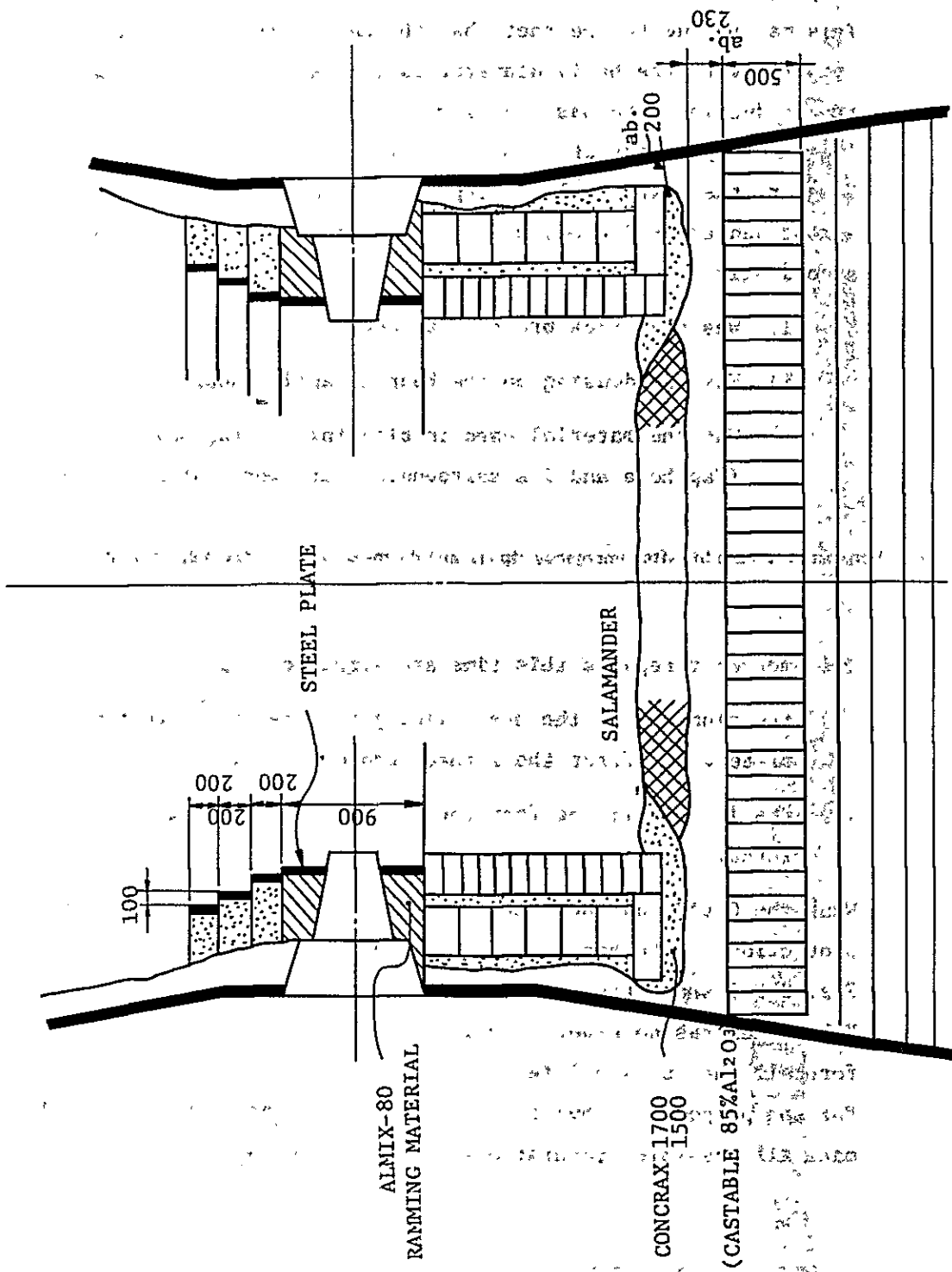


Fig. 2.6-9 Repaired furnace bottom linings

While it is quite understandable that the repairs this time have experienced hardships because of difficulty in procuring materials, they are far from being tolerated so far as our experience dictates. The problems involved in the workmanship are as follows.

Problems

- i) There are great possibilities that the thermal change in the remaining bricks will lead to breaking the joints apart and causing cracks.
- ii) The compatibility of the quality of the bricks used for reinforcement (borrowing of hot stove bricks, for example) and the control of joint widths with reference to the brick shapes are dubious.
- iii) Whether or not the removal of low-fusion point slag encrusted upon the surfaces of the remaining bricks has been perfect. (particularly from the joints of the reinforcing bricks)
- iv) Use of castables
 - a) Slow-heating is necessary in the dehydrolytic region (500°C to 600°C). In the heating-up of the blast furnace, the slow-heating is very hard, and the cracking is a high probability.
 - b) Because of high porosity, the castables are highly susceptible to seepage of slag and molten metal and also to structural spalling.
 - c) The cohesion with the existing line is concerned about.
- v) As illustrated in Fig.2.6-9, the hearth walls are retained by the tuyeres. The tuyeres are not fixed to the furnace body, and are liable to get slackened.
- vi) What has been left of the bricks in the hearth shows serious damage.

The survey mission cannot warrant or forecast the life of the furnace. The COLAR is therefore requested to provide various recommended measures end-to-end for the purpose of extending the furnace life.

Measures to extend the furnace life

- 1) Intensified cooling of the surroundings of tap hole and cinder notch. For the dousing around the tap hole, refer to Fig. 2.6-10.

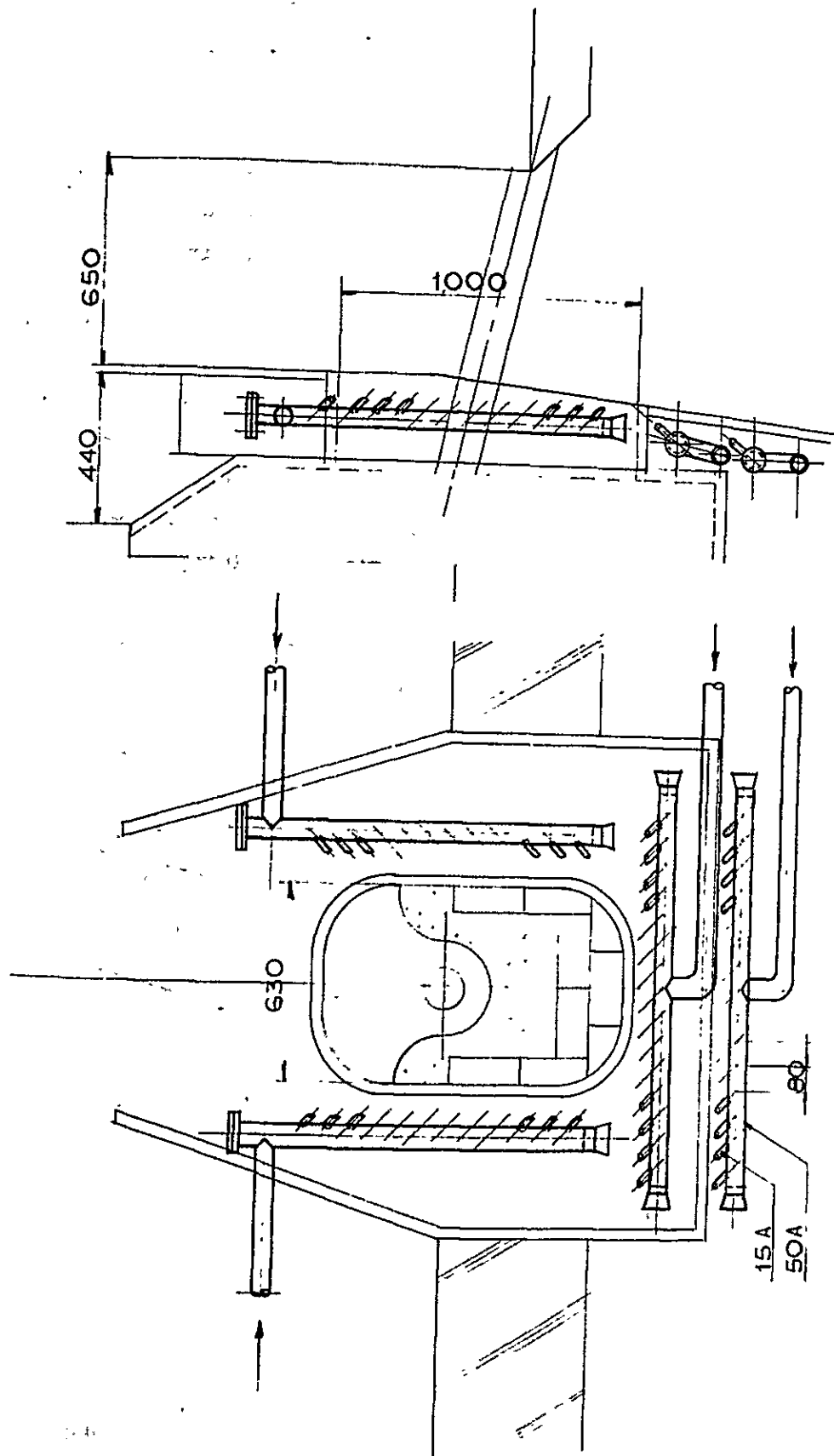


Fig. 2.6-10 Arrangement of dousing cooler around the tap hole

- 2) Intensified cooling of hearth mantle (see Fig. 2.5-23), and removal of iron oxides and other foreign objects from the mantle surfaces for the purpose of increasing cooling efficiency. The intensified cooling of the mantle will shift the solidifying temperature line (1,150°C) of iron toward the furnace center, protecting the walls from the attack of molten iron.
- 3) Increasing of the tap hole depth. To this end, it is necessary to make efforts to channel the slag out through the cinder notch alone for the purpose of minimizing the loss of the tap hole blocking material due to slag. It is also required to improve the quality of tap hole blocking material. At present, the level of the tap hole is extremely low. If the COLAR continues this situation, the lining around the tap hole and the shell might possibly be fail.

Fig. 2.6-11 shows a comparison between Japanese furnaces and COLAR's in relation to furnace capacity and tap hole depth.

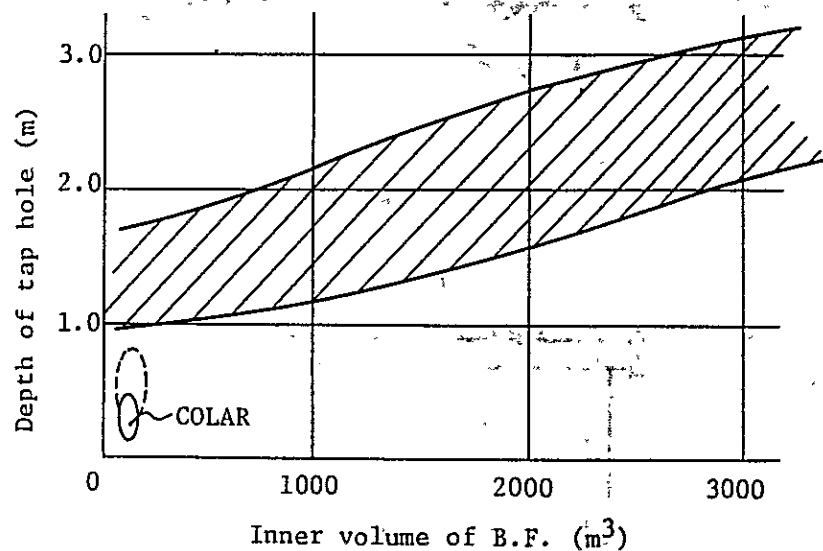


Fig. 2.6-11 Comparison between Japanese furnaces and COLAR's in relation to furnace capacity and tap hole depth

Tap hole blocking material

Required characteristics of tap hole blocking materials

a) Workability

The blocking material must facilitate filling and breaking. The mud should be as hard as can be permitted by the mud gun. It should be noted that even the same material (same in terms of composition and grain size) shows different hardnesses depending on the mixing time and storage period. In such a case, the mud should preferably be on the soft side. (See Fig. 2.6-12)

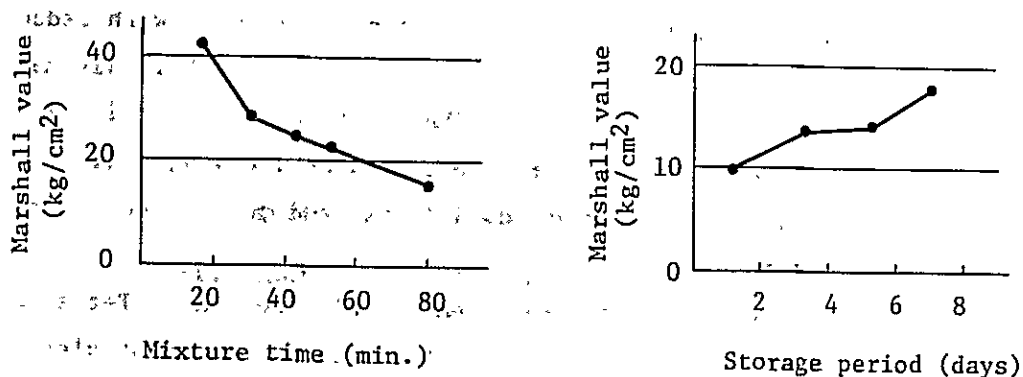


Fig. 2.6-12 Mud hardness vs. mixing time and storage period

The mud which lacks volatile components and water becomes hard. This kind of mud shows a high filling density, and is highly resistant to corrosion because of low porosity.

b) Sintering property

The faster the sintering speed, the better. The sintering speed should be determined to meet the tapping cycle.

If the sintering is insufficient, premature blow-out may take place, jeopardizing the work in the cast house.

The factors determining the sintering speed include moisture content, volatile component, grain size and chemical composition of the material. Excess moisture will impair the sintering property of the mud and reduce the corrosion resistance.

Table 2.6-3 shows the relationships between moisture content and physical properties of the mud.

Table 2.6-3 Relationships between moisture content and physical properties of mud

Moisture content (%)	Apparent specific gravity	Bulk density	Apparent porosity (%)	Compression strength (kg/cm ²)	Tapping time (min)
2.0	2.38	1.55	35.0	95	96
2.3	2.36	1.52	35.3	94	86
2.7	2.36	1.51	35.9	90	79

In Table 2.6-3, the tapping time is extended with reduction in moisture content; this means that so much is discharged from the blast furnace. The volatile component is closely related to the sintering property of the mud, filling density after sintering, durability, and occurrence of premature blowout, etc.

The volatile component stems mainly from tar. Tar should preferably be the one that contains as little naphthalene as possible. Naphthalene leaves no dry residue, but sublimes totally, thus making the mud porous and weak in strength.

c) Corrosion resistance

The mud is required to be chemically stable against molten slag and iron and at the same time resistant against abrasion. The lower the porosity, the higher the corrosion resistivity the mud has. The porosity has much to do with the grain size distribution of the materials mixed and the dose rate of tar. Generally, the more the volatile component the mud contains, the poorer its porosity.

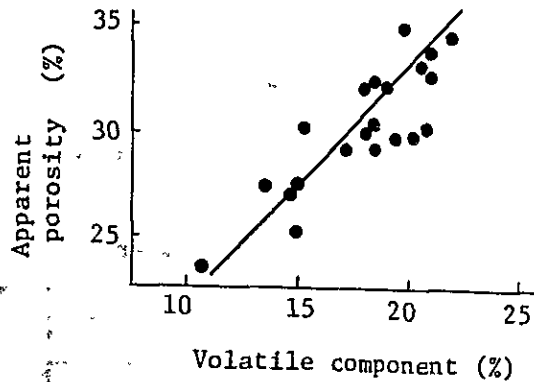


Fig. 2.6-13 Relationship between volatile component and apparent porosity

- d) Important subjects concerning mud production control
- i) Control of refractory materials, coke composition, grain size and moisture content
 - ii) Control of physical properties of tar
 - iii) Mix proportion and mixing order
 - iv) Adjustment of mixing time, temperature and hardness
 - v) Product hardness, moisture content, storage time, etc.

Introduction to the production of mud for Amagasaki No.1 blast furnace

a) Properties of materials used

Table 2.6-4 Properties of materials used

		Clay powder	Chamotte powder	Coke powder		Tar
Chemical composition	Ig. loss	13.78%	2.37%	-		C. 90%
	SiO ₂	55.24	59.60	Ash analysis	53.52	H. 5
	Al ₂ O ₃	29.58	35.51		26.91	N. 0.75
	Fe ₂ O ₃	1.20	1.86		8.05	S. 0.37
	SiC	-	-	ash.	12.62	O. 2.98
	FC	-	-	VM.	1.31	
				FC.	86.07	
	Moisture content	7.2	4.0	12.0		0.2
	24 meshes up	5	21.6	4 meshes up 7		Specific gravity 1.1
	24~48 meshes	25.4	27.1	4~8 meshes 8.9		
	48~200 "	31.2	12.8	8~35 " 52.2		
	Under 200 meshes	38.4	38.5	35~200 " 31.6 Under 200 meshes 5.6		
	Refractoriness	32	32	-		-

b) Mixing conditions

Table 2.6-5 Mixing

	Coke powder	Chamotte powder	Coke powder	Tar	Total
Weight (kg)	120	120	175	112	527
Ratio (%)	22.8	22.8	33.1	21.3	100

c) Mixing operations

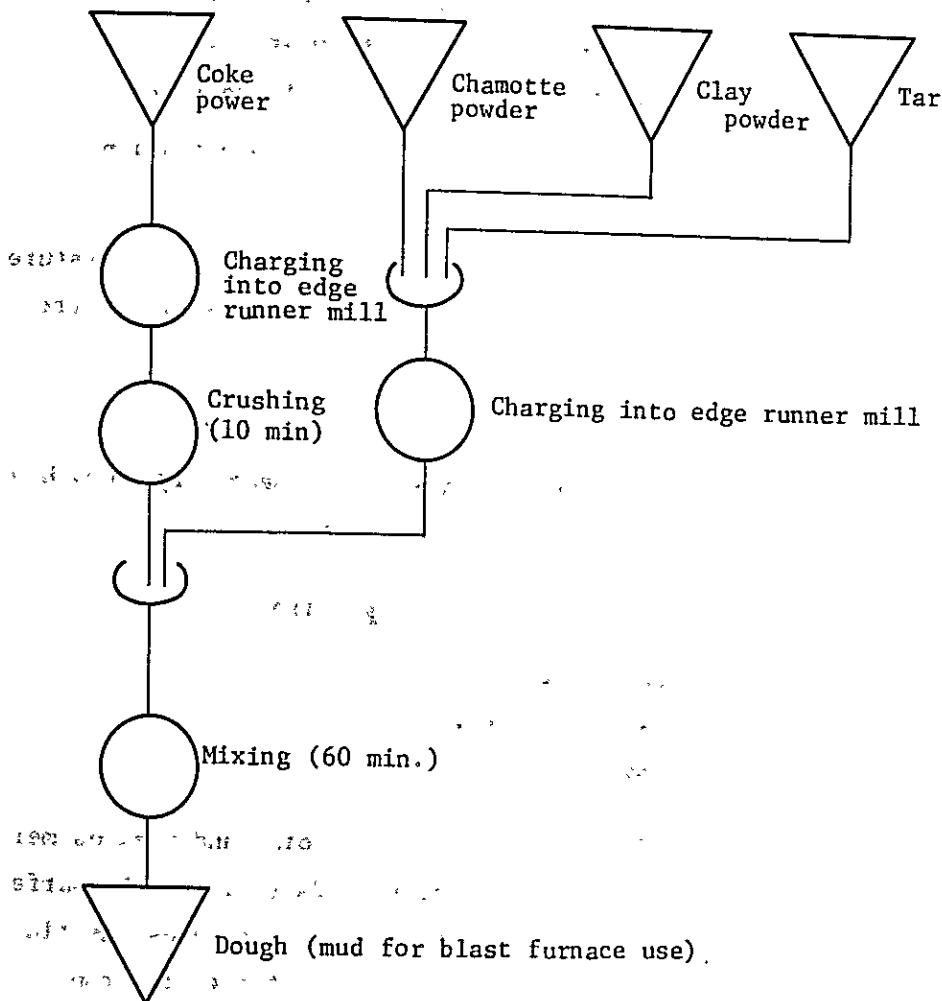


Fig. 2.6-14 Mixing work flow chart

The moisture content in the mud is in the range of 0.1 to 0.2%; namely, each component additive should be dehydrated and dried. The dough should be used in 3 days after production. Since the mud contains tar, it should be handled as a hazardous material from the viewpoint of safety engineering.

4) Pig iron composition

Where it is required to operate a blast furnace whose bottom lining is seriously damaged, utmost care should be paid to the properties of the pig iron to be smeltered.

The desired properties of the pig iron are as follows.

- a) The pig iron should have a higher surface tension so that it may not enter a narrow crack.
- b) The pig iron should have a high solidifying temperature, and should liberate carbon as much as possible in the basin.
- c) The pig iron should have a high viscosity.

To achieve these characteristics, it is necessary to reduce S and P and increase Si a little higher.

Desirable chemical composition of pig iron

S: less than 0.02%

P: The less the better.

Si: more than 2.5%

P : Produces phosphorus eutectoids and reduces melton temperature. Also, P tends to lower the surface tension of the pig iron and increases the fluidity in the solidifying process of the pig iron.

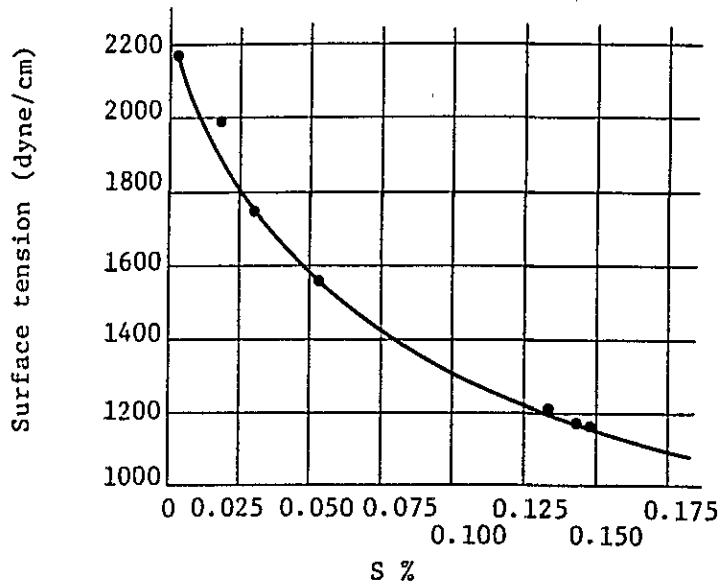
S : Reduces the surface tension pronouncedly (see Fig. 2.6-15). For the purpose of preventing the pig iron fretting into narrow crazes, sulfur should be reduced.

Si : Increase in Si content works to shift the eutectic point of Fe-C family materials toward low C side and sends up the solidifying temperature.

Reduction: Improvement in the indirect reduction ratio in the blast furnace leads to the reduction in FeO content in the fusion and reduces the loss of C in the molten metal.

Where the operating conditions make the temperature of molten metal at the tuyere level high, the molten metal of high carbon saturation will drip into the basin cooled down from around while liberating C. Thus, the protection of the furnace bottom lining is promoted.

If the molten metal has a higher C content compared with Si, Sc-value will increase; when the molten metal of 1,300°C to 1,450°C is flowing while solidifying, its run of length will decrease with increase in Sc if it is hypereutectic ($Sc \geq 1$).



2.6-15 Relationship between S and surface tension of molten metal

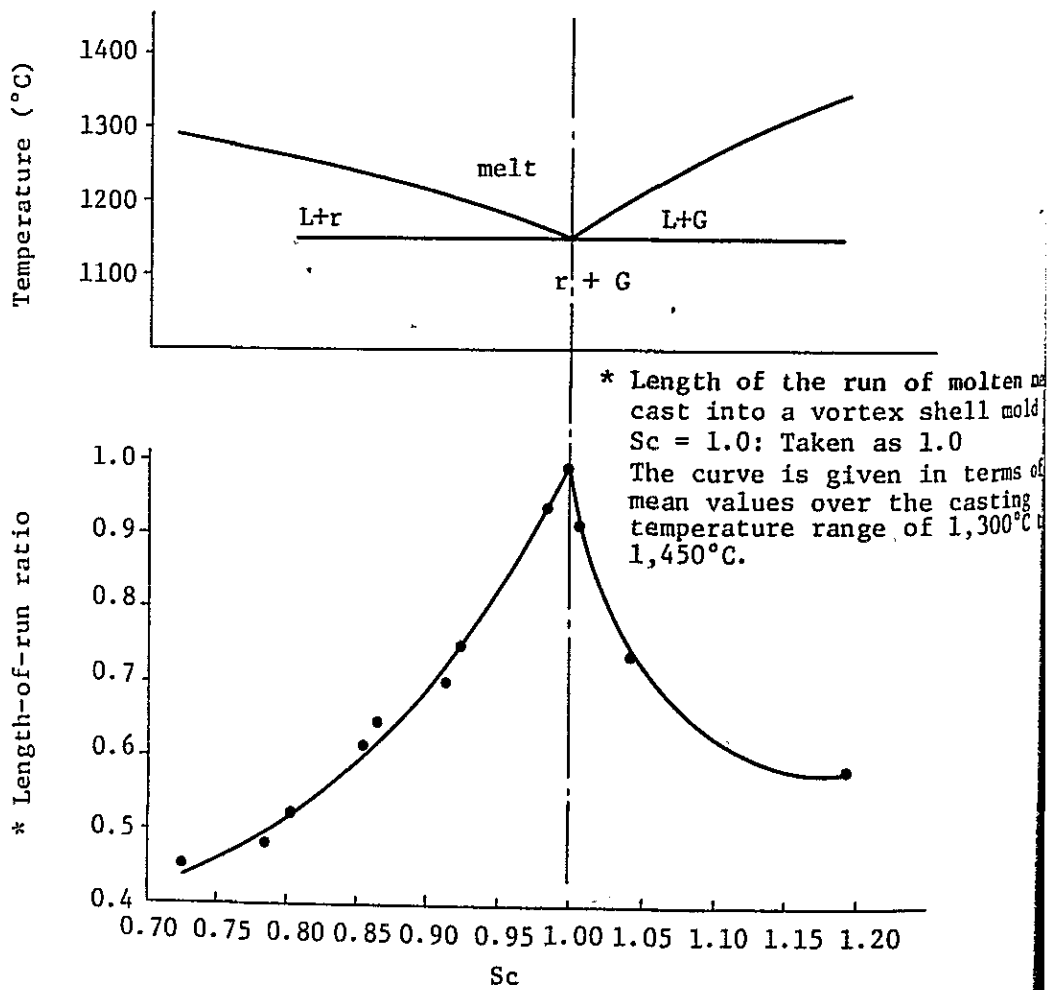


Fig. 2.6-16 Sc vs. length of run

When the molten metal is flowing through a narrow clearance, its length of run into the brick joint will become short if S_c is high, reducing the level of danger, accordingly.

- 5) Measurement of bottom mantle temperature, and action to be taken in the furnace operation

It is recommended to control the mantle temperature by providing a number of thermometers at the mantle surfaces. Where the thermometer is not provided or where the spacing of the thermometers is coarse, the mantle temperature should be detected by the feel. If the temperature is abnormally high, the furnace should be operated with a reduced blast rate while splashing water over the mantle until the temperature goes down to a tolerable value.

This examination by the hand should be carried out frequently. Care should be taken not to make an erroneous diagnosis as the mantle temperature will rise if high temperature drain water from the tuyeres runs down over the mantle.

26.4 Bricks for hot air stove

(1) Damage on hot air stove bricks

In recent years, the damage on the hot air stove bricks is chiefly accounted for by structural rupture resulting from the fact that the blast air temperature is increased more than necessary for the purpose of increased production in defiance of brick specifications.

The structural rupture is due greatly to the lack of the creep resistance of bricks against temperatures.

The Nelly is fed from only 2 hot stoves, but this kind of trouble will be rarely because the hot air temperature is low. The hot air stove trouble this time is developed because fouled furnace gas has attacked and molten down the bricks. The bricks denaturalized under the influence of dust laden in the furnace gas lose their creep resistance markedly.

Generally, the dust in the furnace gas is composed of iron oxides, lime, silica and alkali, etc.; if the hot stove is constructed by high alumina brick, dust deposit will grow to cause clogging. The clayey dust, however, gets vitrified.

Table 2.6-6 shows a chemical profile of dust in the furnace gas.

Table 2.6-6 Chemical composition of dust in the furnace gas

SiO ₂	Al ₂ O ₃	Fe ₂ O ₃	MnO	CaO	MgO	Na ₂ O	K ₂ O	SO ₃
12.7~ 18.9	4.6~ 10.3	12.8~ 60.1	0.35~ 0.9	3.1~ 13.4	1.35~ 2.8	0.1~ 0.35	0.15~ 0.65	0.05~ 1.75
S	PbO	ZnO	Ig. loss					
0.6~ 5.25	0~ 3.65	0~ 18.9	9.6~ 28.3					

In the hot air stove operation, therefore, care should be taken of the following points.

- i) To use fuel gas of high purity

In the case of furnace gas, the purity should be at least 20 mg/m³.

- ii) To prevent the overheat of dome bricks by the proportional control combustion air.

Namely, the temperature should be controlled to within a design value, particularly when clayey bricks are used.

No sample of damaged bricks from the hot air stove has been available to the survey mission, and no definite thing cannot be said about the damage.

An account of Kobe Steel's past experience in a trouble with No. 4 hot air stove for Amagasaki No. 2 blast furnace will provide something of reference for the COLAR.

The furnace gas for No. 2 hot air stove was scrubbed through Theisen washer (secondary gas scrubber).

The furnace gas contained as much dust as 30 to 50 mg/m³.

Coke oven gas was also used to increase the calorific value of fuel gas. Thus, the high-temperature air blast of higher than 1,000°C on the monthly average was achieved for the first time in Japan. However, the upper part of the checker was softened and run down to block up the air passage. Also, the checker bricks were broken down sending up the gas flow resistance. Once the softening took place, the gas flow resistance increased acceleratedly, and it became very hard to attain a desired blast air temperature. The hot air stove had to be shut down and repaired.

The repairs involved the replacement of checker bricks over a range of 1.0 m to 1.5 m.

The time required to repair was as follows.

° Cooling	:	approx. 5 days
° Repairs	:	approx. 3 days
° Heat storage	:	approx. 5 days
Total	:	approx. 13 days

The checker bricks were found to have been denaturalized as shown in Table 2.6-7.

The surfaces of the denaturalized bricks were found vitrified. The extraneous contaminants included Na₂O, K₂O, ZnO, CaO and Fe₂O₃. As a result, highly fusible materials, such as hercynite (FeAl₂O₄), were found developed. The bricks subjected to a high degree of denaturalization got their refractoriness reduced to 1,260°C. Continued operation was no longer possible, accordingly.

Table 2.6-7 Denaturalization of checker bricks

		Original brick	Denaturalized brick			
			A	B	C	D
General physical properties	Water absorption factor (%)	11.8	0.0	0.8	11.5	9.8
	Apparent porosity (%)	23.6	0.0	2.2	23.6	20.8
	Bulk specific gravity (%)	2.06	2.73	2.62	2.06	2.14
	Apparent specific gravity	2.64	2.73	2.68	2.70	2.68
	Refractoriness, (°C)	SK. 33	1260	1620	1720	1710
Chemical composition	SiO ₂ (%)	56.63	50.32	52.12	55.71	54.81
	Fe ₂ O ₃ (%)	2.02	4.53	2.10	2.07	2.37
	Al ₂ O ₃ (%)	40.37	32.75	37.43	38.60	39.77
	TiO ₂ (%)	.	1.17	1.27	1.38	1.40
	CaO (%)	0.14	4.10	0.74	0.24	0.10
	MgO (%)	0.18	0.32	0.16	0.24	0.16
	Na ₂ O (%)		2.87	1.69	0.48	0.63
	K ₂ O (%)		2.66	1.99	0.43	0.67
	ZnO (%)		0.4	0.2	0.1	0.3
	Total (%)	99.34	99.12	97.22	99.25	100.21
Mineral composition			Mullite Corundum Hercynite	Mullite Tridymite Cristobalite Corundum	Mullite Tridymite Cristobalite	Mullite Tridymite Cristobalite

Gasified particles of Alkali, ZnO, etc. produced in the chemical reaction process in the blast furnace are extremely finer than those developed in physical process.

For the purpose of cleaning away these contaminants, the gas scrubber should be designed and constructed with utmost care.

(2) Selection of bricks for hot air stove

The checker bricks are perforce required to be thin for the purpose of procuring a required area of heating surface.

They are heated entirely under loaded conditions, and the wall bricks are the first to yield under creep deformation.

Naturally, it is important to select checker bricks of proper characteristics.

In examining the creep of the hot air stove, the following two points should be taken into account.

- i) The furnace gas is used as a fuel gas. It contains much dust. Thus, the checker bricks should be such ones that stand extraneous contaminants and the resulting creep. SiO₂ bricks and high-alumina bricks are most recommendable in this respect.
- ii) The bricks themselves should have an ample creep resistance at temperatures and under loads which they are to encounter.

Fig. 2.6-17 shows the results of creep test on silica bricks, high alumina bricks and fireclay bricks under 2 kg/cm².

Usually, the creep test on refractories is carried out for a comparatively short period of up to 100 hrs.

However, 300 to 800 hrs. are required to attain a steady creep condition as shown in Table 2.6-8.

Assuming that the safety operating temperature is the one at which the creep quantity after 400 ~ 500 hrs in a steady creep speed is held within 1% in a long-term creep test, it will be as follows.

Silica brick	1,550°C
Al ₂ O ₃ 70% high alumina brick	1,300°C
SK35 fire clay brick	1,150°C

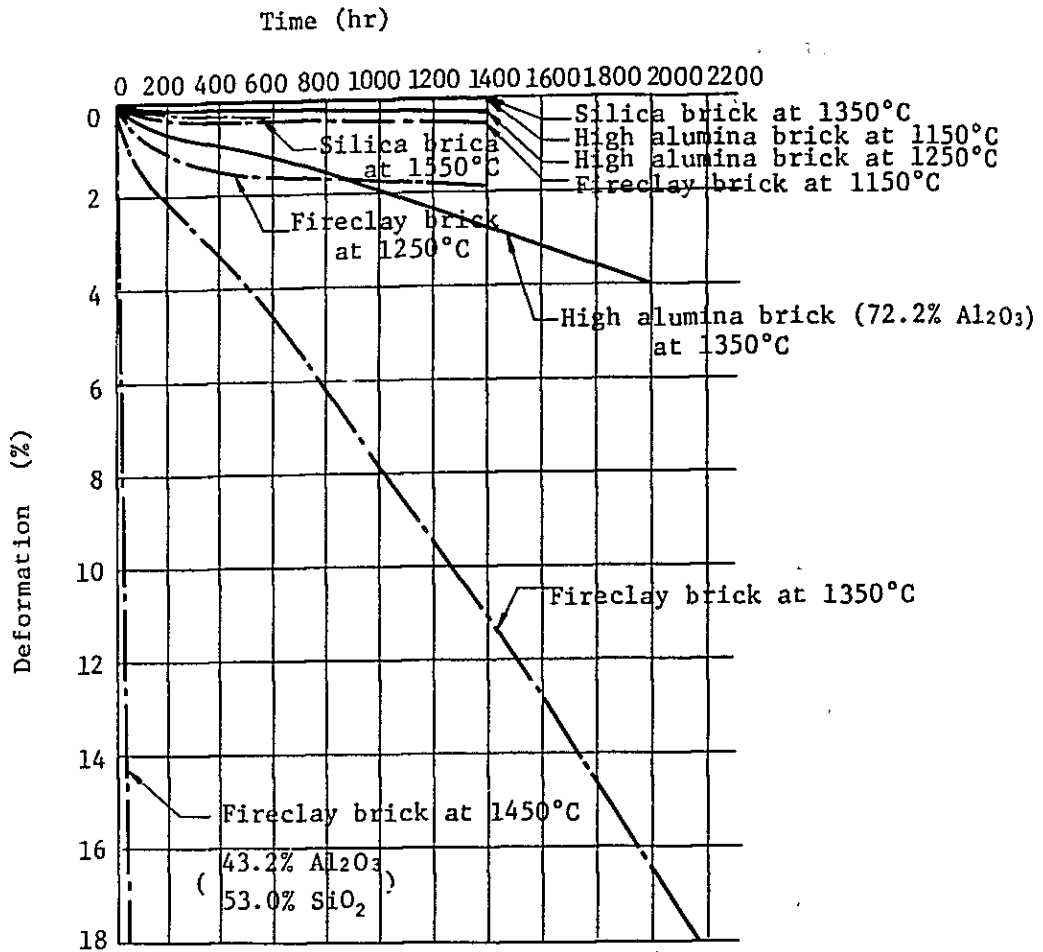


Fig. 2.6-17 Results of creep test at 2kg/cm² load

Table 2.6-8 Time to get steady-state creep rate

Specimen \ Item	Test temperature (°C)	Time to get steady state creep rate (hr)	Steady state creep rate (%/hr)
Silica brick	1550	300	0.0001
High alumina brick (Al ₂ O ₃ 70% class)	1250	600	0.0002
	1350	300	0.0010
Fireclay brick (SK35 class)	1150	400	0.0001
	1250	800	0.0005
	1350	300	0.0070

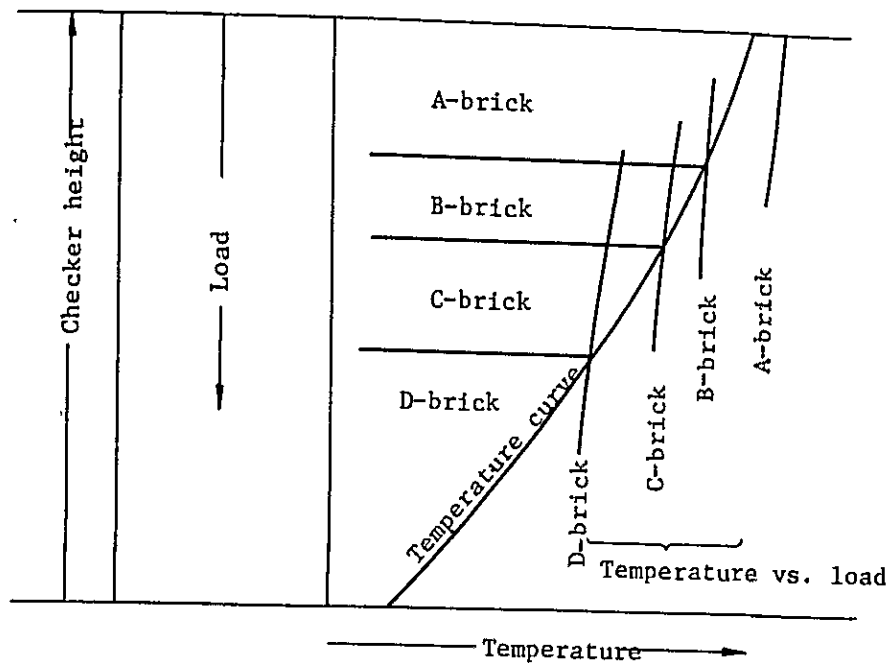


Fig. 2.6-18 A schematic chart showing the method of designing the checker bricks

In order to achieve a proper quality of checker bricks in view of creep resistance, a procedure as illustrated in Fig. 2.6-18 should be followed.

- 1) Determine the load first to meet the checker height.
- ii) Determine the temperature curve according to the checker height
- iii) Determine the temperature vs. load relationship for each specific type of brick.
- iv) Find the checker bricks that coming below the intersection between (ii) and (iii).

In this way, the blast air temperature to be set for the future can be set, or the bricks of the best specifications can be selected.